

UNIVERSITY OF TWENTE.

Faculty of Electrical Engineering, Mathematics & Computer Science

Researching Feasibility of mmWave Solutions for Insect Detection Applications

Nithin Suresh Babu (s2278359)
MSc Electrical Engineering

November 2021

Supervisors:
Prof.dr.ir. Paul J.M. Havinga
dr.ir. Jacob Kamminga
ir. Jeroen Klein Brinke
dr.ir. A.B.J. Kokkeler

Faculty of Electrical Engineering,
Mathematics and Computer Science
University of Twente
P.O. Box 217
7500 AE Enschede
The Netherlands

Abstract

Insect populations have been drastically declining in the past due to the affect of Artificial Light at Night (ALAN). Since nocturnal insects utilise light for migrating from one point to another, the presence of ALAN disrupts their path and largely affects their behaviour. Therefore, it becomes essential to monitor insect populations and investigate the effect of ALAN on them. However, despite the importance of ALAN on insects, there is no technology available to monitor this effect on them. Millimeter Wave (mmWave) radar technologies are non-obtrusive, ubiquitous and do not use light. Furthermore, they have shown promising results in detecting smaller targets because of their short wavelengths and have also known to show robustness in extreme weather conditions.

In this thesis, we research the feasibility and investigate the performance of a state of the art mmWave radar in detecting airborne insects successfully by deploying it in urban and suburban environments. The existing detection algorithm present in the radar system is modified and optimised to process radar returns from insect targets. In addition to this, we also develop an algorithm to estimate an approximate size of an insect target, which may be used to identify airborne insects up to a certain degree.

We were able to obtain an average precision and recall rate of 70% and 60% respectively in detecting airborne insects in distinct environments. The standard deviation and the error induced in validating the true range with the detected range for small targets placed at multiple distances were observed to be minimal in the range of $\pm$ 0.059m and $\pm$ 0.012m respectively. Furthermore, the effect of various external parameters on the performance of the mmWave radar system were also studied and analysed.

Our study revealed that the mmWave radar shows moderate performance in detecting airborne insects in different environments and introduces ecologists around the world to a new domain of monitoring biodiversity and insect abundance by employing state of the art mmWave radar technology.

Acknowledgements

First of all, I would like to thank Prof.dr.ing Paul J.M. Havinga for giving me this wonderful opportunity to work in this thesis project. I am grateful for his valuable assistance during the course of the thesis.

Secondly, I would like to thank my daily supervisors Dr.Ir.Jacob Kamminga and Jeroen Klein Brinke who gave me numerous valuable advice about my thesis project. They were always kind and patient to guide me step by step to finish this thesis. They also provided me with great support during some challenging times and motivated me to think out of the box to solve the problems at hand. During the writing of this thesis, they also patiently reviewed my work and provided me with suggestions to improve it. I am very grateful for their encouragement and support.

Additionally, I would also like to express my sincere gratitude to Dr.Ir.Kamiel Spoelstra from Netherlands Institute of Ecology (NIOO-KANW) and Rotem Kadan Zilber from ARISE for their exceptional help and guidance in conducting the field tests required for our thesis project in Katwijk Aan Zee and Artis Experimental Site respectively. Without their help it would have not been possible to complete this thesis project. They also shared a lot of useful advice and knowledge into the current state of the art technologies utilised in monitoring and detecting biodiversity worldwide.

Last but not least, I express massive gratitude to my family and friends. They gave me the mental courage and strength to face the challenges embedded in this thesis and successfully complete it.

Contents

1 Introduction **13**
- 1.1 Background . . . 13
- 1.2 Motivation . . . 14
- 1.3 Problem Statement . . . 16
- 1.4 Research Goals and Questions . . . 17
- 1.5 Research Approach . . . 17

2 State of the art **19**
- 2.1 Technical Background . . . 19
  - 2.1.1 Conventional Radar Technology . . . 19
  - 2.1.2 mmWave Frequency Radar Technology . . . 23
  - 2.1.3 LiDAR Technology . . . 24
  - 2.1.4 Optoacoustic Technology . . . 26
- 2.2 Literature Review . . . 28
  - 2.2.1 Methodology . . . 28
  - 2.2.2 Conventional Radars . . . 28
  - 2.2.3 Light Detection and Ranging (LiDAR) . . . 32
  - 2.2.4 Optoacoustic Technology . . . 34
  - 2.2.5 mmWave Radar . . . 36
- 2.3 Discussion and Analysis . . . 38
  - 2.3.1 Requirements of the System . . . 39
  - 2.3.2 Literature Study Analysis . . . 40
  - 2.3.3 Summary . . . 41

3 mmWave Radar Theory **44**
- 3.1 FMCW radar . . . 44
- 3.2 Range Measurement . . . 46
  - 3.2.1 Range Resolution . . . 47

3.3 Velocity Measurement 48
3.3.1 Velocity resolution 49
3.4 Angle of Arrival Measurement 50
3.4.1 Angular Resolution 50
3.5 Object Detection with CFAR Algorithm 51
3.5.1 CASO-CFAR Algorithm 51
3.6 Clustering with Gtrack Algorithm 53
3.7 Board Specific Parameters 53
3.7.1 Profile 54
3.7.2 Frame 54
3.7.3 Chirp 55

4 System Methodology **58**
4.1 Introduction 58
4.2 Information Extraction Module 59
4.2.1 IWR6843AoP Module 59
4.3 Radar Front End 60
4.3.1 Maximum Range Estimation 61
4.3.2 Maximum Range Resolution 63
4.3.3 Maximum Velocity and Velocity Resolution 64
4.4 Insect Detection and Processing 65
4.4.1 CFAR Algorithm 67
4.4.2 Gtrack Algorithm 69
4.4.3 Spread Estimation Algorithm 71
4.5 Experimental Setup Overview 73
4.5.1 Setup Components 74
4.6 Annotation of Insect Data 75
4.6.1 Dataset Preparation 75
4.7 Test Environments and Conditions 76
4.8 System Performance Metrics 77

5 Experimental Methodology and Analysis **79**
5.1 Non-Insect Target Detection 79
5.1.1 Data Collection and Performance Analysis 79
5.2 Airborne Insect Detection 83
5.2.1 Data Collection and Performance Analysis 83

6 Results **96**
6.1 Non Insect Target Detection 96
6.2 Airborne Insect Detection 99

7 Discussion, Conclusion and Future Work **102**
7.1 Constant False Alarm Rate (CFAR) Detection Algorithm 102
7.2 Clustering Algorithm 103
7.3 Spread Estimation Algorithm 104
7.4 Performance of the mmWave Radar in Detecting Small Non Insect Targets. 105
7.5 Overall Performance of the mmWave Radar in Detecting Airborne Insects 106
7.5.1 Effect of the Scaling Threshold Parameter 107
7.5.2 Effect of the Size of the Insects 108
7.5.3 Effect of External Environmental Conditions 108
7.6 Conclusion 109
7.7 Future Work and Recommendations 110

A Theory **119**
A.1 Cell-averaging CFAR 119

List of Figures

1.1 Figure depicting the effect of ALAN on various species of insects [12]. . 15
1.2 The vacuum cleaner effect of light on insects, where insects are drawn out of their habitats. 15

2.1 Figure illustrates the numerous frequency bands and their corresponding wavelengths used in radar technologies. 20
2.2 Schematic representation of the working of a pulse-based scanning radar, in which the radar system transmits a burst of pulses to detect targets in its Field of View (FoV). 21
2.3 Schematic representation of the operation of Vertical Looking Radars (VLRs). 21
2.4 Illustrative working of a Doppler based radar which uses the principle Doppler shift of the targets to identify them. 22
2.5 Illustrative working of a Polarimetric radar with dual polarization modes which use the concept of horizontal and vertical polarization components to detect targets. [13] 23
2.6 Schematic representation of a working of a Light Detection and Ranging (LiDAR) system which uses light waves emitted from laser beams to detect targets. 25
2.7 Airborne LiDAR system mapping vegetation over a particular area. 25
2.8 Illustrative working of a Microphone used to record audio data from its surrounding environment. 26
2.9 Working of an Optoelectronic sensor to record data from its surrounding environment and convert it into audio data.. 28

3.1 illustrative graph to show the estimation of the IF signal from the Transmitting Antenna (TX)-Receiving Antenna (RX) chirp [47]. 45
3.2 Range Resolution as a function of Bandwidth 48
3.3 Illustrative working of a CASO-CFAR Algorithm to determine if a detection performed by the radar system is from an actual target source. 52

3.4 Typical Frame Structure of the mmWave radar system in defining a chirp sequence to tranmsit. 55
3.5 Velocity and velocity resolution as a function of chirp interval. 57
3.6 Figure depicts an overview of the transmitted chirp and the important parameters associated with it to define the sensing capability of the system [50] 57

4.1 High Level Overview of the mmWave Radar Module in extracting the surrounding information from its Region of Interest (RoI). 59
4.2 IWR6843AoP mmWave Radar Module 60
4.3 Radar Front End Overview 61
4.4 Graph to depict the variation of Signal to Noise Ratio (SNR) as a function of Range for Different Radar Cross Section (RCS) values. 62
4.5 Configured Range Resolution 64
4.6 Figure depicts the configured velocity and velocity resolution. 65
4.7 Back End Processing Chain of the Radar System to detect targets in the mmWave radar's FoV. 66
4.8 Flowchart to show the process involved in determining if a detection performed from the mmWave radar is from an insect target 67
4.9 Hypothetical Boundary layer as depicted by the clustering algorithm. This boundary layer takes the shape of a cuboid outside which the mmWave radar module would not be able to measure point cloud data. 70
4.10 Experimental Setup considered to deploy the mmWave radar module in different environments. The light trap is used to lure airborne insects near out system and the camera modules are used for validating the data obtained by the mmWave radar system. 73
4.11 System Flow of UART Interface to allow configuration and debugging of data in real time. The UART data port receives the data from the radar system and COM port transmits specific chirp configurations to the radar/ 74
4.12 Figure shows the multiple test environments in which the experiments to detect airborne insects were conducted. 76

5.1 The small insect-like targets that were utilised for evaluating the performance of the mmWave radar. 80
5.2 Figure denotes the detection of various objects by the radar system in the X-Y axis. The black circle indicates the point cloud cluster formed by the object, the grey dotted line indicates the FoV of the sensor, the blue dot denotes the point cloud data reflected by that particular object. The Red box in the center denotes the mmWave radar itself. 81

5.3 Figure denotes an occurrence of an insect target near our experimental setup. This insect target is indicated by the black square box highlighting the insect's outer layer. 84
5.4 Real time coordinates of the insect calculated by the mmWave radar as indicated by red dots in the 3D plot. These coordinates were estimated by the radar at a specific time interval at which the insect was present near our system. 85
5.5 Analysis of Insect data obtained in an Urban Environment. 86
5.6 Figure denoting the position displaced by each insect target as estimated by the mmWave radar module. The Insect ID in legend represents each insect cluster detected by the radar system. 87
5.7 Experimental setup of the mmWave radar deployed in the suburban environment. 90
5.8 Insect recorded by the Video Camera occurring near our system as indicated by the white square box. 91
5.9 3D graph plotting the real time coordinates of the insect indicated by red dots, as calculated by the mmWave radar at a certain point in time. 91
5.10 Experimental setup for the mmWave radar deployed in Artis Experimental site. 93
5.11 Figure denotes the occurrence of two insects near the experimental setup. The insects are indicated by the black circles marking their outer layer in the figure. 94
5.12 3D plot denoting the coordinates of the insects depicted in Figure 5.11 as red and yellow markings at some point in time. 95

6.1 Figure Denoting the maximum range detected by the mmWave radar for different targets utilised in this experiment. 97
6.2 Figure 6.2a 6.2b and 6.2c show the measured range from the mmWave radar with standard deviation as error bars. Figure 6.2d depicts the total standard deviation obtained for each radius of the battery. 98
6.3 Figure depicting the relation between the False Positive Rate and the Scaling Threshold in different test environments. 99
6.4 figure representing the effect of size of the insects on the false negative rate achieved by the system. 100
6.5 Figure illustrates the effect of the external environment on the performance obtained in the system. 101

A.1 Working of the CA-CFAR algorithm 120
A.2 Literature Review Summary 121

List of Tables

2.1 Comparison of various Technologies Based on Requirements of the System. 40
2.2 Decision Matrix Representing the Weights and Total Score for Each Decision Criteria. 41

3.1 Profile Parameters for the System 54
3.2 Chirp Parameters for the System 56

4.1 Table shows the calibration parameters for estimating the maximum range obtained by the system. 63
4.2 Table shows the theoretical estimations from the front end layer 65
4.3 Table depicts the CFAR configuration parameters employed for our work. 68
4.4 Clustering Parameters employed for our work to cluster radar returns from insect targets. 71
4.5 Performance metrics realized for evaluating the performance of the System. 78

5.1 The deviation in range measured by the mmWave radar for the batteries kept at different ranges for a set of 20 continuous measurements. 82
5.2 The environmental conditions observed during the tests performed in an Urban Environment. 83
5.3 Ground Truth for Insects 84
5.4 Evaluation of the performance metrics from the experimental data collected in urban environment. 88
5.5 Environmental Conditions observed during the course of the experiment. . 89
5.6 Analysis of the performance metrics that were estimated from the data collected in Suburban Environment. 89
5.7 The variation in the size of insects that were attracted by the light source during the course of the experiment. 92
5.8 Environmental Conditions observed during the experiment in Artis Zoo. . 92

5.9 Evaluation of the performance metrics for varying Scaling Thresholds. . . 94

6.1 Overall performance of the system in determining the true range of small targets having different radius and size. 97
6.2 Overall performance of the mmWave radar system in detecting airborne insects in all the environments. 99

List of Acronyms

ALAN	Artificial Light at Night
AoA	Angle of Arrival
CASO-CFAR	Cell Averaging Smallest of Constant False Alarm Rate
CA-CFAR	Cell Averaging Constant False Alarm Rate
CCD	Charge Coupled Device
CFAR	Constant False Alarm Rate
CMOS	Complementary Metal-Oxide Semiconductor
CUT	Cell Under Test
CW	Continuous Wave
DBSCAN	Density Based Scanning Algorithm
DSP	Digital Signal Processor
FFT	Fast Fourier Transform
FMCW	Frequency Modulated Continuous Wave
FoV	Field of View
FNR	False Negative Rate
FPR	False Positive Rate
GHz	Gigahertz
Gtrack	Group Tracking

IF	Intermediate Frequency
IWR6843AoP-EVM	IWR6843 Antenna on Package-Evaluation Module
LiDAR	Light Detection and Ranging
MCU	Micro Controller Unit
MHz	Megahertz
MIMO	Multiple Input Multiple Output
mmWave	Millimeter Wave
MTR	Migration Traffic Rate
RCS	Radar Cross Section
RF	Radio Frequency
RoI	Region of Interest
RX	Receiving Antenna
SDK	Software Development Kit
SNR	Signal to Noise Ratio
TDOA	Time Difference of Arrival
TPR	True Positive Rate
TX	Transmitting Antenna
UART	Universal Asynchronous Receiver Transmitter
USB	Universal Serial Bus
UV	UltraViolet
VLRs	Vertical Looking Radars

Chapter 1

Introduction

Ecologists and conservationists have long studied global insect declines in biodiversity. Many insect populations are undergoing rapid and worrying declines, that could have serious implications on ecosystem functioning, ranging from pollination to insectivore bats and birds. One of the main drivers for such declines are ALAN and it mainly affects nocturnal insects as it deviates them from their original migration path. Recent studies conclude that if the current trends continue, 40% of insect species would go extinct in the next 100 years. Despite such frightening rates, there is hardly any research performed on the most effective and compact technology which could be adopted for detecting and monitoring the declining insect species across the globe. As a result, it becomes critical to investigate the most suitable technology for detecting insects attracted to ALAN and assess its performance by deploying it in various environments.

1.1 Background

Biodiversity (biological diversity) encompasses all the variety of life on Earth, from genes to ecosystems, it also includes the developmental, ecological and evolutionary processes that sustain life. Biodiversity is also known to play an important role in ecosystem functioning and is a principal aspect in most of our lives for many reasons. To begin with, biodiversity supplies the organisms that live inside it with essential resources such as food, fuel, and medication in order for them to survive and grow on our planet. Secondly, the various lifeforms associated with it provide crucial services such as climate regulation, nutrient cycling and water purification [1] [2]. As a result, biodiversity must be protected for a better and more sustainable future, given its ever-increasing importance in ecosystem functioning and its function as a human resource.

Insects play an important role in forming the backbone of our terrestrial ecosystem and

biodiversity. Insects are significant due to their diversity, ecological importance, and beneficial effects on agriculture, human health, and natural resources. They are also known to perform a multitude of tasks such as cycling nutrients, pollinating plants, maintaining soil structure, physical decomposition and fertility to regulate our environment and maintain the balance in nature [3]. They are also a key component in the food web and provide a major food source for other species. Furthermore, insects are also an important supplementary source of calories and proteins for humans in many regions of the world, and around 500 species of insects are known to be consumed [3]. The study of insects has produced major advances in our understanding of bio-mechanics, climate change and physiology [4], which has further resulted in scientists and researchers understand the evolution of nature in an effective way. Therefore, it has to be comprehended that insect species are one of the most important species in our ecosystem and its conservation is of utmost importance currently. However, despite the countless benefits insects have brought into this world, previous studies [5][6][7] have revealed that insect populations have been plummeting at an alarming rate. The declination of insect populations worldwide will have numerous drastic and irreversible effects on our environment.

1.2 Motivation

Drastic decline in insect populations have gained increased attention in the scientific community. Recent studies have showed that, insect population has declined 75% over the past three decades. These decline in insect populations is mostly accounted for by large scale factors such as landmass changes, use of pesticides, climatic change and ALAN [5]. ALAN is a widespread phenomenon that strongly impacts insects that are sensitive to light and active at night. Light is an essential cue for insects, and several nocturnal insects utilize light for orientation, navigation, avoidance of predators, location of food and reproductive behaviour [8]. Several Nocturnal insects are extremely sensitive and attracted to various spectra of light such as blue and red, and are most often negatively affected by ALAN because of their exceptional visual abilities in low-light conditions. Therefore, ALAN is intermittently recognized as a possible cause of the observed drop in various species of male and female nocturnal insects such as *Spruce Budworm*, *Choristoneura fumiferana* [9] and moths of *Yponomeuta cagnagella* and *Ligdia adustata* [10]. Recent collaborative studies conducted by Langevelde et al. [11] observed that Moth populations have been declining steadily over the past 30 years in Netherlands as they are nocturnally active and are attracted to light compared to species that are diurnal or not attracted to lights. ALAN has been steadily increasing at an annual rate of 2 to 6% over the past decade [5]. Despite its ubiquity, it is often overlooked when analysing the decline in insect population. ALAN

results mainly, from artificial light sources such as light poles, incandescence lamps, infrastructure light sources and is further amplified by skyglow, i.e. reflection of light in the atmosphere, particularly from clouds [6]. ALAN not only affects insects, but is also known to affect humans, leading to various problems such as obesity, depression and breast cancer [7]. ALAN separates the insect population from their permanent habitat and creates a sense of temporary false habitats for insects near these light sources. As a result, insects exhaust all their remaining energy, creating a flux near light sources and ultimately die, resulting in local population sinks, which eventually affects the population of insects globally. Figure 1.1 depicts how ALAN can affect multiple species of insects ranging from small Beetles to large Bats.



Figure 1.1: *Figure depicting the effect of ALAN on various species of insects [12].*

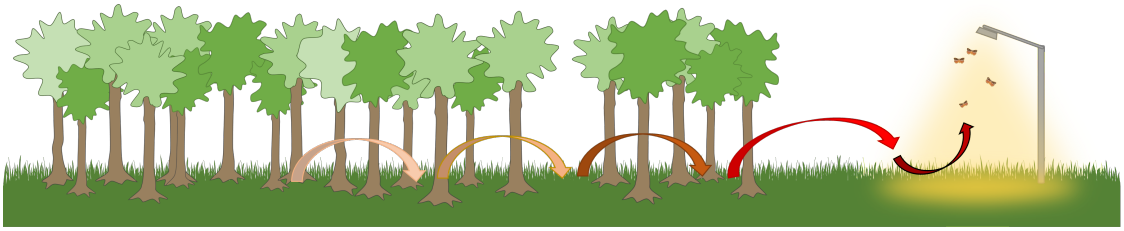


Figure 1.2: *The vacuum cleaner effect of light on insects, where insects are drawn out of their habitats.*

Insect detection applications in the past has heavily relied on either studying insect migration over a specific geographical area or studying insect and pest population densities over agricultural crops. However, there has been very little research on the effect of

artificial light sources on insect population densities and the "**Vacuum Cleaner Effect**". Vacuum Cleaner effect as shown in Figure 1.2 is defined as to how insects respond to light sources, at various distance and locations. Hence, it becomes vital to detect insect populations, flying near artificial light sources, in order to obtain a clear understanding on how they affect different species of insects in different environments. It also becomes fundamental to understand that insect detection and tracking could have its applications in diverse areas such as in

- Estimating the insect population density over a certain geographical area.
- Determining the most common migration path followed by insects and also aid in determining Migration Traffic Rate (MTR) over a certain stretch or an area.
- Provide us with information and insights regarding how various environmental factors such as temperature, rain and wind speeds affect the flight and behaviour of insect species.

Since, insect populations are observed to migrate more frequently in the night time, than during the day and as a result are the most vulnerable species to ALAN and the Vacuum cleaner effect. As a result, it becomes critical to efficiently monitor insect populations accumulating near these artificial sources of light. The respective technology implemented should be independent of light as it has been observed to affect them notoriously. Additionally, it needs to be comprehended that conventional airborne insect traps cannot be used to monitor insects as they have shown to physically harm the insects, alter their usual flight and in the process kill or destroy them. Thus, several researchers and scientists have tried to monitor the impact of artificial light on insects by using several state of the art technologies such as LiDAR, Radar systems, and Optoacoustic technologies, but have yet not achieved the expected results as these approaches have various challenges associated with themselves. Since, conventional insect traps physically harm the insects, a comprehensive research needs to be performed to understand the various challenges associated with each technology and evaluate the numerous trade-offs that would have to be considered in order implement an efficient system to detect airborne insects in real time. Thus, it becomes important to effectively evaluate the performance of the chosen system in detecting airborne insects without physically harming or altering the flight of insects.

1.3 Problem Statement

The technologies used until now for insect monitoring are cost inefficient, intricate to deploy, are enormous in size or weight and require highly complex signal processing algo-

rithms. Therefore, in order to effectively use insect detection and tagging in such applications, it becomes necessary to utilise a technology that allows for unattended continuous sampling, is compact, flexible, cost-effective and could be easily deployed in multiple locations at the same time. Most importantly, the method should be independent of light as any interaction between the measuring technology and environmental light must be avoided. mmWave radars are one such technology that comply with these requirements and have shown exceptional results in various automobile and vehicular applications because of their high performance and efficiency. However, their application has yet not been extensively applied in ecology for insect monitoring applications. Thus, it becomes important to understand the feasibility of the state of the art mmWave solutions in detecting airborne insects and how various parameters such as its transmission range, range resolution and SNR affect the detection capability of the system. It also becomes important to understand the trade-offs that would required to be taken in order to enhance the performance of the radar in detecting and tracking airborne insects in various environments.

In the end, we envision a ubiquitous network of small unobtrusive mmWave sensor nodes that detect and track airborne insects in various environments.

1.4 Research Goals and Questions

This Research proposes to use mmWave radar technology for detecting airborne insects. The primary research question is: **What is the performance of mmWave radar in detecting airborne insects?** The key sub questions are:

- What is the maximum theoretical detection range and the range resolution achieved by the mmWave radar in detecting small targets?
- What is the performance of the mmWave radar in detecting small objects that have equivalent size to that of insects?
- What is the performance of the mmWave radar in detecting airborne insects in urban and suburban environments and what are the main parameters that affect the performance?

1.5 Research Approach

The reasoning and the advantages of using mmWave technology for this application is established in Chapter 2 where the relevant literature available for detecting insects is studied and evaluated based on the requirements of the system mentioned in Section 2.3.

The research will then look to estimate the theoretical maximum detection range and, the radar could achieve in detecting simulated insect returns with a relatively high signal to noise ratio.

The objects chosen for addressing the second research question were spherical metal watch batteries of different sizes. The maximum detection range was then observed for each battery and deviation of the measured range from the true range was then calculated. This observation paved the way for quantifying the mean and the standard deviation of the radar system and thus, depict the error present in the measurement of the system.

The performance of the system in detecting airborne insects was then quantified by validating the number of insects that occured during the course of the experiments conducted in urban and suburban environments and subsequently comparing it with the detection capability of the mmWave radar in detecting them successfully. This was then followed by discussing and analysing the major parameters that affect the performance of the radar in different environments.

Lastly, The limitations of the existing algorithms are discussed and recommendations are provided to further optimise the mmWave radar system and enhance its performance in the near future.

Chapter 2

State of the art

This chapter briefly introduces the technical background of the technologies that have been used in insect detection applications. Next, the readers are introduced to the challenges associated with each technology, it is then followed by conducting a comprehensive literature review, to select the most suitable insect detection and monitoring technology for our study with minimal overhead.

2.1 Technical Background

2.1.1 Conventional Radar Technology

Conventional entomological radar technology have been an important aspect in the study of broad scale species migration in recent years. Conventional radar technology, used in the past to monitor insects were grouped by the following frequency bands as observed in figure 2.1. The choice of a specific frequency band of radar systems can have significant effects on several factors as discussed below:-

- **Physical Size:** The physical size of the antenna is directly proportional to the wavelength of the specific band. The higher the wavelength, antenna sizes will be large and heavy. Whereas, for smaller wavelengths, antenna sizes can be small and packed in small chips, which allows them to operate with less weight and complexity.
- **Transmitted Power:** The amount of power transmitted increases as the wavelengths increase. Therefore, radars employing smaller wavelengths may transmit considerably less power and cover smaller ranges.

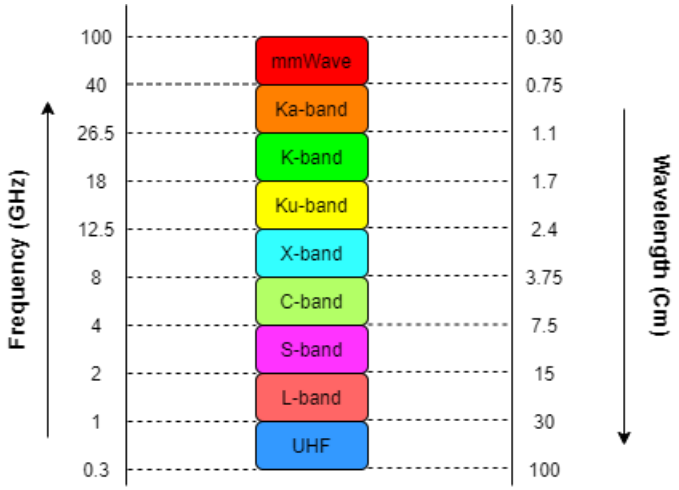


Figure 2.1: *Figure illustrates the numerous frequency bands and their corresponding wavelengths used in radar technologies.*

- **Beamwidth:** Beamwidth refers to the radar's ability to focus radiated energy in a small area and is affected by antenna size and frequency. For a given antenna size, a higher frequency allows the beam to be more closely focused.
- **Radar Cross Section:** RCS of a target is the equivalent area as seen by the radar system. It is the measure of how detectable an object is by the radar system. Therefore, a larger RCS indicates that the object is more easily detected. However, RCS is not directly related to the physical cross-section of the object and depends on a number of factors such as its material, size, angle of reflection and the polarization of the transmitted and received radiation with relation to the orientation of the object.

Based on the above frequency bands, radar systems can be broadly classified into pulse based scanning radars, VLRs, Doppler based radars and Dual polarisation radars.

Pulse Based Scanning Radars

As illustrated in Figure 2.2, in a pulsed based scanning radar, electromagnetic waves are transmitted from the radar antenna in short bursts. These short bursts of waves are interrupted for a period of time, so that the wave can reach a reflecting target and a portion of the energy can return to the receiver before the next burst of waves is transmitted. Thus, the interval between the transmission and reception of pulses can determine the distance to the target relative to the radar's position.

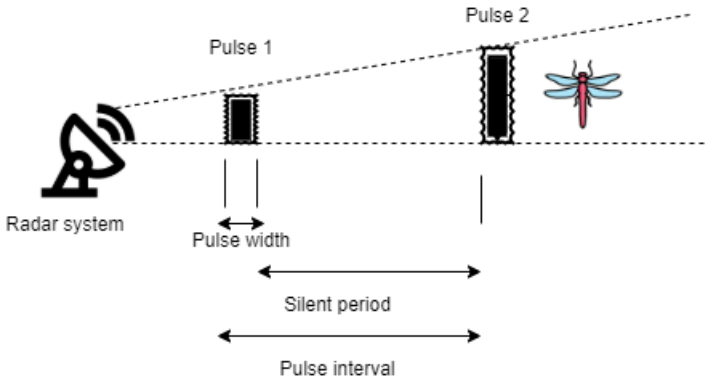


Figure 2.2: *Schematic representation of the working of a pulse-based scanning radar, in which the radar system transmits a burst of pulses to detect targets in its FoV.*

Vertical Looking Radars

VLRs consist of a transreceiver module that emits a continuous narrow cone beam into the sky. When airborne objects fly over the beam, they reflect and scatter the continuous signal. This reflected signal from the aerial objects would have a potential difference with respect to the original wave and would be out of phase. By measuring the potential and the phase difference, it is possible to determine the height at which these objects are detected. Overflying objects modulate a signal in such a way that advanced Fourier transforms can be applied to extract important parameters such as reflectivity coefficient, direction of movement, and angle of arrival of various objects. The transreceiver module is further placed on a rotating platform to enhance the field of view.

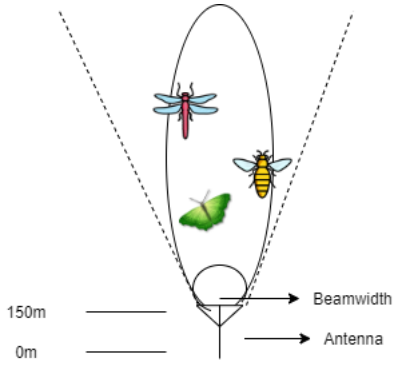


Figure 2.3: *Schematic representation of the operation of VLRs.*

Doppler Based Radar Systems

Doppler radar systems utilise the well-known Doppler effect and are a type of pulse based scanning radar, in which the radar system transmits radio wave pulses in a specific direction and listens for any returned signal. As the radiowaves strike the object, the signal is scattered in all directions and some of the energy is reflected directly back to the radar. By measuring the shift in phase between a transmitted pulse and the received echo, the target's movement from the radar is calculated. This provides a velocity along the direction the radar is pointing, called radial velocity. A positive phase shift implies motion towards the radar and a negative shift indicates motion away from the radar. This phase shift effect is similar to the "Doppler shift" observed with sound waves. As the object is moving towards your location, the frequency of sound is higher due to compression of the sound waves, and when the object moves away from your location, sound waves are stretched, resulting in a lower frequency. Thus, this technology is currently been widely used to monitor bats, birds and insects migration over a large geographical area.

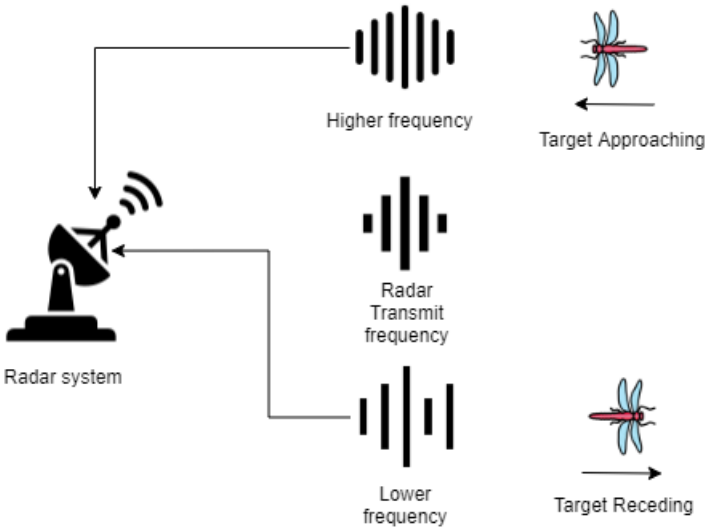


Figure 2.4: *Illustrative working of a Doppler based radar which uses the principle Doppler shift of the targets to identify them.*

Dual Polarisation Radars

A polarimetric radar is another name for this radar technology. The radar system transmits and receives linearly polarized RF signals and alternates between horizontal and vertical polarizations when transmitting individual or a group of pulses. In most cases, these radar systems transmit both polarization orientations simultaneously at the same time.

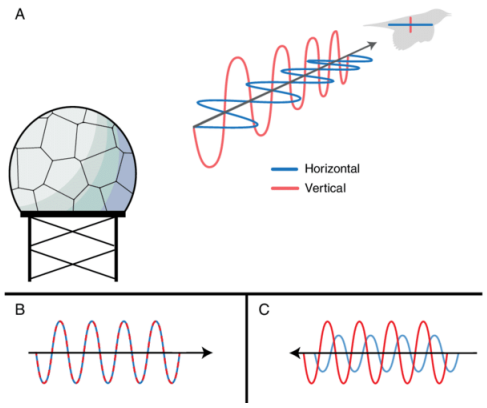


Figure 2.5: *Illustrative working of a Polarimetric radar with dual polarization modes which use the concept of horizontal and vertical polarization components to detect targets. [13]*

2.1.2 mmWave Frequency Radar Technology

mmWave refers to a class of radar technology that uses short-wavelength and high frequency electromagnetic waves. The working of mmWave radar technology is similar to conventional radar systems, where radar systems transmit radiowave signals which are intercepted by targets in the path. By capturing this signal, the system can then determine the range, velocity and angle of the targets.

mmWave radars transmit signals with a wavelength in the millimeter range. This is considered a short wavelength in the electromagnetic spectrum and because of this, the size of system components required such as antennas required to process signals becomes relatively small. mmWave systems generally operate at 40 to 100 GHz frequency range, with a corresponding wavelength ranging from 0.75 to 0.30cm. This small wavelength will enable the system to detect small objects and their movements .

mmWave Harmonic Tags

Recent developments in the field of mmWave frequency radar technology, researchers have considered using harmonic tags tagged to the body of insects to measure and detect their flight pattern and movement. The tag consists of a wire antenna attached to a Schottky diode, which uses the radar signal as an energy source, re-emitting a harmonic of the transmitted wavelength. These harmonic tracking systems comprise of a transponder and the receiver. The tags act as a receiver and a ground based scanning radar acts as a transreceiver module. The signals received in the ground based transreceiver can then be processed to obtain its position and flight pattern.

2.1.3 LiDAR Technology

LiDAR is a technology that employs light waves instead of radio waves for monitoring and tracking insect species and works in the optical part of the electromagnetic spectrum. LiDAR systems utilise a laser to illuminate a target object and a photodiode is used to register the backscattered radiation. A LiDAR system fires thousand pulses of light waves per second. These light waves bounce off objects and return to the LiDAR sensor. The sensor then utilises the time it takes for each pulse to return to calculate distance (time of flight). These pulsed returns can be then fed to advanced processing algorithms to visualise point cloud data and generate a 3D map of the target area in interest.

LiDAR systems, employed in insect and species monitoring applications, commonly use a type of atmospheric remote sensing technique known as Scheimpflug principle, referred to as Scheimpflug LiDAR (sLiDAR) [14]. The working of Scheimpflug principle states that when a laser beam is transmitted into the atmosphere, the backscattering echo of the entire illuminating probe volume is still in focus simultaneously without diminishing the aperture as long as the object plane, image plane and the lens plane intersect with each other [14]. A two dimensional Charge Coupled Device (CCD)/Complementary Metal-Oxide Semiconductor (CMOS) camera can be then used to resolve the backscattering echo of the transmitted laser beam. The transmitting optics used in LiDAR system can direct the laser beam into a specific direction and the receiving optics can enlarge and direct the received backscattered signal into the receiver module. Conventional LiDAR systems for insect and pest monitoring applications employ a Continuous Wave (CW) laser system utilising wavelengths in the range of 808 to 821 nm operating in the near infrared spectral region. A CW system depicts that the transmitter continuously transmits waves of constant amplitude and frequency instead of using short periodic bursts. The major difference between traditional entomological radars and LiDAR systems is that LiDAR systems in the optical spectrum will have the capability to detect even the smallest of insect, because most insects will be much smaller than the wavelengths of radiowaves (2.5 to 3.75cm) used

in conventional lower band radars, but will be larger than the wavelengths of light waves used in LiDAR (for example at 808 nm wavelength) [15][16]. Thus, the proper choice of wavelength plays an important role in efficient tracking and monitoring of insects. The working of a conventional CW LiDAR system is shown in Figure 2.6.

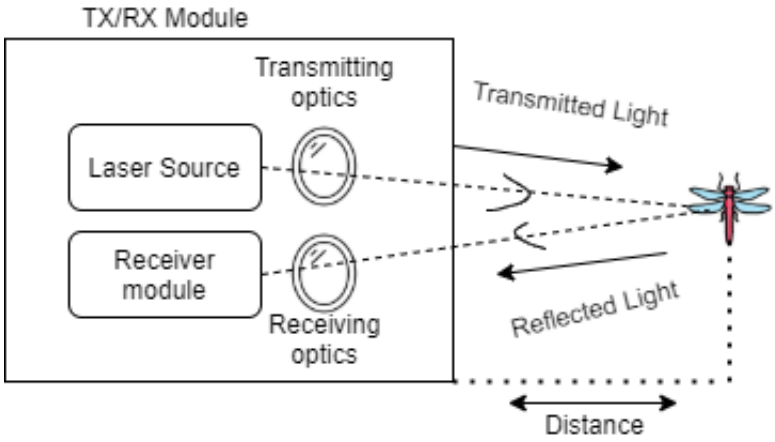


Figure 2.6: *Schematic representation of a working of a LiDAR system which uses light waves emitted from laser beams to detect targets.*

Airborne LiDAR systems as shown in Figure 2.7 are those systems, in which the laser scanner is attached to an aircraft during flight, which further creates a 3-D point cloud model of the landscape it is monitoring. Airborne LiDAR systems have been primarily used to study vegetation, sea ice and ocean surface characteristics which could further depict insect and various species abundance over these areas.

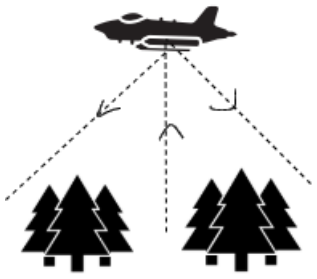


Figure 2.7: *Airborne LiDAR system mapping vegetation over a particular area.*

2.1.4 Optoacoustic Technology

The acoustical properties of flight activities of economically and socially important insects have drawn attention even prior to the wide acceptance of microphones. Acoustic sensors mainly consist of a microphone to record sounds from various sources. The integration of acoustic sensors with optical or Optoelectronic sensors is what has come to be known as Optoacoustic technology. Optoacoustic technologies mainly consist of microphone or an Optoelectronic sensor coupled to a sound recorder to record insect's wing-flap sounds and buzzes generated by the insects.

Acoustic Technology Integrated with a Microphone

Microphones record these data as analog signals, which is further treated by a frequency analyser to convert it into digital format. The converted digital data is then processed by a computer using Fast Fourier Transform to extract specific parameters such as its wing size, proportion and its wing span length. Figure 2.8 Shows the operation of an acoustic technology with an integration of the microphone.

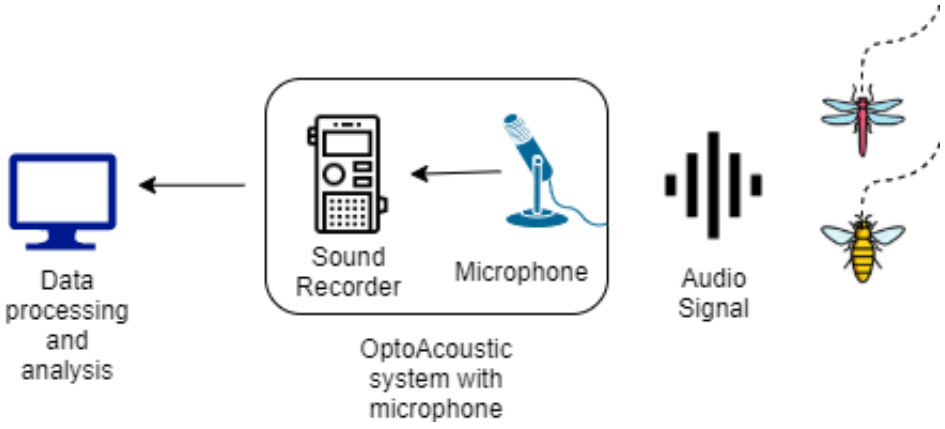


Figure 2.8: *Illustrative working of a Microphone used to record audio data from its surrounding environment.*

Acoustic Technology Integrated with an Optoelectronic Sensor

On the other hand, The optical sensor in most cases emit a laser beam from a transmitter which is received by a photodiode or a phototransistor. As the insect passes through this beam, its wings occlude the light beam and cause small light fluctuations. The light fluctuations are captured by the photodiode as changes in current, and the signal is filtered

and processed by a signal processing algorithm to successfully identify the insects. These approaches can be used to calculate and estimate the fundamental wing beat frequency of various insects. Therefore, Optical and Acoustic sensors work in combination to identify and detect different species of insects.

During digital sound recording, incoming sound waves are transduced into an electrical signal that is recorded at a specific sampling rate (in Hz) and bit-depth (number of bits per sample). These parameters determine a recording's frequency and amplitude resolution, since, most of the insect's wingbeat sounds lie in the higher frequency spectra, higher sampling rates would be required to resolve these frequencies.

Several studies have also integrated Acoustic sensors with opto-electronic sensors to identify insects by their wingbeat frequency [17] [18]. The operation of an opto-electronic sensor is identical to that of an optical sensor, with the exception that an electronic board is employed to filter and process the signal. The output of this electronic board is then fed into a digital sound recorder. In these approaches, opto-electronic sensors have been used instead of microphones to record wing-flaps of insects. An illustrative working of an Optoacoustic technology with an Optoelectronic sensor can be observed in Figure 2.9. The main advantages observed by researchers while implementing Optoelectronic sensors instead of microphones are:

- The opto-electronic devices records an event only when the path from the emitter of some form of light(e.g.. phototransistor, photo-resistor) is interrupted. Whereas, a microphone picks up sound from all directions.
- opto-electronic sensors return a very high SNR, whereas microphones record all sound sources and can become susceptible to external noise.
- Microphones, although can be protected in several weather conditions, are more vulnerable to open field conditions especially in noisy environments.

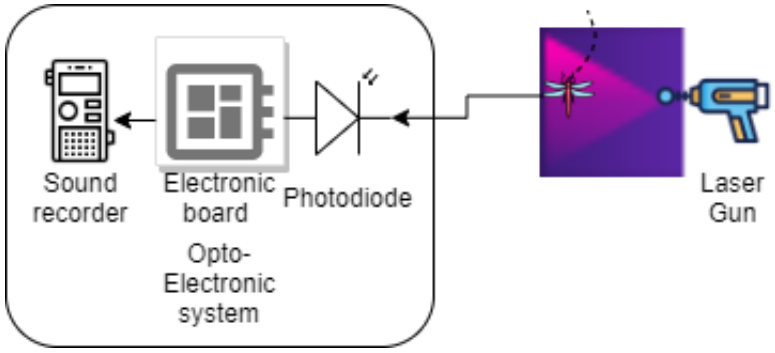


Figure 2.9: *Working of an Optoelectronic sensor to record data from its surrounding environment and convert it into audio data..*

2.2 Literature Review

In the recent years, several technologies have emerged for studying insect migration. These technologies range from traditional military radar systems to state of the art LiDAR, Acoustic and mmWave sensors. However, each technology has its own advantages and disadvantages and have proven to be effective in their own unique ways. This section will briefly discuss the relevant literature performed in existing studies for all the technologies discussed in Section 2.1 and the advantages and limitations associated with each technology will be elaborately explained.

2.2.1 Methodology

The most common keywords and search strings used for searching relevant papers in each field of technology were : ***Entomological Radar Technology***, ***LiDAR Technology***, ***CW Scheimpflug LiDAR***, ***Optoacoustic Technology***, ***FMCW radars***, ***mmWave radars for Insect detection*** and ***High Performance Insect Detection Methodologies***.

2.2.2 Conventional Radars

Conventional radars have been one of the important aspects for the study of broad scale aerial movement of bats, birds and other species related in biological conservation. Depending on the type of radar, distinct information can be gathered on migration and movement of animal species over long distances and has been used in the past to understand the magnitude of airspace used by animals, birds, bats and insects globally. It is interesting to look into bird migration, as birds exhibit a similar behaviour and have similar signal

processing pattern when compared with insects.

Bird Migration

Conventional radars in the past, have been used to measure the migration of birds in highly sensitive areas. It becomes necessary to look into bird migration as birds show similar homologous traits. It is estimated by authors of [19] that around 3 million bird and 20 million insect species pass over a 1km transect annually. Thus, knowledge about bird migration can also provide us with comprehensive information regarding the flight path of various aerial fauna such as insects and give insight into the processing capability of conventional radar systems in extracting information from bird returns.

The first attempt to study bird migration can be traced back to 1967, when Eastwood et al [20], used a short range X-band scanning radar for this specific purpose. Similarly, Ruhe et al [21], utilised a civil air traffic radar to study the spatial and temporal distribution of birds on a national scale. Weather Surveillance Radars (WSRs) have been commonly used in the past to scan large terrestrial landmasses for studying the abundance of birds and further analyse population density, aerial pathways and seasonal movement phenology [22]. Marine radars have also been used to monitor number and flight behaviour of threatened seabird species, such as *Petrels* and *Murrelets* as they travel between breeding and feeding areas [23]. Radars have also been used in systematic studies to monitor migratory flow and density (number of birds flying per unit volume) in order to gain a better understanding of how various bird species migrate over distinct area. This study was performed using fixed or scanning beams and antennas of different shapes, further employing a narrow pencil beam for optimal quantitative recording of data [24]. Swiss Birdradar Solutions BV have also been extensively using BirdScan radar systems to effectively monitor aerial bird and bat fauna. This data allows researchers to quantify the height distribution and temporal pattern of bats and bird with a high spatial and temporal resolution. BirdScan radar systems employ a pulsed X-Band radar. Since the size of multiple bird species fall in the same range of wavelength (2.5cm to 3.75cm) of radiowaves emitted by the radar, X band radars have become popular in various bird migration studies. The transmitter generates hundreds of pulses per second and the antenna combines the pulses into a directed beam. The antenna in this acts as a transceiver to convert the received signal into a digital signal. This data can also be used to calculate MTR and obtain accurate classification of distinct species of bats and birds flying above the radar unit.

Insect Monitoring and Tracking

Conventional VLRs and Weather Radar Systems have been used from 1980s to detect high altitude insect migration and retrieve useful insect parameters such as density, mass, orientation and wingbeat frequency. Furthermore, since insects are unaffected when flying through the radar beam, it provides an exceptional opportunity investigate and process returns from insect targets without harming or altering the flight of insects.

Recent works consider the Ku-band radar. Hu et al [25] analyses RCS characteristics for data measured in the field by using a Ku-band high-resolution insect radar. The Ku-band radar operates in the frequency band of 12-18 GHz and has a corresponding wavelength of 1.6 to 2.5cm. Therefore this wavelength range makes it ideal for the radar to detect insect species less than 2cm in size. In reference [26], researchers proposed a novel method for automatic wing-beat frequency extraction for a Ku-band insect radar system using second order polynomial approximation of the insect's horizontal speed estimation for high resolution and full polarization radar set.

Hobbs et al. [27] developed an Airborne radar system to detect moths at a range of about 1km. The radar system developed was a modified X-band marine radar, employing a peak power of 25kw, pulse length of 100ns and a pulse firing rate of 2560 Hz. The radar beam was focused by a circular parabolic reflector of diameter 0.61m. The radar returns were processed by a signal processor at 48 separate range intervals and this data was further recorded and stored in a tape recorder. This airborne radar was installed in a single-engine aeroplane with its beam focusing towards the ground.

Similarly, Chapman et al. [28] designed a nutating beam, X-band Vertical Looking Radar integrated with autonomous data analysis software for monitoring high altitude insect migration. VLRs are different from conventional scanning radars as they project a narrow conical beam vertically upwards from a stationary reflector. This VLR was deployed at two sites in southern England, one at Rothamsted and the other at Malvern. The VLR emitted a circular symmetric vertical looking beam in which the plane of polarisation was continuously rotated by turning the upward facing wave-guide feed through the vertical axis. The feed was further offset by 0.18°, making the beam oscillate slightly. Furthermore, this produced a conical scanning space emerging from the beam. The radar was capable of detecting around 450000 individual insect species such as *parasitic Hymenoptera*, *tiny Diptera*, and *Aphids* which contained more than 1Mg of biomass within them, by using several range gates which were separated by intervals of 26m. The radar returns were further processed for evaluating insect biomass density, temperature and wind profiles of different insect species.

On the other hand, Poffo et al. [29] developed a Radar system capable of transmitting high power electro-magnetic pulses. The radar system utilised was a C-band polarimetric radar working at a frequency in the range of 3.7 to 4.2 GHz. The radar was capable of emitting both horizontal and vertical polarizations simultaneously. The antenna of the radar emits the pulses to the insects migrating at a certain distance. The backscattered signal was then digitised, amplified and processed in the radar receiver, which was further recorded and displayed to gain detailed information such as the body size and the wingbeat frequency of the subjected target depending on various parameters such as the horizontal and vertical reflectivity of the radar, radial velocity, spectral width, phase difference and correlation coefficient. Dual polarization technology utilised by this radar produces valuable information on the shape and nature of the detected target. The correlation coefficient was considered as an important metric for determining the consistency of target's shapes and sizes within the radar beam. A higher value implied that the size and shapes of radar targets were more consistent, while a lower value suggested that the shapes and sizes of insects showed higher heterogeneity.

Challenges

The major challenges associated with various Bird migration radars are the limitations of the radar, such as their size, cost, high power consumption, low energy efficiency and the complex data processing algorithms required for successfully quantifying radar returns. Since, traditional entomological radars utilised the X-band frequency for monitoring and detecting aerial fauna, incorporating this particular wavelength limited the radar to detect larger species alone. Since the size of most of the insects are small, the RCS will be very small and thus cause difficulty in producing a good SNR in the backscattered signal, leading to a large number of false positives and degradation of accuracy. Furthermore, these radars are labour intensive to operate as they require frequent maintenance, since, they are prone to various environmental constrains such as rain, fog, wind and thunderstorms and hence, are unsuitable for long term monitoring of insects. On the other hand, The limitation with VLRs is that they do not provide coverage below 150m because the parabolic dish consisting of the Transmitter and the receiver module are placed at altitudes above 150m to enhance its beam transmission capabilities and mitigate ground clutter. They also do not provide high range resolutions in differentiating multiple targets [30]. VLRs can also succumb to interference caused by natural terrain features, human-made structures and vegetation. Due to various technical limitations, most entomological radar studies have been pursued for studying the high-altitude behaviour of insects Hence, lower altitudes mainly below 150m have been ignored and entomologists had to rely on swarm

detection or flock of insects rather than focusing on detecting insect species flying closer to the ground [28].

2.2.3 Light Detection and Ranging (LiDAR)

LiDAR, on the other hand, uses light for detecting and ranging in a form of pulsed laser to measure ranges and distances to the earth. LiDAR systems work in a similar manner to radar, but uses light waves instead of radio waves. As discussed in Section 2.1, LiDAR systems often emit laser beams in the nanometer range (808-821 nm) and as a result unlike radar systems, LiDAR systems could be employed to study species migration closer to the ground (less than 150 metres) and investigating the abundance of multiple organisms and the surrounding vegetation on which various species of insects and bats prey on.

Forestry and Vegetation Monitoring

It becomes important to look into the applications of LiDAR systems in forest monitoring and vegetation sensing as insect abundance is positively related to multi layered vegetation in forests. It can be inferred from various studies that higher the density of vegetation in forests, the more number of different species of insects can be observed in that area. This is due to the presence of unevenly aged, mixed species forest areas that promote total insect abundance [31][32]. LiDAR systems have been primarily used in the past for forestry and other applications. Turner et al. [33] developed an Airborne LiDAR system for remote sensing of biodiversity at a certain geographical area. Similarly, Lim et al. [34] reviewed the developed application within a forest area to acquire information regarding canopy and tree height, biomass and volume. LiDAR systems mainly focused on the forest vertical structure , where Lefsky et al. [35], utilised a LiDAR system in CW Scheimpflug arrangement to estimate the forest canopy height with an RMSE(Root mean square error) of 5m in varied forest types including evergreen needle leaf and deciduous broad-leaves in tropical evergreen forests located in Brazil.

Insect Abundance Studies

Zhu et al. [36] utilised a continuous wave LiDAR system operating in Scheimpflug arrangement to monitor insect abundance in a rice field located in southern China. The system operated with two perpendicularly near-infrared lasers, activated intermittently, and the backscattered signal from targets was measured using a linear array detector placed after a linear polarizer. The LiDAR system comprised of Laser beam emitters and a termination box. The laser beam was directed at a height of 3-5m from the ground and was terminated at low reflectance, black neoprene foam sheets, known as the termination box.

The termination box was placed at a distance of 513m from the laser transmitter. The results obtained from the LiDAR system showed that the fundamental wingbeat frequency obtained from 22810 samples of detected insects were in the range of approximately 160 Hz. However, the measurements were performed during rainfall, and the authors found it complicated to filter signals obtained from raindrops from that of insects. The authors, also observed that insect abundance was at the peak, during dusk (Just after sunset) than at dawn, when the activity is reduced after sunrise. This phenomenon is also in accordance with the flight behaviour of nocturnal migrant insects observed with entomological radars. The authors also observed higher insect density during rainfall. However, the authors inferred that rainfall brought many of the high flying insects lower to the ground, which attributes to the higher number of insect count during rainfall.

Kirkeby et al. [15] conducted a study to determine and analyse the spatio-temporal distribution of insects, and classify them based on their wingbeat frequency and body wing proportion using a high resolution LiDAR system. The LiDAR system comprised of an 808nm near-infrared Laser beam, UltraViolet (UV) light trap (320 to 420nm wavelength) for attracting insects and a termination box. The termination box was placed at a distance of 140m from the laser transmitter. The UV light trap was placed halfway from the laser transmitter. The experiment was conducted during the night from the 20th to 21st of July in southern Sweden. The authors observed that a group of small insects (Wingbeat Frequency > 300Hz) were abundant near the light trap from dusk to around 22:00. The abundance slowly started to deteriorate around 23:00. On the other hand, The authors also observed that a group of larger insects (Wingbeat frequency < 300Hz) were abundant near the LiDAR system during the evening and then moved towards the light trap from around 22:00 until 23:30. The authors also observed that the most abundant clusters of insects were small and large *Trichopetra*, *Aphididae* and *Heteroptera*. The authors inferred, that this numerous cluster of insects were abundant in that location because of mating and predator avoidance. The authors also observed great overlaps in body wing proportions and wingbeat frequency and thus, used a species recognition algorithm to accurately classify the insects.

Challenges

LiDAR systems are particularly being used for low altitude insect monitoring. Studies have showed that, LiDAR systems have the potential to accurately detect multiple insect species simultaneously with an sampling volume of order 1 m^3 [15]. Despite this benefit, the preceding analysis show that Airborne LiDAR systems are cost inefficient and are intricate to deploy on open areas. They can also produce elevation errors due to its inability

of penetrating very dense forests. In some cases, where the canopies are dense, LiDAR pulses may not be able to completely penetrate them, thus returning incomplete data to work with. They are also significantly affected by rainfall and low hanging clouds, because of the effects of refraction. Since they use various light traps for attracting insect species, the light emitted from these traps can have its own effect on the insects and thus lead to inaccurate measurements for our application. Several studies have also shown that insects have accumulated near the laser beam emitted by these systems [15][16][36], causing a "memory of attraction" effect on insects, where insects would accumulate around the laser beam even after the laser was switched off, for a short period of time [16]. Thus, using LiDAR systems will make our system more complex, expensive and more prone to the surrounding environment. As a result, these shortcomings make it unsuitable for our use, as our application requires a monitoring and detecting device that is independent of light and the surrounding environment.

2.2.4 Optoacoustic Technology

Sound has proven to be an effective medium for detecting and classifying insects in the recent era. Several studies have shown that microphones or optical sensors integrated with sound recorders have successfully achieved accuracies in the higher range($>$90%) [17] [18][37]in detecting and classifying insect species in indoor and outdoor environments.

Insect Detection and Classification

Raman et al. [37] developed an Acoustic insect flight detector, constructed from a noise cancelling microphone, integrated to an sound recorder capable of recording for 10 hours. The focus of this work, was mainly on mosquito detection as mosquitoes are the most common species of flying insects and contribute to a large number of diseases worldwide. This system comprised of a noise cancelling microphone connected to a preamplifier and a high pass filter designed by the authors [37]. The output of the high pass filter was then fed into a sound recorder and the data from the sound recorder was stored in MP3 and WAV audio format files for up-to 10 hours. The system was deployed from May to August 2004, for 250 hours over the course of 30 days in a high noise urban and suburban environment. Multiple approaches were performed to detect insect flight tones. These approaches, involved sensing the first and second harmonic frequencies of mosquitoes, but the authors observed this lead to large number of false positives because of other ambient sounds involving those from birds, human voices, frogs and automobiles. The authors observed that a total of 726 insect buzzes were detected by the algorithm, in which 6.5% were false positives. However, when the authors combined first four harmonics obtained from mosquitoes, the total number of insect buzzes detected increased to 784, an increase

by 8% from the previous approach. But simultaneously, increased the number of false positives upto 28% from the previous approach.

Chen et.al [17] conducted an comprehensive study on classifying insects using inexpensive sensors. Firstly, the authors conducted an extensive research on why there has been lack of progress in and none of the previous research using acoustic sensors has had a lasting impact on the current entomological research. This can be attributed to factors such as high sensitivity of microphones to ambient noise in the environment, Building classification models with very limited data, and over reliance on one single feature, the wingbeat frequency of insects. Secondly, the authors design a novel system to record sound of insect flight in short distances. This system is setup inside a chamber in a lab based environment. The sensor used by the authors consists of a phototransistor array connected to an electronic board, and a laser pointing at the phototransistor array. When an insect flies across the laser beam, its wings occlude the light, causing small light fluctuations. The light fluctuations are then captured by this array as changes in current and voltage, and the signal is then processed by the electronic board. The output of electronic board is then fed into a sound recorder as audio data in MP3 format. Bayes classifier was then used by the authors to classify insects. The authors achieved an accuracy of 98.99% in classifying a certain species of house fly, and an accuracy of 98.27% in classifying a specific species of Mosquito.

Challenges

Acoustic or Optical sensors coupled with microphones have proven to be effective in detecting and classifying insects by extracting their wingbeat sound or frequency inside a lab based environment [17][18], where insects are trapped inside a chamber, and their flight is restricted. Although, these tests have achieved accuracy up to 99% in classifying certain common species of insects such as *Houseflies* and *Mosquitoes*, they have not been effective in open field tests, as microphones are sensitive to ambient and wind sound. Hence, it becomes intricate to filter these external sounds from those which are generated by insects as highly advanced signal processing algorithms are required which further complicates the functionality and efficiency of the overall system [37]. Similarly, Optoelectronic sensors could also pick up noise and static signals during deployment in outdoor environments and would ultimately result in a large number of false positives and affect the efficiency of the whole system.

2.2.5 mmWave Radar

mmWave frequencies, combined with traditional radar systems have achieved exceptional results. The main idea behind using mmWave frequencies is that, radar cross section is inversely proportional to the fourth power of radar wavelength and therefore, reducing the wavelength offers the advantage of increasing the effective size of smaller insects, birds and bats, making them viable radar targets.

Bird Monitoring and Detection

Klein et al. [38] developed a 94 GHz mmWave radar for dedicated bird detection at airports and airfields during final approach and departure of flights. The radar classifies the bird flock significantly by their bio mass which is in turn proportional to the RCS and further identifies the range, azimuth angle and elevation position of the birds. The maximum range of detection achieved by the radar was observed to be 4.8 kilometres.

Rahman et al. [39] developed radar system operating in the W-band frequency of 94 GHz to obtain distinct micro Doppler signatures to differentiate drones and birds. The authors observed that the phase coherence method of radar system can retrieve highly reliable signatures of flying targets compared to the amplitude coherence method.

Insect Detection and Migration Studies

In 1992, Riley [40] developed a 8.8mm radar system capable of detecting individual small insects weighing less than 2mg upto a distance of 1km from the radar. The radar developed was a conventional, thyratron-driven pulse radar. The operating frequency was in the ka-band range of 26.5 to 40 GHz. The author used a horn antenna rather than dipole antenna which was more commonly used during those times to mitigate the losses occurring during signal transmission. The first field trials conducted by the author were to calculate the maximum range for detection of planthoppers. A maximum range of 1.3km was observed by the authors. Furthermore, the authors were able to observe 1000 to 1200 targets of different species of insects on the radar's scanning space.

On the other hand, Tahir et al. [41] developed a mmWave harmonic sensor for tracking small insects. The use of mmWave frequencies in harmonic tags significantly decreases the weight and size of the corresponding tags, compared to previously used X-band harmonic tags. These low cost harmonic sensors can be attached on the back of insects and can be tracked using a harmonic radar. The frequencies of reception and transmission for

the harmonic tags were designed to be at 38.5 and 77 GHz respectively. The authors observed that, the harmonic tag could be detectable by the radar upto a distance of 200m. The author's also inferred that, the fixation of these harmonic radars to Unmanned Aerial vehicles (UAVs) could increase the range for upto 1km in excess to the previous range achieved. However, the authors of [42] have acknowledged that harmonic radars use big transponders which may affect the insect behaviour to a certain extent and affect their flight or movement.

Similarly, Yang et. al [43], developed a millimeter wave vertical looking entomological radar system operating at 34.5 GHz continuously detecting targets flying at a maximum distance of 200m above the ground. The radar emits a vertical looking and a circular symmetric beam by mechanically rotating the waveguide with 6 times per second. The vertical-looking beam is offset by 0.18°around the vertical axis to get a wider coverage. The VLR system works 24 hours a day on a 15-minute period with 5-minute data capturing and 10-minute data processing capabilities. The radar returns were processed by a signal processor implemented on an Altera FPGA board with ADS249 ADC. The data after conversion enters into a FIFO buffer, where it is then processed by Fast Fourier Transform (FFT) algorithm. The radar returns could then be extracted to gain the target's size, shape, position and speed with respect to its orientation to the radar beam.

Wang et al. [44] proved that wingbeat information could be extracted from radar returns, because both the components of the signal, its amplitude and phase can be modulated by wing-beating. The authors implemented a W-band and S-band coherent radar to measure the wingbeat frequency. W-band radar was operated at a wavelength of 3.2mm whereas the S-band radar was operated at a wavelength of 90mm. The coherent radars utilised were a type of VLRs which would transmit a radio-wave vertically upwards and insect echo could be acquired when insect flew within the radar beam. The W-band radar utilised a Frequency Modulated Continuous Wave (FMCW) wave for the transmitted signal waveform with a sweep time of 0.5ms. The signal bandwidth available was 1.2 GHz, which provided a range resolution of 0.125m. The S-band radar adopted a stepped-frequency pulse train (SFPT), generating a bandwidth of 320 MHz and providing a range resolution of 0.47m. Micro-Doppler analysis with FFT was used for signal processing and removing noise from the received signals. The authors observed that the wingbeat induced amplitude information from the W-band radar is more intense than that of the S-band radar. The authors also observed that not only amplitude modulation, but also phase modulation could be used to measure the wingbeat frequency. The authors concluded that the W-band radar showed better performance on both the measurement precision and the measurable minimum size of the insect.

Advantages

mmWave radar systems provide large sampling volume compared to traditional detection methodologies. Furthermore, mmWave radar systems are also insensitive to external environment unlike Acoustic and LiDAR systems, as they are not effected by rain or absence of light. They also do not affect flight, visibility, and movement of insects and don't have a direct influence on their behaviour. Several studies have achieved accurate monitoring of insects using mmWave radar systems [43][40]. FMCW and Doppler based mmWave radars are compact, flexible and can easily be deployed for this specific purpose. The deramping frequency of FMCW based mmWave radars allows it to have a higher range resolution and a better scanning range [45]. FMCW radar system's continuously transmit and receive signals and thus, can provide full lossless coverage of signals. In addition to this, they are also cost effective and have a reduced form factor in which the Digital Signal Processor (DSP), Micro Controller Unit (MCU) and the Transceiver antenna module are etched into a single unit. This radar technology demands more research attention in entomological research, due to its promising results in the automation industry [46] and its capability to detect different targets precisely, in adverse weather conditions. Therefore, mmWave sensors could prove to be a reliable solution for detecting insects with minimal cost and higher efficacy.

2.3 Discussion and Analysis

The study of existing literature enabled us to gain knowledge on the previous work accomplished in various insect detection solutions. Most of the existing solutions in detecting insects were inferred to be focused on incorporating a large form factor for hardware design and involved advanced signal processing algorithms to process insect returns. This has resulted in complex systems with high costs and labour intensive maintenance to felicitate requirements such as high performance and reliability. Thus, it is necessary to implement a system that is capable of detecting airborne insects flying close to the ground and can be readily deployable in different environments and adverse weather conditions. In this research, a system that is capable of detecting insects and effectively processing its returns will be implemented by adapting certain methodologies and strategies from existing work.

The selection of the most suitable sensor technology for detecting insects is one of the important decision that needs to be taken. Fundamental performance metrics such as its precision and false positive rate will have a direct influence on the results achieved by the system. The best suited technology for our system is selected by comparing each

technology based on specific parameters that are identified to be the crucial requirements for this research.

2.3.1 Requirements of the System

The requirements of this current research can be formulated to be following parameters :

- **Range**: The maximum distance at which a specific system recognises the target is known as range. Although, a high range is preferred but for our research,a short range system will also be suitable as the main focus of the sensor is to detect close range airborne insects affected by ALAN. This research will investigate the maximum detection range that can be achieved for detecting insect targets.

- **Range resolution**: Range resolution is defined as the ability of a system to distinguish between two or more targets present on the same distance but at different angles. Range resolution depends on the bandwidth of the transmitted pulse, higher the bandwidth higher will be the range resolution. This research requires a system with high range resolution such that multiple small insects flying close to each other can be easily differentiated.

- **Precision**: Precision is defined as the ability of the system to detect insects efficiently in adverse environments. This research requires a system that could achieve a high precision in reliably detecting insects.

- **External sensitivity**: External sensitivity is defined as the impact of external environmental factors on the overall performance of the system. This research requires a system with minimal external influence that provides reliable performance across adverse environmental conditions. This requirement is essential because, the system will be set up during unfavourable weather conditions such as fog, rain,and wind in a terrestrial environment with large trees and plants that promote difficult conditions.

- **Cost**: Cost is defined as the budget required to purchase the hardware components required to construct the experimental setup. The cost required for the system will mainly depend on the range obtained by the system in detecting insect targets. a low range implies that the cost would be high as multiple sensor nodes will be required. However, for this research large amounts of money can be spent if required and hence, the cost of the system would not be a significant factor in determining the acceptability of the system.

2.3.2 Literature Study Analysis

It can be inferred from the literature review that there has been very little research on applying mmWave radar technology in airborne insect detection applications without using harmonic tags. As a result, this research will look at the functioning of mmWave radar technology and examine its effectiveness in detecting insects, and subsequently evaluate its performance.

Table 2.1 provides an overview of the distinct parameters of each technology. This table has been constructed depending on the requirements of the system to be implemented. It can be observed that even though LiDAR has similar advantages compared to mmWave sensors, it has higher external sensitivity to the outside environment and hence can lead to imperfect measurements in our application. mmWave sensors have shown robustness and promising results in performing effectively in adverse environmental conditions and hence, can be a possible solution for our application. mmWave sensors available currently are cost-effective and provide high reliability in efficient detection of small objects as they utilise millimeter wavelengths and wide bandwidths. As a result, wide bandwidths also provide high range resolution to successfully detect multiple targets simultaneously.

Requirement	**Conventional Radar**	**LiDAR**	**OptoAcoustics**	**mmWave Radar**
Range	Moderate	High	Low	Moderate
Range Resolution	Moderate	Moderate	Low	High
Precision	Moderate	High	Moderate	High
External Sensitivity	Low	High	High	Low
Cost	High	High	Moderate	Low

Table 2.1: *Comparison of various Technologies Based on Requirements of the System.*

Table 2.2 realises a decision matrix table for the given technologies to choose the virtuous technology from the available alternatives. The weightage for the parameters varies from 1 to 5, 1 being the poorest and 5 being the most suitable solution. Reliability and performance have been considered as the significant parameters for this application and therefore have been given a weightage of 5. Complexity has been given a weightage of 4 as it depends on the design and the Software Development Kit (SDK) of the sensor, taken care of by the manufacturing company. Since mmWave radar technologies have shown better performance and reliability in outdoor environments, they have been given a high score compared to the other alternative technologies. The complexity of the technologies depends on a number of factors such as its hardware feasibility and physical constraints.

Based on these factors and literature review studied, mmWave radars have shown promising results in reducing the complexity of the overall system by decreasing the physical size of the antenna compared to conventional radar technology where antenna sizes are large and furthermore, integrating DSP and MCU functionality in a single board and employing low complex signal processing algorithms to filter clutters from received returns. Conventional radar technologies would require multiple subsystems to employ various signal processing algorithms and eventually would increase the complexity of the system. As a result, mmWave radar technology has been provided with a higher rating. The reliability of the system often depends on the recall, precision and redundancy achieved from the data obtained from the overall system. mmWave radars have shown significant improvements in detecting targets with approximately $>80\%$ precision. mmWave radars substantially consist of multiple transmitters and receivers to provide low redundancy and enhance the reliability of the system.

Criteria	**Weight**	**Conventional Radar**	**LiDAR**	**OptoAcoustics**	**mmWave Radar**
Reliability	5	4	4	3	4
Performance	5	3	4	3	4
Complexity	4	2	2	3	3
Total		43	48	42	52

Table 2.2: *Decision Matrix Representing the Weights and Total Score for Each Decision Criteria.*

The weightage and scoring for each decision criteria for Table 2.2 is based on the literature review studied and analysed in this thesis. It can be inferred from Tables 2.1 and 2.2 that mmWave radar outweighs all the other alternative solutions in the most significant parameters required for choosing our sensor node.

2.3.3 Summary

One of the oldest technologies for detecting insect population is conventional radar technology. While traditional radar technology in the X and S band of frequencies have proven to be efficient in tracking and detecting birds, bats, and certain large insects, their large wavelengths restrict the radar's ability to detect small insects as they have a relatively small RCS. These radar systems have a large form factor and are very difficult to operate with limited labour and maintenance. Conventional radar systems also have only been successful in detecting insects flying at a high altitude of 150m, and therefore insects flying at low altitudes are missed. As a result, these radar systems are ineffective for continuous

and long term detection and monitoring of small insects.

On the other hand, even though LiDAR systems have produced acceptable results in detecting and tracking low-altitude flying insects, they are highly cost inefficient and are affected by external environmental factors such as rainfall and cloudy weather. LiDAR systems use laser beams for detecting and mapping targets in region of interest. This property of LiDAR systems makes it unsuitable for our research as it ultimately leads to a measurement bias and hinders our primary goal of detecting insects without the influence of light from the sensor.

Acoustic sensors basically use sound to detect insects. Although, Optoacoustic technology have shown favourable results in detecting and identifying different species of insects inside a lab based environment, with minimal external interference, they have not shown accurate results in detecting insects in an open field. Since, sound is a highly sensitive feature, emitted by all the living creature on the planet, Microphones and Optoelectronic sensors associated with Acoustic sensors can easily pick up these sound signals from an open field and overlap with those generated by insects. As a result, complex metrics and algorithms would be required to filter the signals produced by insects, which would be strenuous, given the scarcity of reference data for various insect species. To account for within-class variability and background sound, large training datasets are required to efficiently detect insects with high precision and reliability. As a result, optoacoustic technology is not a viable option for our research as it is highly sensitive to the external environment.

mmWave radar technology employ smaller wavelengths, that make it easier to detect smaller targets such as insects. The utilization of radio waves for detection results in having minimal to no effect on insect targets and achieving low sensitivity from external environmental factors. Since mmWave sensors employ wider bandwidths, they provide higher range resolutions compared to traditional radar systems. As discussed in Section 2.3.1 this property of the radar system helps in distinguishing multiple targets close to each other and thereby, enhancing the detection performance of the radar. mmWave sensors also have a smaller form factor compared to traditional radar systems and thus, are easier to deploy and operate in difficult environments. Several studies [43] [44] [40] have showed that mmWave sensors can also generate accurate returns from its targets. Therefore, it could be regarded as the most favourable solution for continuous and long term monitoring and detection of insect species. This study demonstrates a correlation between radar returns obtained from traditional radar systems. However, these returns are very complex to be evaluated and thus, requires further enhancement, which would be one of the main

focus of this research.

Chapter 3

mmWave Radar Theory

In this chapter a short introduction will be given on the physical principles behind the working of the mmWave radar technology utilized during the course of the research. First, the functioning principle of a FMCW radar will be discussed, then a short introduction will be provided on important characteristics and algorithms employed inside the mmWave radar system.

3.1 FMCW radar

mmWave radar technologies in most cases incorporate a continuous wave technology known as FMCW. The underlying concept behind this technology is the transmission of electromagnetic signals that objects or targets reflect in its path. In an FMCW radar signal, the frequency increases linearly with time. This type of signal is known as a chirp. It can be observed in Figure 3.1 that as time increases, the frequency of the system also linearly increases with respect to time. The basis of FMCW modulation is that the reflected signal from a target is combined with the transmitted signal producing an Intermediate Frequency (IF) tone. The combined IF can be given by the formula:

$$IF_{freq} = sin[(\omega_1 - \omega_2)t + (\phi_1 - \phi_2)] \tag{3.1}$$

Where ω_1 and ω_2 denote frequency and ϕ_1 and ϕ_2 depict the phase difference of the TX and RX signal respectively.

A chirp signal is a fundamental part of a FMCW system as it can be used to calculate the range or distance at which a target is present. This relation can be given by the phase difference obtained from the IF signal. The delay present in the RX chirp is directly proportional to the distance of the target. A chirp signal can also be used to differentiate

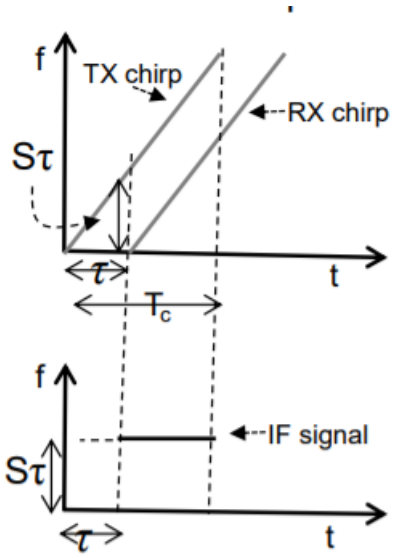


Figure 3.1: *illustrative graph to show the estimation of the IF signal from the TX-RX chirp [47].*

between multiple targets based on its phase difference and the delay obtained from the IF signal. The FMCW radar system transmits a chirp signal continuously and captures the signals reflected by objects in its line of sight. It can be observed in Figure 3.1, that the delay τ generated by the RX chirp can be given by the formula

$$\tau = 2d/c \tag{3.2}$$

Where d is the distance of the detected object and c is the speed of light. The initial phase of the signal (ϕ_o) is defined as the difference between the phase of the TX chirp and the RX chirp at a time corresponding to the start of the IF signal, which can be given by the formula:

$$\phi_o = 2\pi f_c \tau \tag{3.3}$$

Where f_c is the operational frequency of the radar.

In addition, for an object at distance d from the radar, the IF signal generated will be a sine wave given by the equation:

$$IF_d = Asin(2\pi f_o t + \phi_o) \tag{3.4}$$

Where A is the amplitude of the signal.

It now becomes important to look into how each parameter such as the range, range resolution, velocity and velocity resolution are estimated and calculated by an FMCW radar system.

3.2 Range Measurement

Range is an important parameter for a radar system as discussed in Section 2.3.1. Range basically defines the maximum distance at which the radar is able to detect a certain target. The maximum range of a radar system can be limited either by the SNR of the received signal or the maximum IF bandwidth supported by the radar system.

The beat frequency is defined as the frequency difference between the transmitted and the received chirp. The beat frequency is directly proportional to the distance of the system. A larger beat frequency corresponds to a larger distance of the target. The beat frequency (f_b) yielded by the RX chirp in the intermediate frequency band can be given by the formula

$$f_b = \frac{S2d}{c} \tag{3.5}$$

Therefore from equation 3.5 we can derive that the maximum range R_{max} of a radar system, depending on its maximum IF bandwidth can be given by

$$R_{max} = \frac{IF_{max}c}{2S} \tag{3.6}$$

where c is the speed of light and S is the slope of the transmitted chirp. Slope is the rate at which the frequency of a chirp transmitted increases linearly with respect to time. Slope is typically measured in MHz/µS. The slope of the system can be given by the formula

$$S = \frac{f_b}{\frac{2d}{c}} \tag{3.7}$$

However, as discussed earlier, the maximum detectable range can also be limited by the SNR of the received signal. This mainly depends on Radio Frequency (RF) physical parameters of the radar device such as its TX output power, receiver noise figure, system loss, RCS, chirp duration and the number of chirps transmitted in a frame. Antenna parameters such as gain of the TX and RX and the number of receivers and transmitters will also play a significant role in determining the maximum range obtained by the radar system. All of these fundamental factors can be formulated into a equation which can be given by:

$$R_{max,SNR} = \sqrt[4]{\frac{P_{Tx}G_{Tx}G_{Rx}(\lambda)^2\sigma T_c N_c N_{TxRx}}{(4\pi)^3 K T_e \eta L SNR}} \tag{3.8}$$

Where P_{Tx} is the TX output power, G_{TX} and G_{Rx} are the transmitter and receiver antenna gain respectively, σ is the RCS of the detected target, T_c is the chirp time for each chirp, N_c is the number of chirps in a particular frame period, N_{TxRx} is the number of transmitters

and receivers respectively, η is the receiver noise figure, k is the Boltzmann Constant and T_e is the ambient temperature assumed for the radar system.

However, the maximum IF bandwidth of a system is also limited by the ADC sampling rate in the system.

$$IF_{BW} = 0.9 * ADC_{sampling} \tag{3.9}$$

This limitation of Bandwidth will in succession reduce the range obtained by the radar system.

Therefore, it becomes necessary to program and assume these parameters in an efficient way to obtain a maximum detectable range for small targets such as insects. The assumptions considered for obtaining a maximum range in the mmWave radar system will be explained briefly in Chapter 4.

3.2.1 Range Resolution

Range resolution as previously explained in 2.3.1 an important requirement of the current system, and is defined as the ability of the radar to distinguish multiple targets present at the same distance. When two or more targets move closer to each other, at a certain point the radar system would be incapable of distinguishing them as separate targets. The closest point at which they can be readily distinguished is the range resolution of the system. However, Fourier Transform states that the resolution obtained can be enhanced by increasing the length of the IF signal.

To increase the length of the IF signal, the bandwidth of the system must also be increased proportionally. This resultant IF signal results in an **!** (**!**)IF spectrum with two separate peaks. The two IF signal tones can be resolved in frequency as long as the frequency difference satisfies the relationship given by

$$\Delta f > \frac{1}{T_c} = \frac{S2\Delta d}{c} \tag{3.10}$$

In equation 3.10, the separation distance Δd can be represented by

$$\Delta d > \frac{c}{2B} \tag{3.11}$$

Where c is the speed of light, T_c is the chirp time, S is the slope, and B is the bandwidth of the radar system.

Therefore, the range resolution (d_{res}) of the radar system depends on only the bandwidth swept by the chirp signal which can be given by

$$d_{res} = \frac{c}{2B} \tag{3.12}$$

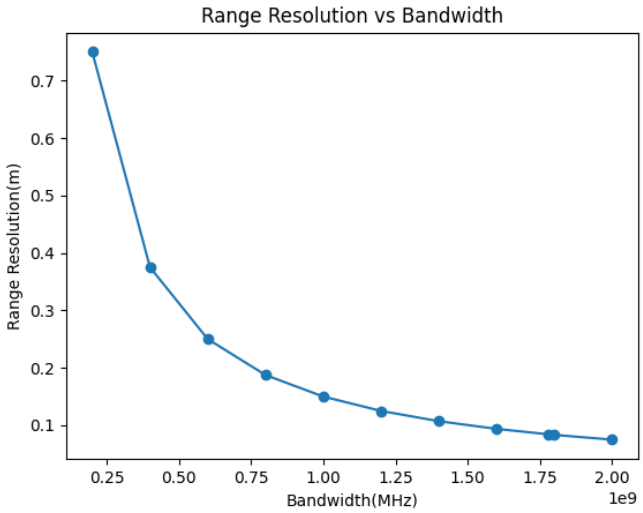


Figure 3.2: *Range Resolution as a function of Bandwidth*

Where B = ST_c.

Figure 3.2 shows how the range resolution decreases as the bandwidth of the system increases. Lower range resolutions enhance the system's efficiency in detecting multiple targets close to each other.

3.3 Velocity Measurement

Velocity is defined as the speed at which a target is approaching or receding from a radar system. This can also be defined as the component of the target's motion that is along the direction of the radar beam.

In order to measure velocity, an FMCW radar transmits two chirps simultaneously separated by time interval T_c. Each reflected chirp is processed by a Range FFT algorithm to calculate the range of the object. The range corresponding to each reflected chirp will have peaks in the same location, but with a different phase. Thus, this phase difference could be measured to estimate the velocity of a target.

Thus, the maximum relative velocity (V_{max}) measured by two chirps spaced T_c apart can be estimated by:

$$V_{max} = \frac{\lambda}{4T_c} \tag{3.13}$$

Where λ is the wavelength of the FMCW radar. Since, maximum velocity estimation is

inversely proportional to the interval between chirps, accurate velocity estimations would require shorter transmission times between chirps.

However, the limitation with this method is that it would not work if multiple targets are moving at the same distance from the radar. Since, they are at the same distance, they will generate reflective chirps with identical IF frequencies. Therefore, as a consequence, the range FFT would result in a single peak which represents the combined signal from all of the equidistant targets.

Therefore in order to mitigate this problem, the radar system should transmit more than two chirps. As a result, the radar system transmits a set of N equally spaced chirps. This set of chirps is known as a chirp frame. As a result, the range FFT processes the set of N reflected chirps each with a different phase incorporated with the phase distribution from both the targets. Therefore, a second FFT, known as Doppler FFT is performed on the N chirps to resolve the two targets. Thus the velocity estimations of both the targets v_1 and v_2 having $\omega 1$ and $\omega 2$ as their respective phase difference can be given by the equations 3.14 and 3.15

$$v_1 = \frac{\lambda \omega_1}{4\pi T_c} \tag{3.14}$$

$$v_2 = \frac{\lambda \omega_2}{4\pi T_c} \tag{3.15}$$

3.3.1 Velocity resolution

Velocity resolution is defined as the minimum velocity difference required between two targets detected at the same distance to be resolved as two different targets. Therefore, for a FMCW radar system, the velocity resolution can be given by

$$V_{res} = \frac{\lambda}{2T_f} \tag{3.16}$$

where T_f is the frame period can be calculated by

$$T_f = NT_c \tag{3.17}$$

where N is the number of chirps transmitted and Tc is the time interval between the chirps.

The velocity resolution of the radar is inversely proportional to the frame period (T_f) and thus, lower frame periods can result in a higher velocity resolution for the FMCW radar system.

3.4 Angle of Arrival Measurement

Angle of Arrival (AoA) is defined as the direction from which the the signal reflected from a target will arrive into the antenna array of the radar system. The direction of the signal beam is determined by Time Difference of Arrival (TDOA) between the individual components of the antenna array of the radar. The TDOA measurement is calculated by measuring the difference in received phase at each element in the antenna array.

In order to locate the object in 2D space, it becomes important to know the angle of the object along with the distance. The signal observed at each receiver that are spaced apart with a distance d are delayed by (τ) which can be given by the formula :

$$\tau = d * \sin(\theta). \tag{3.18}$$

This delay causes a phase shift (ϕ_{shift}) which can be given by the formula:

$$\phi_{shift} = \frac{2\pi d \sin(\theta)}{\lambda}. \tag{3.19}$$

Furthermore, this phase shift can be used to estimate the angle of the target. The measurable angular field of view (θ_{FoV}) from the radar system for the maximum spacing between the receiver pair can be estimated by:

$$\theta_{FoV} = \arcsin \frac{\lambda}{2d} \tag{3.20}$$

The maximum spacing between the receiver antenna can be given as $\frac{\lambda}{2}$ and therefore, it can be theorized that the maximum field of view achievable by the radar is $\pm 90°$.

3.4.1 Angular Resolution

Angular resolution is the minimum angle at which the radar would be capable of resolving two targets close to each other. The angular resolution of the radar system mainly depends on the number of the receiver antennas available. The higher the number of antennas available, higher will be the resolution achieved by the radar. The angular resolution θ_{res} is given by the equation 3.21.

$$\theta_{res}(radians) = \frac{\lambda}{dN_{RX}\cos\theta} \tag{3.21}$$

Where d is the spacing between the receiver antenna pairs, N_{RX} is the number of receiver pairs available and λ is the wavelength of the radar system. The maximum angle resolution for our system at minimum azimuth angle(θ) = 10°, N_{RX} = 12 and d = $\frac{\lambda}{2}$ will be approximately around 12°.

3.5 Object Detection with CFAR Algorithm

CFAR is a detection algorithm used in various radar systems. This algorithm uses an adaptive algorithm to detect viable target returns against background noise, clutter and interference.

The role of the CFAR detection algorithm is to determine a power threshold above which above which a radar return can be considered to originate from a expected target, which in our case are airborne insects against other dynamic targets in the scene. If the threshold is set too low, then more real targets will be detected, resulting in an increased number of false positives. On the other hand, if the threshold is set too high, then fewer targets will be detected resulting in a higher number of false negatives, which eventually affects the end functionality of the system. Therefore, this trade-off needs to be considered in an optimal manner to enhance the performance of the system.

There are multiple CFAR detection approaches used in radar systems such as the Cell Averaging Constant False Alarm Rate (CA-CFAR) algorithm, Cell Averaging Smallest of Constant False Alarm Rate (CASO-CFAR) detection algorithm, square law detection and the ordered-statistic CFAR. However, our research will only focus on the principle of the CASO-CFAR detection algorithm. The main benefit of adopting this algorithm is that previous studies [48] [49] performed in evaluating different CFAR algorithms concluded that CASO-CFAR detection algorithm has a higher capability in distinguishing targets with weak signal to noise ratio from immediate noise sources and multipath reflections. Since Insects are generally assumed to be targets with weak signatures, CASO-CFAR algorithm can be reliable in detecting them more effectively than other CFAR detection algorithms in noisy environments. However, other reasons for the implementation of this algorithm will be further discussed in Section 7.1.

3.5.1 CASO-CFAR Algorithm

CASO-CFAR algorithm is used to filter out the required target measurements from other noise and interference signals in the environment. In this algorithm, the average noise level for the cells to the left and the right of the Cell Under Test (CUT) is calculated separately and the smallest of these averages is then compared with the scaling threshold to decide if the detected point is a valid target. The CUT is a range cell for which the power level needs to be determined to consider it as an viable target. Each range bin around the CUT is termed as an range cell. This method can improve the detection performance of the radar system when there is clutter present to the immediately adjacent areas of the CUT. The 1D CASO-CFAR algorithm is applied across the range and angle domains for target detection. The noise power is estimated as the average power of the reference cells within

a configured window around each CUT. This algorithm makes an assumption that the reference cells on which the average noise power is computed do not contain any signals from targets. The guard cells prevent power levels from signals leaking into the reference cells from the target peaks. The detection algorithm performs a scan on range and angle bins to achieve multi level validation to confirm a valid target. The CFAR algorithm first conducts a scan across on range azimuth heatmap and checks the condition across all the range bins. For each detected point, a second CFAR pass check is conducted across the angle bins to confirm the first pass detections.

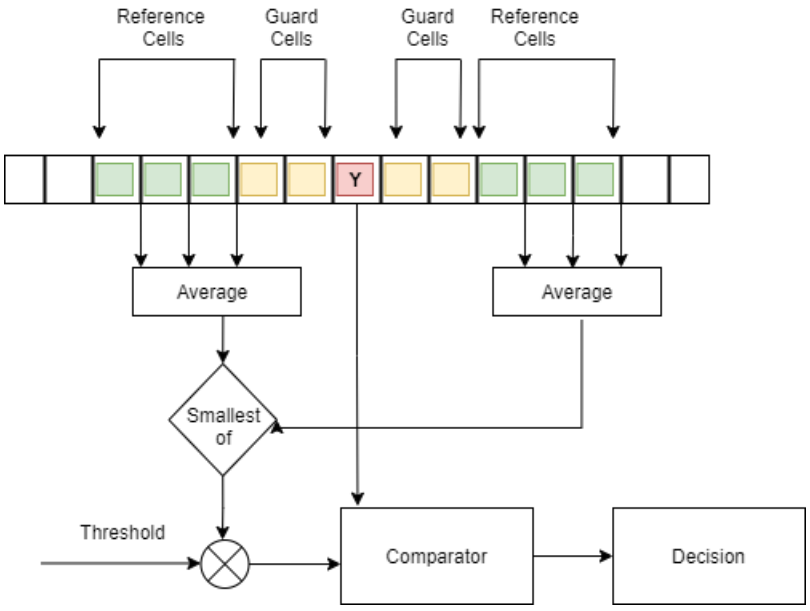


Figure 3.3: *Illustrative working of a CASO-CFAR Algorithm to determine if a detection performed by the radar system is from an actual target source.*

Figure 3.3 shows the working of a CASO-CFAR algorithm, where the green boxes are represented as reference cells and the yellow boxes are represented as guard cells. A comparator is then used to compare the average power level of the cell under test and the threshold is multiplied by the smallest of average noise level from the reference cells. If the average power level of the CUT is greater than the average noise level, then it is regarded as an viable target. The final detection threshold is calculated by estimating the noise level from both the reference cells and combining it with the scaling threshold.

3.6 Clustering with Gtrack Algorithm

Clustering is the process of grouping a set of objects that are similar to each other and pass certain user defined thresholds. Cluster analysis is a common application in exploratory data science fields such as pattern recognition, computer vision algorithms, information retrieval and statistical data analysis. Clustering is typically performed on the detection layer data to group similar set of data. This is essentially done to reduce the number of point cloud data from the detection layer to limit the memory requirements of the radar's internal processor and prevent depletion of the memory resources. Clustering also aids in reducing a large number of ghost detections that occur.

Point cloud data is a set of measurement vectors obtained after the CFAR detection is performed in the radar system. Each measurement in the point cloud data contains the target's positional coordinates, AoA, Doppler velocity and SNR. These similar set of measurement points are grouped by the clustering algorithm. The clustering algorithm defines a specific boundary inside which the measurement points would fall into. Those points that fall outside the boundary are tagged and ignored for further processing. The boundaries in our case define an area or a region of interest where the radar is focused and the probability of insect detection is higher.

The mmWave radar system's SDK employs the Group Tracking (Gtrack) algorithm for clustering. This algorithm was designed and developed by Texas instruments and was included in the mmWave radar's SDK by default to enable ease of processing. In this algorithm, first a random measurement point is chosen as an initial point with which the other measurement points inside the boundary are compared to for initialization of a cluster set. Each leading measurement point is then checked if it passes a certain number of thresholds. These thresholds include comparing the measurement point with a minimum velocity, SNR and distance between a consecutive point cloud measured. If the point cloud data exceeds these thresholds, then the measurement points are added to a cluster.

3.7 Board Specific Parameters

The transmitted signal from the radar system depends on the configuration of the profile, frame and chirp parameters. These constant assumptions for these parameters and the underlying importance of each parameter will be studied in this section.

3.7.1 Profile

A profile is a template for a particular chirp and consists of various parameters that are associated with the transmission and the reception of the chirp. This includes multiple important transmission parameters such as chirp time, number of chirps, center frequency and reception parameters such as range resolution and bandwidth. These parameters intermittently affect the maximum range and velocity that is obtained by the radar system in processing target returns. Table 3.1 gives an overview on the profile parameters for the system.

Parameter	Value
Start Frequency (GHz)	60.75
Center Frequency (GHz)	63.01
Idle Time (µS)	30
Number of ADC Samples	96
Frequency Slope (MHz/µS)	54.71
ADC Sampling Frequency (ksps)	2950
ADC Start Time (µS)	25

Table 3.1: *Profile Parameters for the System*

The start frequency parameter configures the valid bandwidth occupied by the FMCW beat signal to be utilised in the detection layer. Thus, a lower start frequency will enable the system to have a higher bandwidth. The number of ADC samples affects the chirp time and the IF bandwidth as observed in Equation **??**. Increasing the number of ADC samples will result in a wider bandwidth and improve the range resolution. The frequency slope of the system determines the rate at which the frequency increases linearly in the chirp. Therefore, higher the frequency slope, higher will be the rate at which the slope will cover the chirp bandwidth and result in an improved range resolution. However, since insects are highly non linear in their movement and fly at higher velocities, the capability of radar system in detecting insects is still under question and therefore, this limitation will be overcome by varying the scaling threshold of CASO-CFAR detection algorithm the processing block of the radar system.

3.7.2 Frame

Frame can be constructed by defining a sequence of chirps using the previously defined configurations in Tables 3.1 and 3.2. In our system, the frame is constructed using 96

chirps with an inter chirp time of 267µS. This frame can be used as an observation window for radar processing and generating the chirp signal. The frame in our system is run in continuous mode as to continuously keep transmitting a chirp in the specific frame rate. The frame rate is defined by the idle time given in Table 3.1 with 30µS. Thus, chirps with lower idle time will have lower chirp periodicity. This lower chirp periodicity will evidently result in higher maximum relative velocity estimation in accordance with Equation 3.13 for our system. The frame periodicity configures the frame rate of the processing chain. The frame periodicity is defined at 55ms. This lower frame periodicity rate will enable the radar system to detect more number of targets and reduce miss detections.

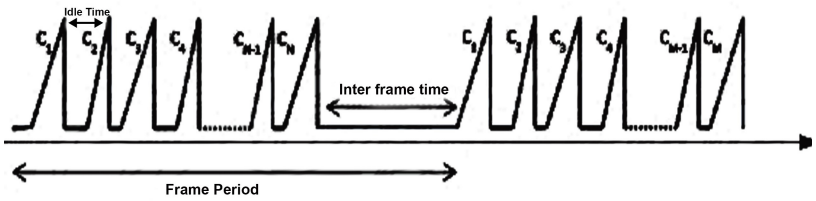


Figure 3.4: *Typical Frame Structure of the mmWave radar system in defining a chirp sequence to tranmsit.*

A frame structure for N number of continuous chirps can be observed in Figure 3.4. C denotes each chirp in a frame and frame period denotes the number of chirps in a frame. Inter frame time denotes the time interval between the consequent frame.

3.7.3 Chirp

A chirp type is associated with a profile and acquires all the properties of the profile parameter. In addition, it also includes the necessary information on the TX antennas on which the chirp should be transmitted. Since our system consists of three transmitters, three consecutive chirps can be transmitted simultaneously by the radar system employing a Multiple Input Multiple Output (MIMO) configuration. In the MIMO mode, the receiving elements must be able to separate the signals corresponding to each transmitter antenna. Therefore, the orthogonality is achieved by employing a time-division multiplexing technique. Hence, Utilizing the MIMO mode improves the angular resolution of the radar system. As shown in Table 3.2 a chirp profile with 96 chirps having a chirp time of 32.5µS with all the three TX antennas enabled were used. The concept of TX Beamforming is to simultaneously transmit the chirp through multiple TX channels and achieve higher gain and longer range in the FoV. However as the FoV is increased, the range of detection is decreased. This is because, the wider the beam becomes, more its power

will be spread across the beamwidth, and therefore, resultant beam will have a reduced range of detection. As denoted in Equation 3.3.1 the velocity resolution of the system depends on the chirp time and the number of chirps used in the configuration. The maximum velocity and velocity resolution is inversely proportional to the chirp interval and the number of chirps, and therefore for having a higher velocity estimate and a reduced velocity resolution, it is recommended to have higher number of chirps and chirp interval in our system. Therefore, a trade-off between the maximum velocity and the chirp time needs to be considered.

Parameter	Value
Chirp Bandwidth (MHz)	1780
Chirp Time T_c (μS)	32.5
Inter-Chirp Time T_r (μS)	267
Number of Chirps	96
Center Frequency (MHz/μS)	63.01
Beat Frequency (MHz)	2.66
Velocity Resolution (m/s)	0.0928

Table 3.2: *Chirp Parameters for the System*

The maximum velocity will now have a relation with the start frequency (f_c) of the system. Thus, from Equation 3.13, we can derive that the maximum velocity will be equal to

$$V_{max} = \frac{c}{4 f_c T_r} \tag{3.22}$$

Where T_r is the chirp interval between two consecutive chirps of the system.

Similarly, the velocity resolution can be given by

$$V_{Res} = \frac{c}{2 N_c f_c T_r} \tag{3.23}$$

Where N_c is the number of chirps defined in the system.

Figure 3.5 shows the variation of Maximum velocity and Velocity resolution with respect to varying chirp intervals. As chirp interval increases, the maximum velocity of the system decreases. On the other hand, the velocity resolution does not vary much. This is due to the dependence of velocity resolution of the number of chirps as well which is assumed to be a constant value.

Figure 3.6 depicts an overview on how the distinct parameters of profile and chirp configurations are fundamental in transmitting an effective chirp for detection of targets in the region of interest.

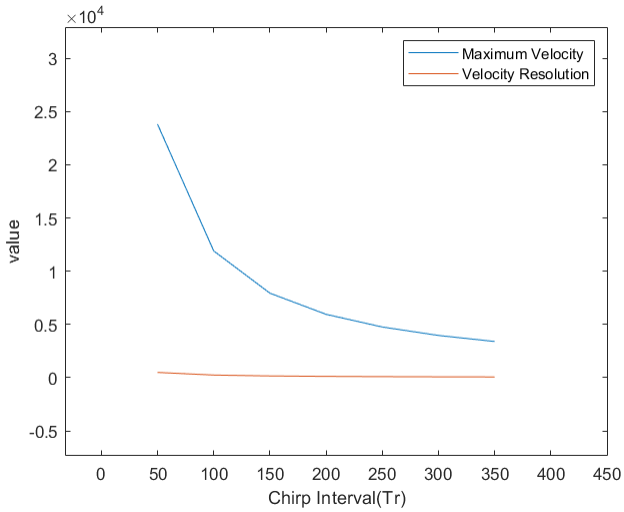


Figure 3.5: *Velocity and velocity resolution as a function of chirp interval.*

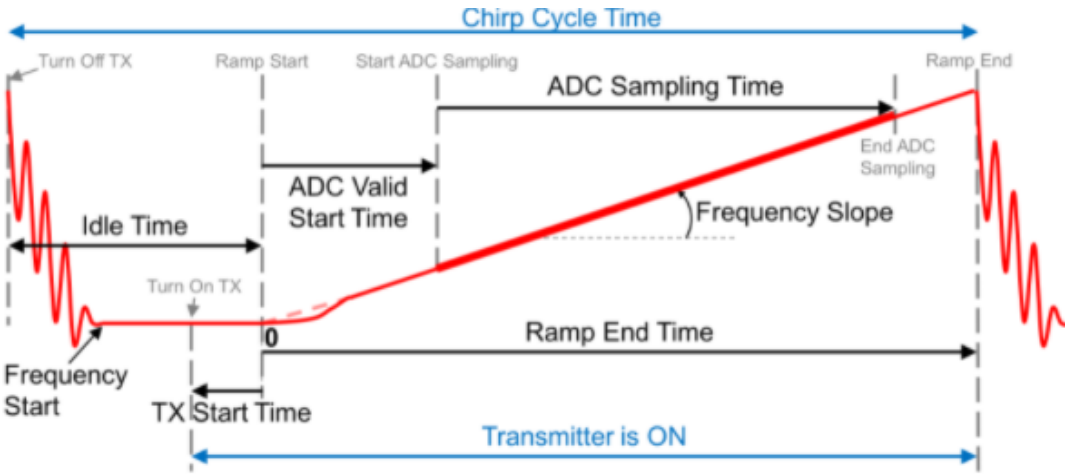


Figure 3.6: *Figure depicts an overview of the transmitted chirp and the important parameters associated with it to define the sensing capability of the system [50]*

Chapter 4

System Methodology

This chapter describes the mmWave sensor employed and the methodology adopted for detecting airborne insects and processing their returns in an effective manner to enhance the performance of the system.

4.1 Introduction

The overview of the overall system can be observed in Figure 4.1. The information extraction module retrieves information from dynamic targets in the region of interest. The information extraction module is namely the mmWave radar module and consists of the front end and the back end processing modules. The front end module consists of transmitting and receiving antennas to transmit the chirps in specific configurations to the region of interest and receive the scattered signals from targets respectively. This raw data is then sampled and sent to the back end processing module where further processing of the signal takes place to retrieve the required important information from target returns. A computer was used to configure the transmitted chirp depending on the interested targets and simultaneously visualize the processed data from the back end processing module. The configuration and design of the radar test bed for our current application involves two important tasks namely, configuring the front end of the radar system to transmit the required chirp and process the radar returns from the reflected target in the back end and determine if a return is from an insect target.

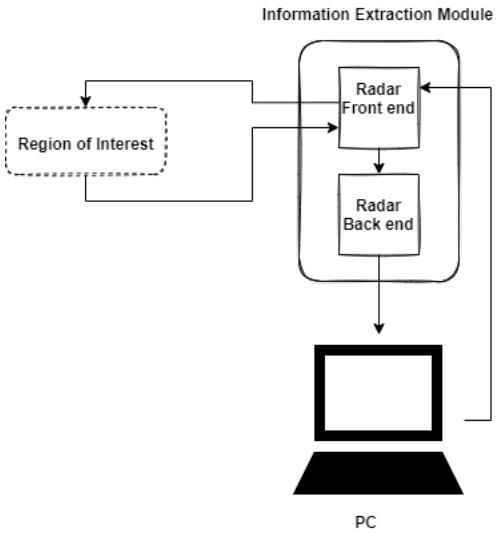


Figure 4.1: *High Level Overview of the mmWave Radar Module in extracting the surrounding information from its RoI.*

4.2 Information Extraction Module

4.2.1 IWR6843AoP Module

mmWave sensors from Texas Instruments, have been primarily used in the past for various applications such as for gesture recognition, heart rate monitoring, logistics and automotive applications and have produced exceptional results. However, this technology has not been extended to be applied in the field of entomological research. Therefore, applying this technology in insect detection is a novel approach. The IWR6843 Antenna on Package-Evaluation Module (IWR6843AoP-EVM) has been chosen as the mmWave TI radar module because of its wider field of view and its enhanced capability of detecting smaller targets owing to its shorter wavelength. This radar sensor utilises the MIMO technology with a FMCW transceiver consisting of four integrated receivers and three transmitters, all being patch antennas employing a 120°field of view. This radar sensor operates in the frequency range of 60 to 64 GHz and subsequently has a bandwidth of 4 GHz to determine the range, speed and angle of the objects within its FoV. The wavelength λ of this radar system can be given by the formula:

$$\lambda = \frac{c}{f} \tag{4.1}$$

Therefore, it can be observed from Equation 4.1 that the wavelength of the system

ranges from 5mm when the frequency is 60 GHz to 4.68mm when the frequency is 64 GHz. The mmWave sensor simplifies the implementation of the system by integrating various subsystems such as RF radios, MCU and a C674x DSP. Thus, by integrating these subsystems, this system mitigates the problem of discretely implementing them and as a result reduces the power and the cost complexity of the system. mmWaveICBOOST is an additional module, which is integrated with the IWR6843AoP-EVM sensor to provide user connectivity for initial radar configuration and debugging of the data captured by the sensor in real time. The name IWR highlights that this sensor belongs to industrial range of sensors and the additional interfaces present in the automobile range of sensors are not required for this particular application requirement. This device enables unmatched levels of integration in an extremely small form factor and is an ideal solution for low power, highly precise radar systems in the current industry.

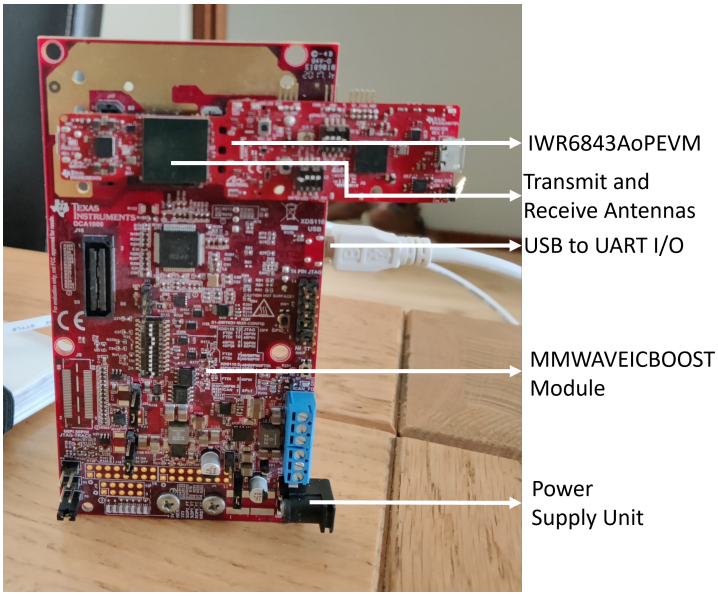


Figure 4.2: *IWR6843AoP mmWave Radar Module*

4.3 Radar Front End

The radar front end is an important layer of the mmWave radar module which defines the sensing capabilities of the system. The radar front end as observed in figure 4.3 transmits the required chirp based on the profile and the frame configurations observed in Table 3.1

and 3.4 respectively. The TX chirp is designed to achieve maximum range resolution within the available range with minimal power and computational complexity.

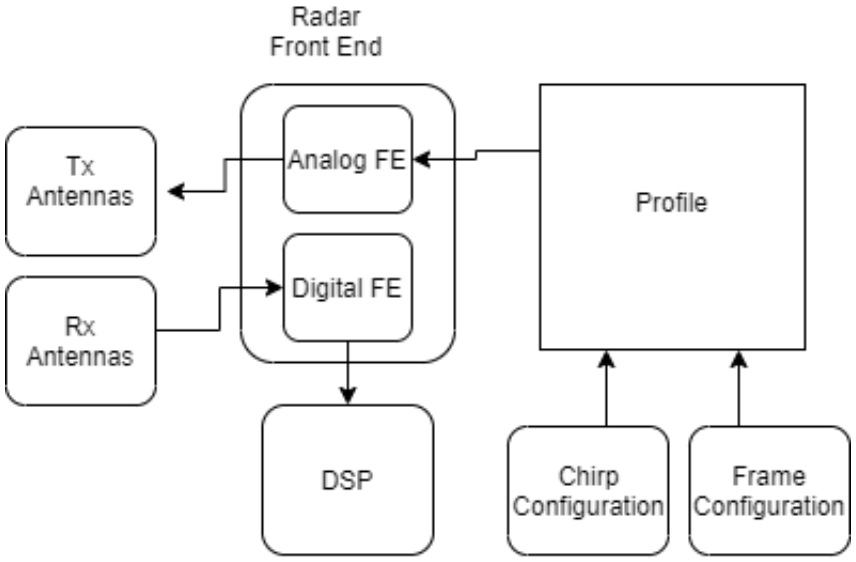


Figure 4.3: *Radar Front End Overview*

However, before we look into the chirp configuration and parameters it becomes important to first estimate the maximum theoretical detection range that could be obtained for a typical target having an RCS similar to that of an insect. As discussed in Section 3.2 the maximum detectable range is limited by the SNR obtained from a target in the region of interest and hence, needs to be considered for estimating the maximum range of our system.

4.3.1 Maximum Range Estimation

Figure 4.4 shows the variation of range as a function of SNR for different Radar cross section values. This figure was plotted by using the Equation in 3.8 which gives the variation of SNR for varying range. The calibration parameters could be observed in Table 4.1. It becomes necessary to know that RCS is not always related to the physical size of the objects. Since RCS depends on the target cross section of insects, it would be irrational to have a constant RCS to accommodate all the insects as they vary substantially in size and as a result, their cross section would also differ considerably. It can be inferred from [51] that for a Centimetre Wave (Cm) wave radar operating at 8-12 GHz, the RCS values measured for an insect or a bug was found to be 0.00001m^2. Additionally, it also needs to be

comprehended that RCS is also a function of the frequency. As the frequency of the wave increases, the wavelength becomes shorter and the target area incident to the transmitted wave becomes larger. Therefore, with increasing frequencies, the RCS value reflected from a small target such as an insect will also increase. Therefore, for this particular research, the RCS values assumed can be observed in Table 4.1. It can be observed from Figure 4.4 that in the worst case scenario when RCS is 1e-6m^2, the maximum detectable range where the SNR remains above the 0dB threshold is approximately around 2m.

This detection range seems to be suitable for short range insect detection as the radar will be mounted near ALAN to detect insects being attracted to its immediate surroundings and a network of sensor nodes may be deployed to further increase the range of detection.

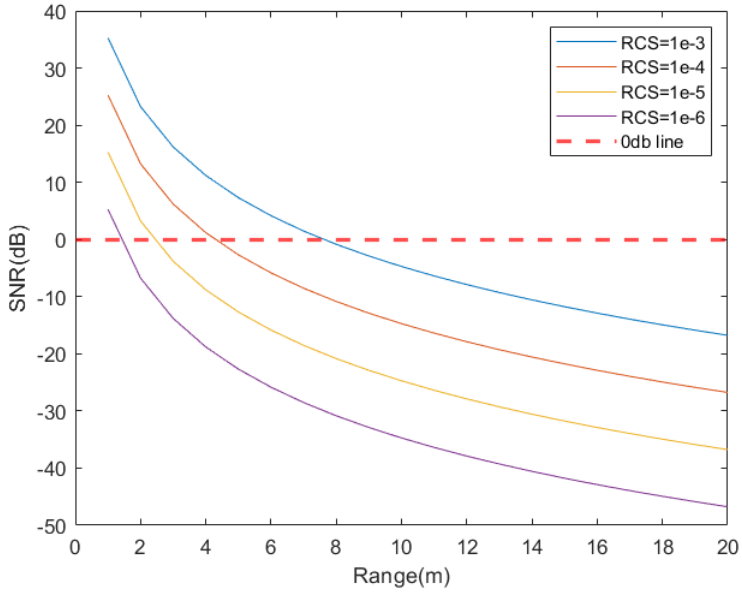


Figure 4.4: *Graph to depict the variation of SNR as a function of Range for Different RCS values.*

Parameter	Value	Parameter	Value
P_t	-10 dBm	K	1.38e-23
G_{Tx}	1 dB	T	290 K
G_{Rx}	16 dB	Bandwidth (B_r)	1780 MHz
λ	0.00476 m	Noise Figure (η)	16 dB
N_{TxRx}	12	System Loss (L)	5 dB
Number of Chirps (N_c)	96	Chirp Time (T_c)	32.5 uS
RCS (m^2)	1e-3 to 1e-6		

Table 4.1: *Table shows the calibration parameters for estimating the maximum range obtained by the system.*

4.3.2 Maximum Range Resolution

Equation 3.12 deciphers that the range resolution of the system is limited by the bandwidth occupied by the chirp. Range resolution is defined as the minimum separation distance required by the radar to resolve multiple targets flying at the same range. From Table 3.2 we can observe that the chirp bandwidth is defined to be 1780MHz. The chirp bandwidth is calculated by the Equation 3.2.1 and therefore, depends on the Slope (S) and Chirp Time (T_C) of the chirp signal. From this, we can infer that the range resolution is inversely proportional to the chirp time and the slope of the transmitted chirp. The range resolution for our system can be calculated to be 8.4cm. This range resolution seems to be sufficient for our research as it is assumed that insects would not be flying closer than 8cm in range to each other and would eventually fly away from each other in the consequent time frame. Figure 4.5 shows the configure range resolution in the theoretically calculated range resolution plot discussed in 3.2. Since previous studies for detecting insects [52] [53] have achieved higher range resolutions in the order of 20cm to 1m, the resolution obtained in our system shows significant improvement from previous studies. However, the chirp bandwidth could be increased to further improve the range resolution. On the contrary, this will increase the memory requirements of the system and thus, affect the performance of the system. .

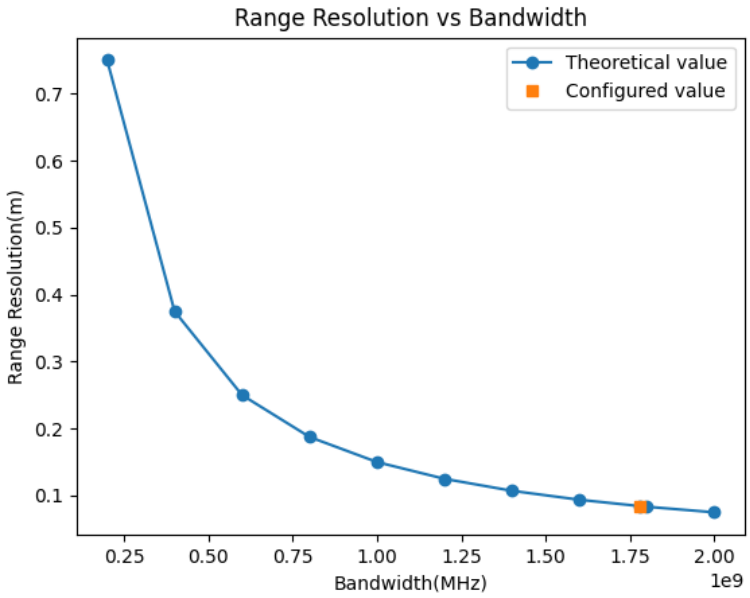


Figure 4.5: *Configured Range Resolution*

4.3.3 Maximum Velocity and Velocity Resolution

The chirp parameters defined for our system can be observed in Table 3.2. The target velocity according to Equation 3.7.3 is estimated from the chirp interval using the Chinese remainder theorem [53]. The velocity resolution obtained by this configuration can be calculated to be 0.36Km/hr which is equal to 9.28cm/s. Thus, this infers that two targets travelling at a velocity difference of 9.28cm/s from each other can be detected by the radar system. The maximum unambiguous velocity calculated in our system is equal to 4.45m/s. This is assumed to be an ideal estimate for our system as it complements the average maximum velocity observed for insects observed to be in the range of 2 to 5m/s [54]. As a result, this chirp configuration will enable the system to detect insect targets travelling at a maximum speed of 4.45m/s with respect to the mmWave radar module.

Figure 4.6 is derived from Figure 3.5. This graph provides an insight on how this configuration will enable us to detect moving targets present in the region of interest.

Table 4.2 gives an overview on the theoretical parameters estimated for the selected chirp configuration for this research. Thus, this study of estimating the maximum value for each parameter addresses our research question **What is the maximum theoretical detection range and the range resolution achieved by the mmWave radar in detecting small targets?**

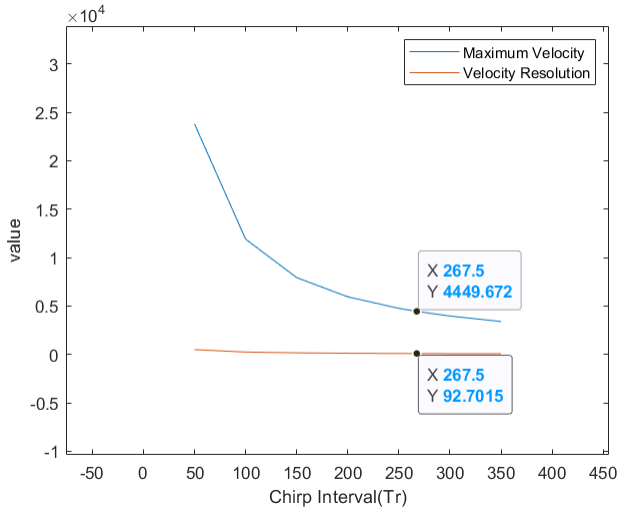


Figure 4.6: *Figure depicts the configured velocity and velocity resolution.*

Parameter	Value
Maximum Detection Range (m)	2.0
Range Resolution (m)	0.084
Maximum Velocity (m/s)	4.45
Velocity Resolution (m/s)	0.0928

Table 4.2: *Table shows the theoretical estimations from the front end layer*

4.4 Insect Detection and Processing

The back end processing chain of the radar system incorporates all the data processing requirements of the mmWave radar operation to provide a well defined interface for application integration. The process of detecting insects and other targets mainly involves taking ADC samples obtained from various targets post analog filtering from the front end as input and transferring useful information regarding the position of targets to the host computer through the Universal Asynchronous Receiver Transmitter (UART) Interface.

The block diagram of the insect detection processing chain can be observed in Figure 4.7. This chain describes how each reflection of the TX frame is processed in order to obtain useful information regarding an insect target from the external environment.

The input from the front end channels are obtained in the Range- FFT block and 1-D-FFT is performed for each antenna to estimate the range for each reflected target. Capon Beamforming algorithm is then used to generate a range/azimuth angle heatmap from

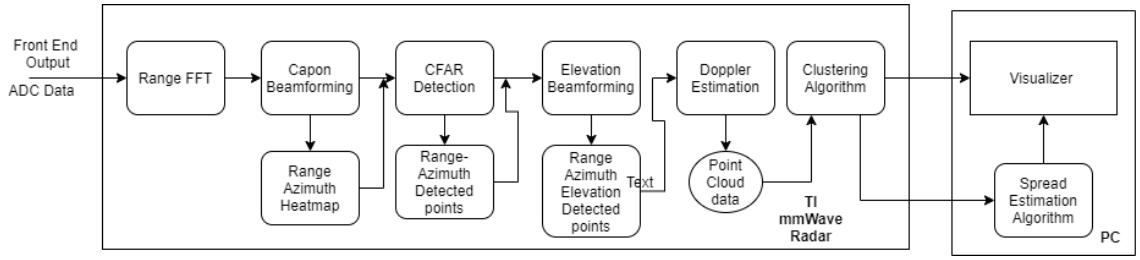


Figure 4.7: *Back End Processing Chain of the Radar System to detect targets in the mmWave radar's FoV.*

the Range- FFT data. The Range/Azimuth heatmap is then fed into a two pass CFAR detection algorithm in the range and the angle domain to estimate the strongest points from the heatmap and compare it with a scaling threshold to determine a valid detected point. The detected points are then fed into another Capon Beamforming algorithm to generate an Elevation angle heatmap, where 1-D elevation spectrum is utilised to detect the strongest peak in the elevation heatmap and estimate the elevation angle of the target. A Doppler- FFT algorithm is then applied on the strongest detected points of the Range/Azimuth/Elevation data by finding the maximum peak in the power spectrum. This Doppler estimation generates a point cloud data with Range/Azimuth/Elevation and Doppler Velocity. Thereby, this processing chain generates the required point cloud of an insect target embedding its position, range, velocity, AoA and SNR into the data frame. This point cloud data is further fed into the clustering algorithm to group the received point cloud data into a specific cluster group and tag the clusters respectively.

The flowchart in Figure 4.8 depicts how a certain point cloud cluster obtained from the clustering algorithm can be determined to be originating from an insect target in the region of interest. It can be depicted that the main parameters that affect the process are the CFAR detection and the Clustering algorithm.

Furthermore, a spread estimation algorithm defined in Section 4.4.3 has been designed to estimate an approximate size of an insect cluster by calculating the distance between the maximum and minimum coordinates in the point cloud cluster. This algorithm is however not accurate and can only provide us with a basic estimation of the distance between the 2-D coordinates in a point cloud cluster. The limitations and possible improvements of this algorithm will be further discussed in Section 7.3. The output from the back end processing chain is then fed into a host controller where it can be further visualized through the Universal Serial Bus (USB) to UART terminal in the host PC. A Python GUI designed by Texas Instruments has been employed to visualise and store the data obtained from the mmWave radar in real time.

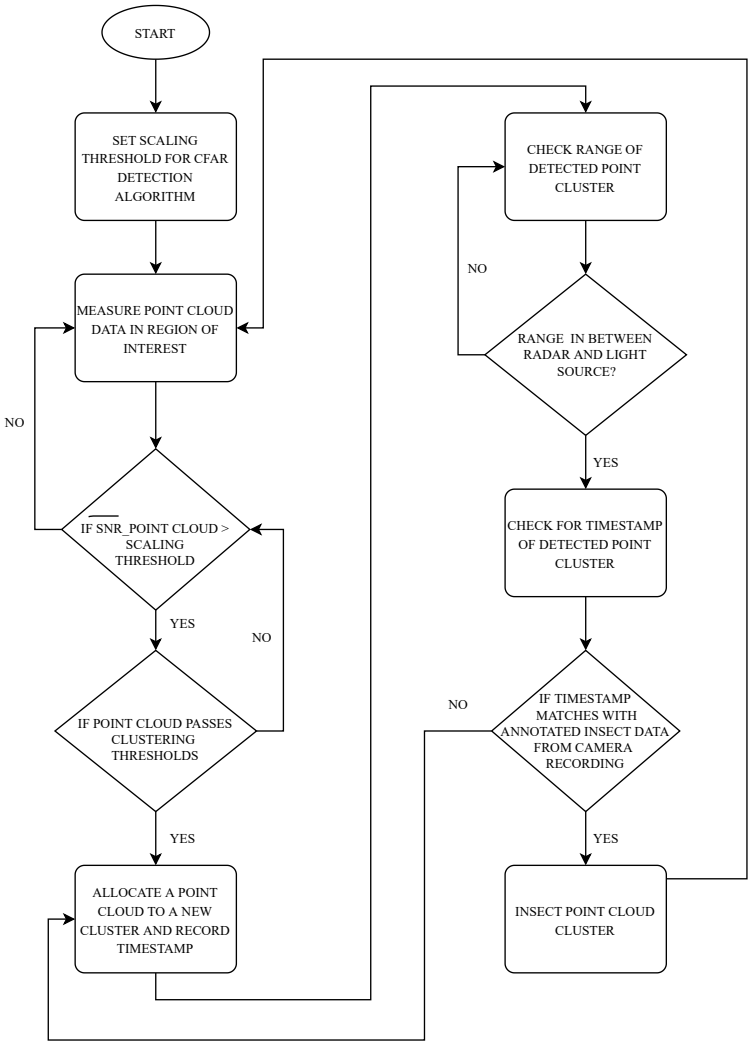


Figure 4.8: *Flowchart to show the process involved in determining if a detection performed from the mmWave radar is from an insect target*

4.4.1 CFAR Algorithm

The working of a CASO-CFAR algorithm can be followed up in section 3.5.1 and a diagrammatic representation can be visualised in Figure 3.3.

The CASO-CFAR uses the smallest noise floor of the point with higher and lower indexes than the detected point. This is done in order to minimise the over filtration of bins with the desired target in the initial stage, as it may result in reduced detectability of

targets and affect the performance of the system.

The Scaling Threshold is one of the key parameters that affects the detectability performance of the radar system. Therefore, this parameter needs to be carefully assigned. In our application, it is necessary to maintain a low threshold for the scaling factor as insects are relatively small in size and enabling a higher threshold might eliminate radar returns from insect targets, treating them as false alarms and noise. This scaling threshold parameter is varied in our research as it is important to determine an optimal threshold for detecting insect returns to enable a higher detection ratio and generate a relatively small number of missed detections. In addition, it is also important to understand that, the scaling threshold parameter also depends on the surrounding environment as relatively low thresholds enhances the capability of the radar system to detect environmental clutter at a higher rate. Thus, this parameter needs to be assigned in such a way that the radar system does not assume insect returns as environmental clutter and discards them. The scaling threshold parameter was varied from 5dB to 25dB for multiple test scenario's and the performance of each scaling threshold on accepting returns from insect targets were evaluated.

The reference and guard window sizes significantly affect detection performance and should be carefully tuned according to the range parameters configured above. A higher chirp bandwidth results in a sharper peak in the range FFT output, and therefore, the guard window size can be reduced to improve the noise estimation accuracy. The configuration parameters for the CASO-CFAR algorithm can be observed in the Table 4.3. A value of 4 in guard window size implies that the four cells immediately adjacent to the CUT will not be considered into estimating the average noise level of the range bins. Since insect species vary in sizes, we do not want larger insects in those areas to be counted as noise samples. Thus, this way there will be a richer point cloud from the multiple range cells and this further allows us to estimate the range and angle of target returns with finer coarse grain.

Parameter	Range Bin	Angle Bin
Reference Window Size	8	12
Guard window Size	4	8

Table 4.3: *Table depicts the CFAR configuration parameters employed for our work.*

The Peak in range, angle and Doppler direction are grouped together and are represented by the highest peak, after the CFAR detection algorithm to reduce reporting of redundant cluster neighbouring points. This further reduces the number of points detected per frame and enables clustering and tagging of point clouds with unambiguous peaks. The static clutter from the environment could also be eliminated from the environment to reduce further computational load for the radar system. The static clutter removal function

is performed by the Capon Beamforming algorithm in the back end processing of the radar system.

4.4.2 Gtrack Algorithm

As discussed in 3.6, the Gtrack algorithm is used to estimate the clusters from the processed point cloud data in the back end processing of the radar system. In our research, we will mainly focus on the steps described below. Various parameters pertaining to the Clustering algorithm have been modified to meet the application requirements for our research. The output of the clustering algorithm is a single point, incorporating the multiple similar points depending on the allocation threshold reflected from a certain target in the region of interest. The fundamental importance of the clustering algorithm in our research is to tag unique clusters denoted by the single point generated from the grouped point cloud data. This tagging from the clustering algorithm generates a unique ID for each insect cluster which makes the analysis of data simpler.

Scenery Parameters

The scenery parameters are the boundary parameters that define the space in which the point cloud data obtained will be processed, clustered and tagged correspondingly. The Scenery parameters can be divided into the left wall, right wall, front wall, ground and the ceiling. The scenery or the boundary for the clustering area can be represented as a rectangular prism or a cuboid. The dimensions of the cuboid when the radar is placed at the origin of its X-face can be depicted in Table 4.4a. In our research, the boundary parameters have been assigned depending on the dimensions of the test environments, where most of the tests were conducted and have been varied accordingly to the changing external test environments. A typical boundary layer as visualized in the Python GUI can depicted in Figure 4.9.

Allocation Parameters

The Allocation parameters define the fundamental characteristics of the clustering algorithm. The allocation parameters are used to cluster the point cloud data into new clusters by following a certain set of defined rules and thresholds. Maximum Distance Threshold and Maximum Velocity Threshold determine whether a detected point cloud can be added to the cluster. The minimum SNR Threshold, Points Threshold and maximum Velocity Threshold determine whether a point cloud detected needs to be allocated to a new cluster or an existing cluster set. These parameters can be shown in Table 4.4b. These parameters have been assigned based on interested targets such as insects. Since insects will reflect

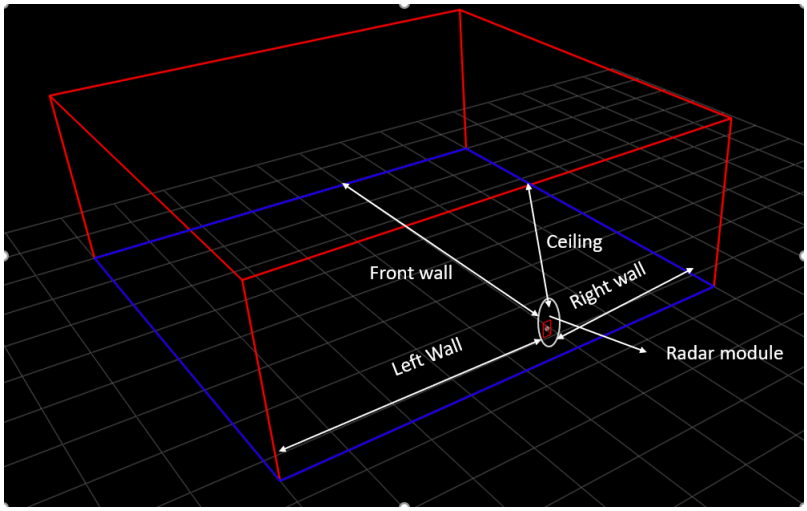


Figure 4.9: *Hypothetical Boundary layer as depicted by the clustering algorithm. This boundary layer takes the shape of a cuboid outside which the mmWave radar module would not be able to measure point cloud data.*

and produce a relatively a low SNR, a low threshold of 3dB is assumed for the cluster set. This defines that a set of point clouds will be associated into a cluster only if the cumulative SNR of the point clouds is greater than the set threshold (which is 3dB in our case). This also depends on the scaling threshold parameter defined in the detection layer. As long as the SNR threshold of the cluster set is higher than the scaling threshold parameter (5dB), new clusters would be formed effectively. Similarly, other parameters have also been assigned in such a way that the system effectively forms clusters for small dynamic targets in the RoI.

Gating Parameters

The gating parameters define define the maximum volume and velocity of a tracked cluster. The most important parameters in this are the gain, length limit, width limit, height limit and velocity limit. Gain determines the amount of clustered points that can grow to create the gating function. Each dimension (X-Y-Z) and velocity can be multiplied by the gain to generate a gating function for the cluster, which is the space where new points can be associated with a pre-existing cluster. The length and width limits determine the physical size of the object and thus limit the size of the cluster formed. The velocity limit limits the velocity of the tracked cluster to the velocity of the interested target in the RoI. These parameters can be observed in Table 4.4c. These parameters have been assigned keeping

in mind, the approximate dimensions of an insect target. The dimensions are assumed to be 1mm in length, width and height respectively. The velocity determines the speed at which the cluster will be tracked and has been assigned a value of 3m/s keeping in mind the average velocity of a swarm of insects [54].

Parameter	Value
Left Wall (m)	-4.0
Right Wall (m)	4.0
Front Wall (m)	2.0
Ground (m)	0.25
Ceiling (m)	3

(a) *Scenery Parameters*

Parameter	Value
Min SNR Threshold (dB)	3.0
Min Radial Velocity Threshold (m/s)	0.25
Min Points Threshold	2
Max Distance Threshold (m)	0.07
Max Velocity Threshold (m/s)	5

(b) *Allocation Parameters*

Parameter	Value
Gain (m)	2.0
Length Limit (m)	0.001
Width Limit (m)	0.001
Height Limit (m)	0.001
Velocity limit (m/s)	3

(c) *Gating Parameters*

Table 4.4: *Clustering Parameters employed for our work to cluster radar returns from insect targets.*

4.4.3 Spread Estimation Algorithm

The spread estimation algorithm gives the distance between the maximum and the minimum locations of all the associated points in a cluster. In the X-Y domain, this information may estimate the target size depending on its coordinates in general but does not accurately match the physical dimensions of the target itself. For an instance, when an insect target is moving at high speeds and its thorax is perpendicular to the antenna beam, then only few points will be associated with the target and the point cloud spread could give an incorrect measure of the estimated spread compared to the actual size of the target. One other reason that may attribute to this fact is that since, insect targets are relatively small in size, in some cases they might only reflect one point from their body cross-section to the radar system. In such cases, the spread of the cluster cannot be estimated and it depends on more than one point to be reflected from an insect target to determine the spread between the maximum and the minimum point. However, there are some cases in which the X

and Y coordinates would lie in the negative quadrant. In such cases, an absolute value of the spread is calculated in order to convert the negative values into positive values and improve the working of the algorithm.

Algorithm 1 Spread Estimation Algorithm

Get $PointCloudCluster$
Initialize $SpreadParameter = 0$
Check for $NumPoints$ in $PointCloudCluster$
if $NumPoints$ > 1 & $NumPoints$ <= 10 **then**
    for Each $PointCloudCluster$ **do**
        Calculate $MaxPoint$
        Calculate $MinPoint$
        Calculate $\sqrt{(MaxPoint - MinPoint)^2}$
        $SpreadParameter$ = $\sqrt{(MaxPoint - MinPoint)^2}$
        if $SpreadParameter$ < 0 **then**
            $Abs(SpreadParameter)$
            $SpreadParameter$ = $Abs(SpreadParameter)$
        end if
    end for
else if $Numpoints$ <= 1 **then**
    Get Next $PointCloudCluster$
end if

The Pseudo-code for the spread estimation algorithm can be shown in Algorithm 1. This algorithm further provides a third layer of validation apart from range and timestamp as explained in Figure 4.8 to check if an point cloud cluster is from an insect target. However, there are certain problems associated with this algorithm, such as vegetation clutter such as leaves and flowers moving in front of the radar. As the spread of leaves and flowers would be similar to that insects and would further introduce a lot of false positives for this algorithm. In addition to this, there are other limitation of this algorithm will be further discussed in Section 7.3 where possible solutions will be provided to improve this algorithm.

4.5 Experimental Setup Overview

This section explains the overview of the setup considered to perform the relevant tests and experiments throughout the course of this thesis. As observed in Figure 4.10, the experi-

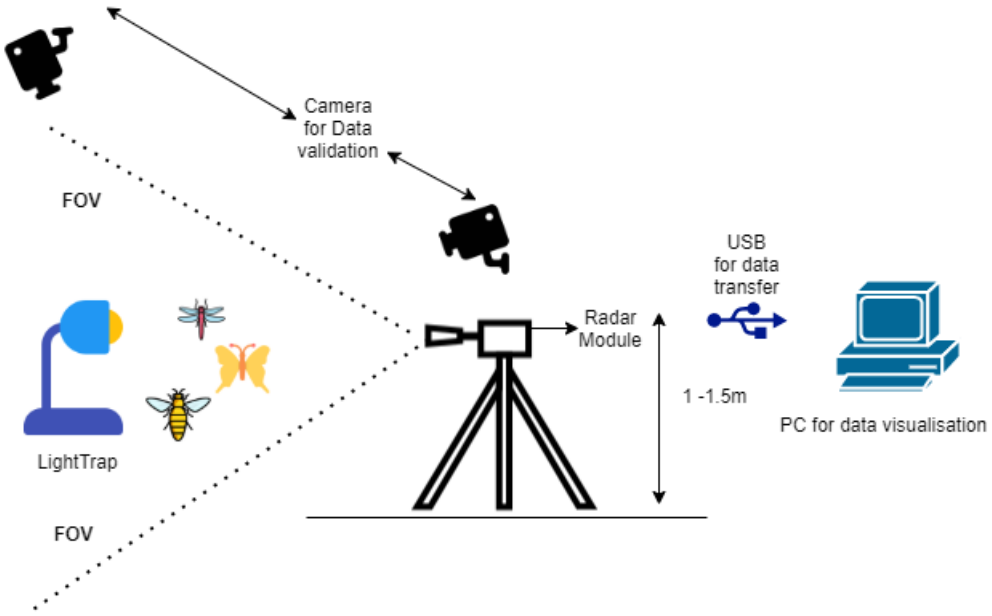


Figure 4.10: *Experimental Setup considered to deploy the mmWave radar module in different environments. The light trap is used to lure airborne insects near out system and the camera modules are used for validating the data obtained by the mmWave radar system.*

mental setup consists of the mmWave radar module for detecting and tagging insect returns continuously for long periods. The radar module is mounted on a tripod stand. A UV light source has been used to attract insects near the radar system. The light source has been used as a stimuli because in an open field, insects are really hard to identify and the setup has physical constraints such as power requirements and cables which makes it intricate to carry around the field and identify insects. Therefore, a UV lamp source operating at lower wavelengths has been utilised for attracting insects near the test environment. Two camera modules have been used for validating the ground truth and verifying the detection capability and the performance of the radar in detecting insects. The camera modules are placed in such a way that they cover the entire FoV of the radar module and subsequently do not miss capturing and recording any insect flying into the FoV of the radar system. The UART interface is then used for bidirectional communication between the radar system and PC. The PC in the system is used to start and stop the mmWave radar and visualize

the data gathered by the radar in real time.

4.5.1 Setup Components

- **Radar Module**: As discussed in Section 4.2, the IWR6843AoP-EVM mmWave sensor has been used as the primary radar module for our application.
- **Light source**: The lamp used for this research is a Sylvania UV-A 20W fluorescent insect attraction lamp. This lamp emits an UV radiation at 368nm which is widely accepted as the most important frequency for the attraction of numerous insect species.
- **Camera Module**: In order to accurately validate and compare radar data, two camera modules have been used to record insects concurrently with the radar system. The two cameras utilised were Sony 4K UHD camcorders with built in night vision mode. Since most of the tests were performed during dusk and night, the camera modules were enabled with night vision recording to increase the pixel resolution of insects flying across the system at nights.
- **USB to UART Interface**: In order to view the data captured by the radar system, an USB to UART interface was utilised to connect the PC and the radar. As observed in Figure 4.11 there are two ports namely, the data and the COM port established for communication between the mmWave radar and the PC. The data port is used by the radar module to send data towards the PC and the COM port is used to send multiple chirp and profile configurations to the mmWave radar module. The USB to UART interface enables easy integration of the radar and PC system with minimal physical constraints and requirements.

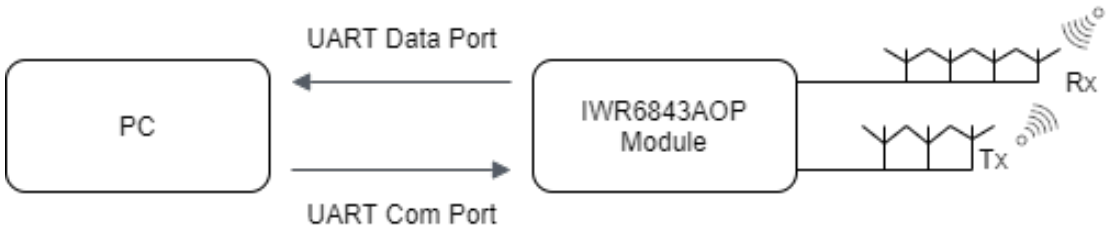


Figure 4.11: *System Flow of UART Interface to allow configuration and debugging of data in real time. The UART data port receives the data from the radar system and COM port transmits specific chirp configurations to the radar/*

4.6 Annotation of Insect Data

The mmWave radar and the camera module operate in tandem with each other. The camera module continuously records the video in the RoI. The recording from the camera module is later observed to look for insects approaching in the camera frame. The manual eyeballing of data from the raw camera recording enabled us to identify the time intervals at which an insect occured in the camera frame. These specific time intervals were then compared with the system clock timestamps generated from radar detection data to term it as a valid insect detection. The camera recordings were visualised with the help of a video player and the respective time periods of insect occurrences were penned down.

A second level of validation can be achieved by recording the radar's visualizer for the duration of the experiment. This recording can then be displayed along with the camera recording to check if the radar system performs a detection when an insect occurs in the camera frame in real-time. Thus, this process allows us to annotate insect data subsequently from both the recordings. However, this method is highly user-dependent as it becomes intricate to look at multiple recording screens simultaneously.

4.6.1 Dataset Preparation

The mmWave radar system continuously monitors the RoI for any dynamic targets. As soon as a target appears in front of the radar, it performs a detection and stores its data frame into a CSV file. The data frame of the radar will consist of the following parameters:

- Timestamp of the detection performed.
- Target ID.
- Number of point cloud data reflected from the target.

Each point cloud data estimated by the radar system, consists of the following variables of information namely,

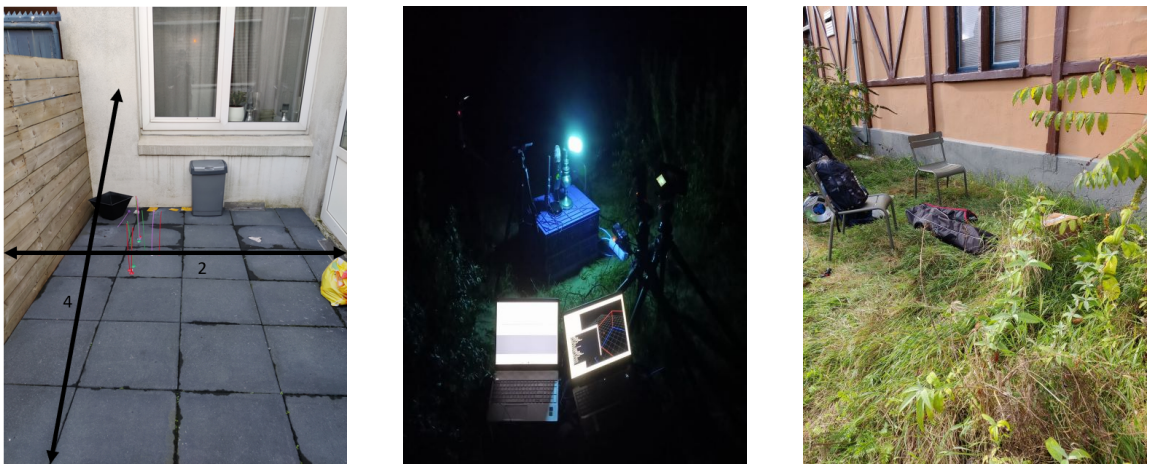
- 3D position of the target at the time of detection.
- Azimuth and elevation angle of the target.
- Range of the target at the time of detection.
- Doppler velocity of the target.
- SNR obtained from the target.

4.7 Test Environments and Conditions

The research is mainly concerned with evaluating the response of insects to the artificial light sources at night, Therefore, higher proportion of tests were conducted at night either after sunset or during dusk. The tests were largely conducted during the proceeding months of August, September and October. The Temperature recorded during most of the tests were observed to be between 18 and 25°C. The wind speed, start time, end time and the distance between the radar and the light source pertaining to each experiment were recorded during the course of the test.

The tests were mostly conducted in urban and suburban environments. The urban environment is namely the backyard of our house and is rectangular in shape. The dimensions of the backyard were measured to be 4x2m. The suburban environment tests were conducted in the inner dune area at Katwijk Aan Zee and Artis Zoo as they were considered as the richest places for finding insects in the surrounding area. The performance of the system in detecting insects at these environments is evaluated and discussed briefly in Chapter 6.

The methodology and the conditions during the experiments will be provided in Chapter 6 where, each experiment conducted along with its results will be discussed in an elaborate manner.



(a) *Urban environment* **(b)** *Suburban environment* **(c)** *Artis Experimental site*

Figure 4.12: *Figure shows the multiple test environments in which the experiments to detect airborne insects were conducted.*

4.8 System Performance Metrics

Performance metrics are used to measure the ability of the system to perform a particular task. In our case, the task is to detect an insect target successfully. These metrics measure and evaluate the parameters that impact the performance of the system. The parameters that impact the detection performance of our system are given by:

- **Number of occurrences of an insect (N):** This parameter defines the number of times an insect has occured in the camera frame. An insect is considered occured and counted when it flies into the FoV of the camera. This occurrence is discarded when the insect exits the FoV and the subsequent insect flying into the next frame is considered as a new insect target.
- **True Positive (TP):** This Parameter defines the detection of an insect target by the radar system when the target is visually present in the corresponding camera frame.
- **False Positive (FP):** This parameter defines a detection by the radar system when there is an absence of an insect target in the corresponding camera frame.
- **False Negative (FN):** This parameter defines the inability of the radar system to detect an insect target when it is visually present in the camera frame.

It becomes necessary to know that our system will not have True Negatives as a performance parameter. The main reason for this omission is the tedious process involved in segmenting insect data as samples from the camera recording. This process would then involve accurate manual eyeballing of the exact time an insect target spends near the light source from the recording videos and comparing them with the frames obtained from the radar system. If a large number of insects occur during the experiment, then this would be a time-consuming process and eventually lead to measurement errors in determining the performance of the system. Therefore, the number of detections performed by the radar compared to the number of insects that occurred during the experiment was taken into consideration. The radar will only detect when there is a dynamic object moving in front of the antenna. This is due to the removal of signals from static or non-moving targets in the detection layer of the radar system. Therefore, when there is no moving target present, the radar system would not perform any detection in its RoI.

These parameters are intermittently important and they will have a drastic impact on the overall performance of the system. These parameters will give an insight into major metrics such as Recall and Precision of the overall system in detecting insect targets and estimating the overall performance of the detection system. The fundamental performance metrics as observed in Table 4.5 are utilised to evaluate the True Positive Rate (Recall), Precision, False Positive Rate and False Negative Rate.

- True Positive Rate (TPR): This metric determines the ratio of correct detections by the radar system to the total count of insects occured during the course of the experiment. This metric gives an insight regarding the sensitivity of the device when insects fly across the radar beam.
- Precision: This metric gives an indication of the positive detections performed. This metric gives an insight on the ratio of positive detections to the total number of detections done by the radar system.
- False Positive Rate (FPR): This metric determines the ratio of incorrect detections performed by the radar system during the course of the experiment. This metric gives an insight on the error that we could observe when the system is deployed in extreme noisy environments.
- False Negative Rate (FNR): This defines the ratio of the missed insect detections by the radar system to the total number of insects occurring during the experiment.

Metric	Formula
True Positive Rate (Recall)	$\frac{TP}{N}$ (4.2)
Precision	$\frac{TP}{(TP+FP)}$ (4.3)
False Positive Rate(FPR)	$\frac{FP}{(TP+FP)}$ (4.4)
False Negative Rate (FNR)	$\frac{FN}{N}$ (4.5)

Table 4.5: *Performance metrics realized for evaluating the performance of the System.*

Chapter 5

Experimental Methodology and Analysis

This chapter describes the methodology on how the experiments were performed to address our research questions and also introduces the reader to the significant data collected from each environment. A comprehensive analysis is then performed on the collected data to evaluate the performance of the mmWave radar in each environment.

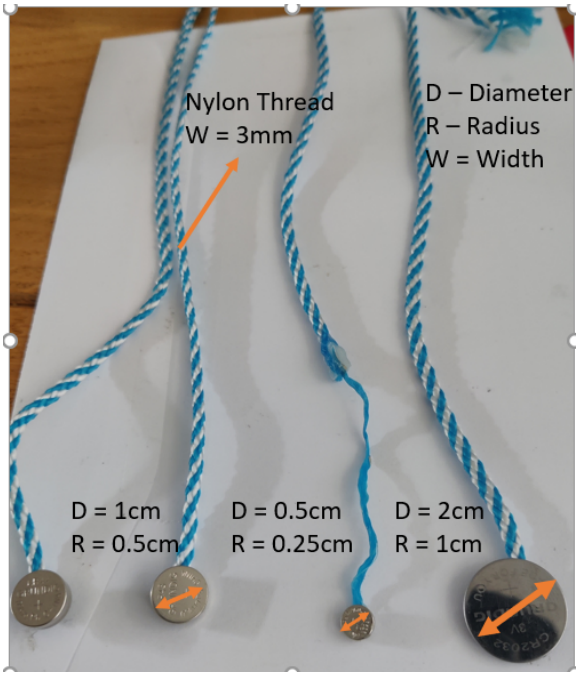
5.1 Non-Insect Target Detection

It becomes necessary to evaluate the performance of the radar initially with non insect targets such as small watch batteries to estimate the practical maximum detectable range of the radar and also verify the authenticity of data for small targets in practical scenarios. A python GUI developed by Texas Instruments was used to visualise the range calculated by the radar. A measuring tape was used to measure the actual range of the objects and validate the ground truth. These results were further analyzed to make the required improvements in measuring actual insect targets with high precision. This experiment addresses our second research question: **What is the performance of the mmWave radar in detecting small objects that have equivalent size to that of insects?**.

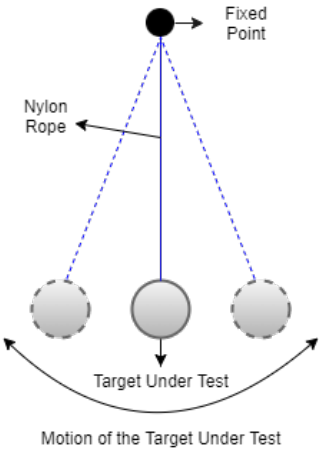
5.1.1 Data Collection and Performance Analysis

The first test performed was used to detect spherical watch batteries of different radius ranging from 0.25cm to 1cm. According to [53] The RCS of a typical sphere can be calculated by the formula πr^2. where r is the radius of the sphere. The spherical metal batteries

were suspended to a Nylon rope having a width of 3mm. Since metals are considered as a highly reflective materials, they produce a high electromagnetic signature for the radar to detect. Therefore, it becomes necessary to have a target which is made from a non-reflective material with a low reflectivity index such as rubber and therefore, dome shaped black rubber earbuds were also used to determine the capability of the radar. The batteries and earbuds were placed at an initial distance of 20cm from the radar system and after initial detection, the distance was increased in small increments of 5cm upto the maximum distance at which the target was detected.



(a) *Spherical batteries utilised for this experiment with their respective radius and attached to a rope to suspend them.*

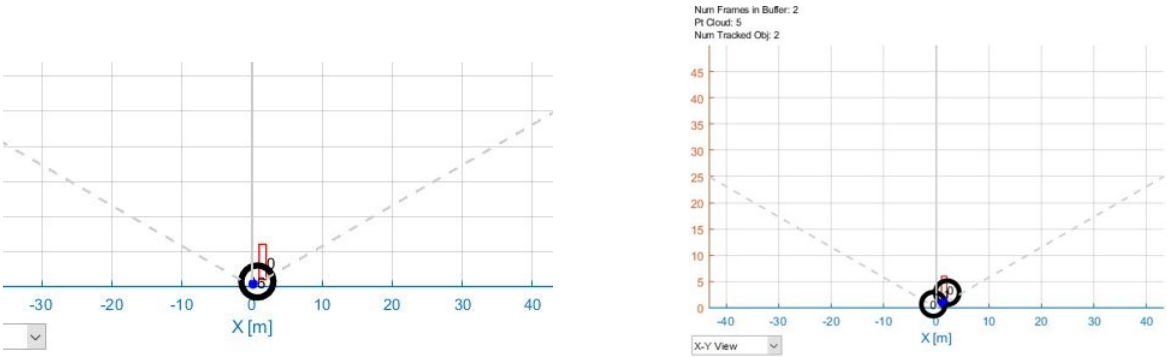


(b) *Figure denoting the pendulum motion of the targets under test. The equilibrium position of the target is the centre point denoted by the solid line and the consecutive positions of the targets are denoted by dashed lines.*

Figure 5.1: *The small insect-like targets that were utilised for evaluating the performance of the mmWave radar.*

The targets suspended under test were dynamically moved in an orthogonal pendulum motion in front of the radar and the respective range plots were visualized in the radar system. The pendulum motion was considered because it would mimic an insect target flying into the frame to a certain extent. The orthogonal motion of the battery indicates that the angle covered during its motion can be ignored as there would only be a minor

difference in the range obtained during its motion from its initially set true range. The scaling threshold factor for the CFAR algorithm was configured to be at 5dB for the targets under test as this threshold detected the targets with a higher probability compared to the other threshold values. The Targets that were utilised for this experiment can be observed in Figure 5.1 and the pendulum motion of the targets is shown in Figure 5.1b.



(a) *Detecting a Single Object* **(b)** *Detecting Multiple Objects*

Figure 5.2: *Figure denotes the detection of various objects by the radar system in the X-Y axis. The black circle indicates the point cloud cluster formed by the object, the grey dotted line indicates the FoV of the sensor, the blue dot denotes the point cloud data reflected by that particular object. The Red box in the center denotes the mmWave radar itself.*

The radar was also able to detect multiple targets at the same time. The radar would be able to detect multiple objects as long as the minimum separation distance remains greater than the theoretical range resolution achieved by the radar. As discussed in Section 4.3.2, the radar system was estimated to have a maximum range resolution of 8cm. Figure 5.2a shows how a single target detected can be visualized from the radar system. Figure 5.2b shows how multiple targets when kept at a minimum distance of 9cm from each other are detected as multiple targets by the radar system.

The performance of the mmWave radar in detecting non insect targets was evaluated by calculating the standard deviation and the margin of error present in the measured average range compared to the true range of targets by taking 20 samples of detection performed by the mmWave radar.

Table 5.1 analyses the performance of the system from the data collected the mmWave radar in detecting the targets under test at various distances. The standard deviation S and

the margin of error of each measurement can be given by Equation 5.1 and 5.2 respectively.

$$S = \sqrt{\frac{1}{N-1}\sum_{i=1}^{N}(x_i - \bar{x})^2} \tag{5.1}$$

Where N = Number of samples
x_i = True range
$\bar{x}$ = Average Range Measured

$$ErrorMargin = \frac{S}{\sqrt{N}} \tag{5.2}$$

Radius (cm)	True Range (m)	Average Range Measured (m)	Standard Deviation (m)	Error Margin (m)
0.25	0.5	0.58	0.040	0.008
	1	1.07	0.067	0.014
	1.5	1.54	0.071	0.015
0.5	0.5	0.57	0.046	0.010
	1	1.11	0.072	0.012
	1.5	1.51	0.077	0.017
1	0.5	0.54	0.046	0.0102
	1	1.05	0.062	0.013
	1.5	1.52	0.082	0.017

Table 5.1: *The deviation in range measured by the mmWave radar for the batteries kept at different ranges for a set of 20 continuous measurements.*

It can be interpreted that the margin of error obtained from the standard deviation is considerably low for all the detections performed. It can be inferred from Table 5.1 that as the distance from the radar increases, the standard deviation also increases. This error observed could be attributed to various factors such as the external environmental conditions, scaling threshold of the CFAR algorithm and the movement of the target under test. This information provides us with an approximate insight on how the performance of the radar will be in detecting actual range of insect targets, as validating the true range with the measured range obtained from insects will be a tedious task and could also lead to larger measurement errors than the ones observed in the spherical battery experiment. An elaborate discussion pertaining to this experiment will be discussed in Section 7.4.

5.2 Airborne Insect Detection

This section describes the data collected to evaluate the performance of the mmWave radar in detecting airborne flying insects in different noisy environments. This performance evaluation will provide us with an insight on the number of true and false positives detected by the radar and its ability to acquire insect data such as its range and SNR. These experiments and analysis will address our third research question: **What is the performance of the system in detecting airborne insects in urban and suburban environments and what are the main parameters that affect the performance of the system?**.

5.2.1 Data Collection and Performance Analysis

Urban Environment -Backyard

The first experiment with actual insect targets were conducted at the backyard of our house. The environmental conditions during the experiments can be observed in Table 5.2. The temperature recorded during the experiments were observed to be around 15 - 20°C. The recorded wind speeds were considerably low and are generally labelled as gentle breeze. The wind speeds should not have a major affect on the flight of the insects. The scaling threshold has been varied for each test and the number of true and false positives were analyzed. A wider field of view is employed during the experiments as the main goal of this experiment was to detect as many insects as possible flying in between the radar system and the light source.

Parameter	Value	Value
Date	08/09/2021	10/09/2021
Weather (°)	20	18
Wind Speed (BFT)	2	3
Start Time	22:05	21:30
End Time	23:05	23:00
Duration (hrs)	01:00	01:30
Distance between Radar and Light Source (m)	0.7	0.7
CFAR Scaling Threshold (dB)	7	5

Table 5.2: *The environmental conditions observed during the tests performed in an Urban Environment.*

The total number of insects that were present during the experiments conducted on both the days is shown in Table 5.3. The ground truth for insects was validated from the camera recording. Insects flying into the camera frame were counted as a single insect and were discarded when they left the camera frame.

Day	Date	Number of Insects
1	08/09/2021	33
2	10/09/2021	36

Table 5.3: *Ground Truth for Insects*



Figure 5.3: *Figure denotes an occurrence of an insect target near our experimental setup. This insect target is indicated by the black square box highlighting the insect's outer layer.*

Figure 5.3 shows an occurrence of an insect target near our system. Figure 5.4 shows the real time coordinates of the insect calculated by the radar system at a particular time interval.

Figure 5.5 shows different plots with respect to the data captured by the radar system. Figure 5.5a provides a relation on how insects are distributed over the course of the duration of the experiment. The entire duration of the experiment has been divided into time intervals of 10 minutes. Out of the total count of 69 insects that occured, 37 insects were detected by the radar system and 32 were not detected by the radar system. This could be due to many reasons such as, the size of insects present during those time windows were

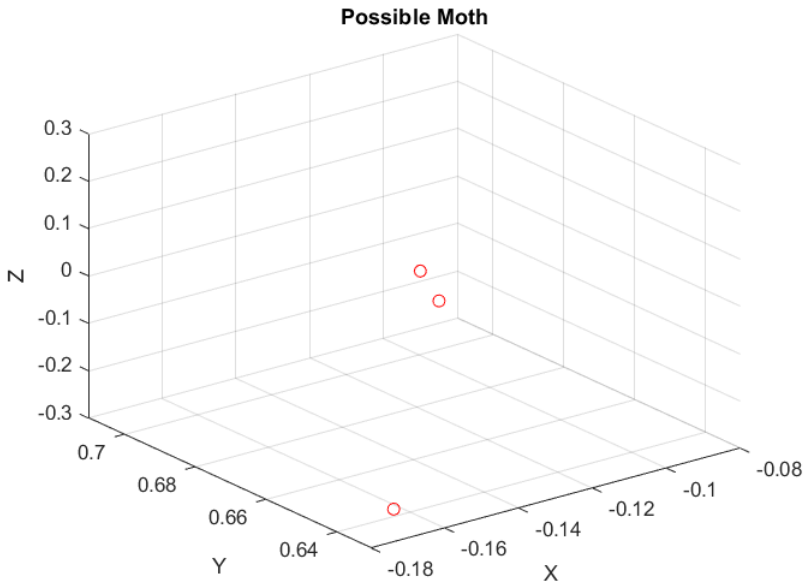
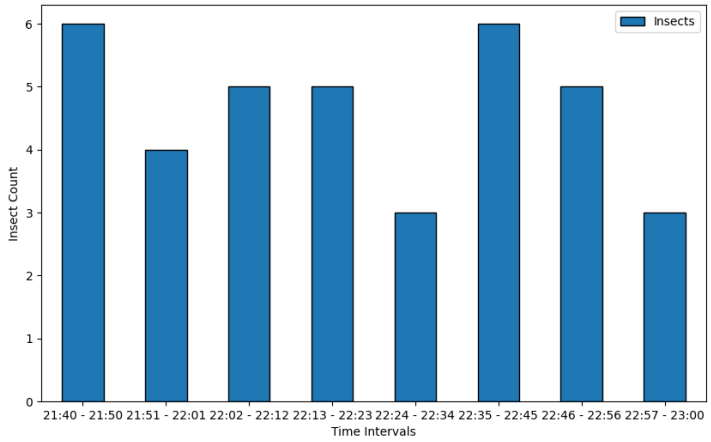


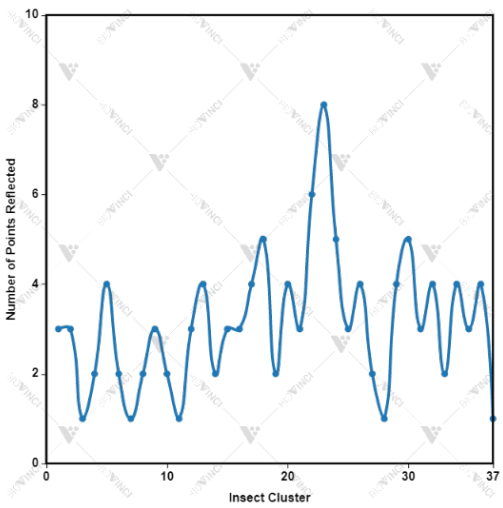
Figure 5.4: *Real time coordinates of the insect calculated by the mmWave radar as indicated by red dots in the 3D plot. These coordinates were estimated by the radar at a specific time interval at which the insect was present near our system.*

smaller in size and hence produced a relatively weak signature which was comparatively less than the set threshold and hence, were not detected by the radar system. One other reason could be that the range at which these insects were present was farther than the radar's theoretical maximum detection range and hence, were not detected by the radar system. This graph can further provide an inference on the distribution of insects over multiple time intervals during the course of the experiments conducted.

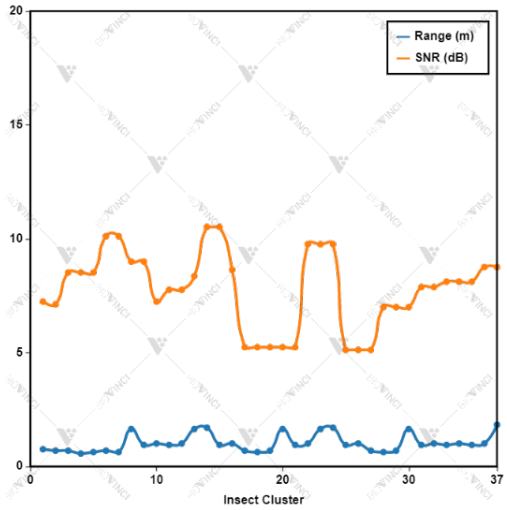
Similarly, Figure 5.5b provides an inference on the size of the insect targets based on the number of points, the insect reflects back to the radar system. Each point cloud data associated with an insect target will have information embedded such as its position, SNR, range and angle. The accumulation of these point cloud data into a cluster point is known as an insect cluster. An insect cluster will consist of all the point cloud data reflected from an insect target. Thus, the more number of points are reflected from an insect target, more data could be deduced regarding their position displacement and flight. The number of points an insects reflect back depends on a number of factors. Larger the size of the insect, larger will be the area of cross-section of the insect and hence the more number of points it would reflect. Similarly, it will also depend on the time the insect spends near the radar



(a) *Insects detected at specific time intervals.*



(b) *Number of points reflected by each insect target.*



(c) *Variation of SNR and Range for each Insect target.*

Figure 5.5: *Analysis of Insect data obtained in an Urban Environment.*

system. Longer the insect will be flying near the system, the more number of points it would be reflecting at different time intervals. It also becomes necessary to know that, number of points reflected from an insect can also depend on the incident and the reflected angle. The incident angle is typically the angle at which the radar beam hits the proportion of the target. The incident angle depends on the shape and the orientation of the target to

the radar source. The reflected angle, is the angle at which radar beam deflects after hitting a target. Thus, a larger difference between angle of incidence and reflection will result in a lower number of reflected points from a larger insect target.

On the other hand Figure 5.5c provides an observation on the variation of the SNR and Range of detection for multiple insect clusters obtained. The variation of SNR and the range for each insect cluster can also provide us with an estimation and information on the displacement and flight of the insects from its initial point of detection.

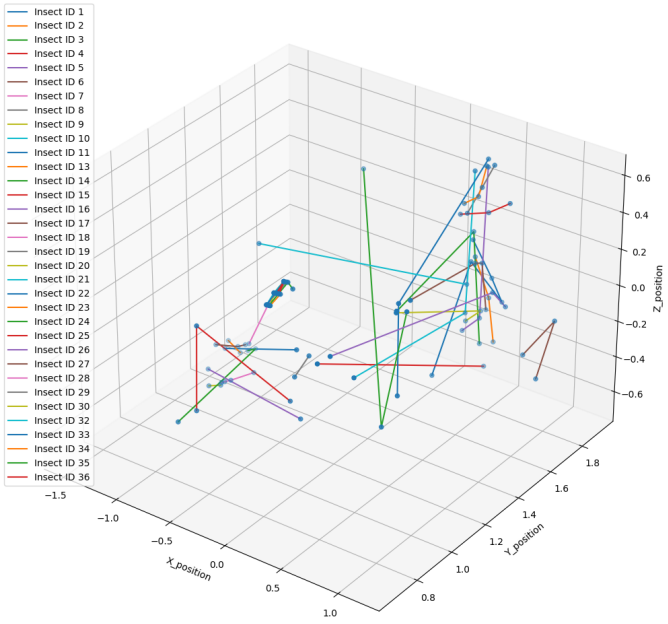


Figure 5.6: *Figure denoting the position displaced by each insect target as estimated by the mmWave radar module. The Insect ID in legend represents each insect cluster detected by the radar system.*

Displacement is defined as the change in position of a specific target from its initial position to its final position in a time frame. The mmWave radar module can be assumed to be at origin (i.e) (0,0,0) and the first detection point of an insect target is assumed as its initial point. The multiple points associated with each insect are tagged until it disappears from the frame.

$$\Delta P = P_f - P_i \tag{5.3}$$

Where ΔP is the change in position in three dimensional Cartesian coordinates and (P_f) and (P_i) are final and initial positions respectively. Insect clusters tagged by the clustering algorithm in the mmWave radar system, reflecting multiple points from each insect can generate an approximate trajectory determining change of position of an insect and in addition also provides us with the information regarding the gradual movement of an insect.

Figure 5.6 shows the real time dynamic coordinates of all the insect targets that occured in the urban environment with respect to its initial and final position. It can be observed from Figure 5.6 that the movement pattern of a certain insect can overlap with another insect. It can also be observed from the graph that the track of an insect can be followed efficiently when there are more number of points reflected from the insect cluster. This attributes to the fact that the insect was tagged by the mmWave radar system for a longer period of time and hence, can be followed more effectively.

Table 5.4 depicts the **performance analysis** for the tests conducted in an urban environment. The Scaling Threshold in the CFAR detection algorithm was varied during the course of the experiments and the performance metrics were evaluated for each threshold. The total recall factor was calculated to be 55% respectively. The total precision could be observed to be around 75% for the observations recorded. Simultaneously, the system has recorded a low number of false positives. The total false positive and negative rate is calculated to be 24% and 46% respectively. The reason behind the higher number of false negatives and the false negative rate will be elaborately discussed in Section 7.5.

Scaling Threshold(dB)	N	TP	FN	FP	Recall	Precision	FPR	FNR
7	33	15	18	4	0.45	0.78	0.21	0.55
5	36	22	14	8	0.61	0.73	0.26	0.38
Total	69	37	32	12	0.54	0.75	0.24	0.46

Table 5.4: *Evaluation of the performance metrics from the experimental data collected in urban environment.*

Suburban Environment - Katwijk Aan Zee

Table 5.5 denotes the environmental conditions at the time of the experiment. A scaling threshold of 5dB was chosen for this experiment as it was contemplated as the most optimal threshold from the previous experiments conducted in 5.2 which generated a higher detection rate for insects. This experiment was conducted in a suburban area surrounded by grasslands and vegetation. However, the area between the radar and the light source

did not consist of a larger amount of vegetation, leaves and other obstruction which would degrade the performance of the radar system. As the experiment was conducted in an open field, a wider field of view of 90°was chosen to cover a broader area and possibly detect all the probable insects occurring near the radar system. The experiment lasted for an hour and approximately data from 51 insect targets was analysed. Figure 5.7 shows the system setup for the experiment conducted.

Parameter	Value
Date	16/09/2021
Weather (°C)	17
Wind Speed (BFT)	2(N)
Start Time	21:30
End Time	22:30
Duration (hrs)	01:00
Distance B/W Radar and Light Source (m)	1.0

Table 5.5: *Environmental Conditions observed during the course of the experiment.*

Figure 5.8 shows a typical insect in the surrounding area attracted by the light source and Figure 5.9 depicts the dynamic coordinates of the particular insect as detected by the radar system. This insect can be observed to be a large insect and hence, reflected more than a single point cloud for the radar to detect.

Table 5.6 shows the **performance analysis** of the data collected during the course of the experiment. The recall and the precision rate was calculated to be 66% and 87% respectively. Since the experiment was conducted at a place surrounded by vegetation and grasslands, a large number of insects were attracted to the light source and were present near the radar system for long periods. The majority of these insects were large in size. The false positive rate and false negative rate are observed to be 12% and 33% respectively.

Scaling Threshold(dB)	N	TP	FN	FP	Recall	Precision	FPR	FNR
5	51	34	17	5	0.66	0.87	0.12	0.33

Table 5.6: *Analysis of the performance metrics that were estimated from the data collected in Suburban Environment.*

It can be observed that the precision of the system has also increased substantially from the previous experiment. This increase could be attributed to the higher number of true



Figure 5.7: *Experimental setup of the mmWave radar deployed in the suburban environment.*

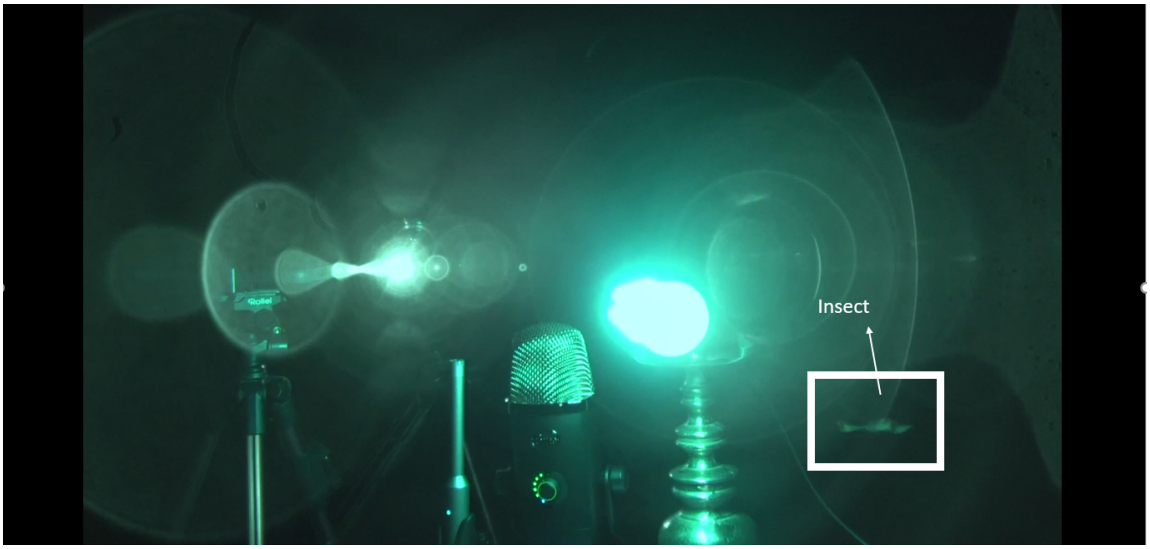


Figure 5.8: *Insect recorded by the Video Camera occurring near our system as indicated by the white square box.*

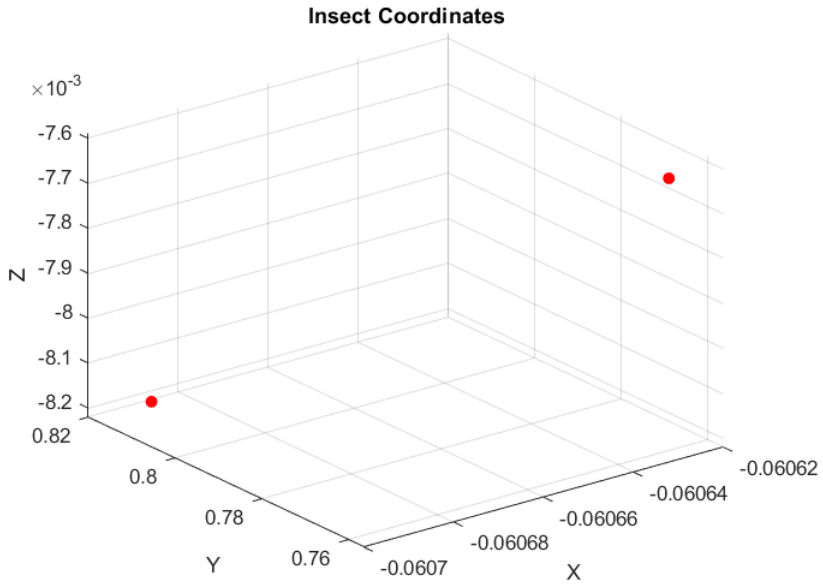


Figure 5.9: *3D graph plotting the real time coordinates of the insect indicated by red dots, as calculated by the mmWave radar at a certain point in time.*

detections and lower number of false detections. Since the area between the radar and the light source did not have any interference such as leaves and trees, the false positive rate decreased correspondingly. Thereby, increasing the performance of the system.

Table 5.7 gives an insight into the different types of insects that were attracted to the light source. There were around 36 large insects exceeding 2cm (approximately from camera data visualized) in size.

Insect	N	TP	Recall
Large Insects(> 2cm in size)	36	30	0.83
Small Insects(< 2cm in size)	15	4	0.26

Table 5.7: *The variation in the size of insects that were attracted by the light source during the course of the experiment.*

Artis Zoo Experimental Site

The third field test was conducted in a foliage in Artis Zoo. The environmental conditions present during the course of the experiment is observed in Table 5.8. The experimental setup can be visualized in Figure 5.10. The restrictions in the opening and closing time of the Artis zoo meant that the experiment had to be conducted during daylight and therefore, a large number of insects could not be attracted by using the insect lamp at hand, as the sunlight was more brighter than the light generated by the lamp. There were also several spells of rain during the experiment which further restricted us in conducting a continuous experiment.

Parameter	Value
Date	06/10/2021
Weather (°C)	13
Wind Speed (BFT)	3
Start Time	10:00
End Time	16:00
Duration (hrs)	06:00
Distance B/W Radar and Light Source(m)	1.0

Table 5.8: *Environmental Conditions observed during the experiment in Artis Zoo.*



Figure 5.10: *Experimental setup for the mmWave radar deployed in Artis Experimental site.*

It can be observed from the setup that the area between the radar and a light source and its surroundings consists of a large number of leaves and shrubs. This condition of the test environment will eventually generate a large number of false positives for the system. The large number of false positives will be generated due to the environmental clutter produced by the leaves and shrubs moving in front of the radar during extreme windy conditions. The scaling threshold parameter plays an important role in this experiment and lower thresholds might generate a large number of false positives for our system as discussed in Section 3.5.1. Thus, a trade-off between the scaling threshold and the environmental clutter needs to be considered. Therefore, the scaling threshold was varied during from 5dB to 25dB as the experiment progressed. At each scaling threshold, the performance of the system was evaluated.



Figure 5.11: *Figure denotes the occurrence of two insects near the experimental setup. The insects are indicated by the black circles marking their outer layer in the figure.*

Figure 5.11 shows typical insects flying near our system. A large proportion of insects that occured during the experiment were typically of the same size as shown in Figure 5.11 which can be visually observed to be greater than 2cm in size.

The **performance analysis** of the data collected during this experiment can be depicted in Table 5.9. The radar system can be observed to have an overall recall factor of 65% and a precision of 24% in detecting insects from the surrounding clutter present. The combined false positive and negative ratio can be perceived to be 75% and 34% respectively.

Scaling Threshold(dB)	N	TP	FN	FP	Recall	Precision	FPR	FNR
5	2	1	1	20	0.50	0.047	0.95	0.50
10	5	3	2	17	0.60	0.15	0.85	0.40
20	12	8	4	13	0.66	0.38	0.61	0.33
25	10	7	3	9	0.60	0.43	0.56	0.40
Total	29	19	10	59	0.65	0.24	0.75	0.34

Table 5.9: *Evaluation of the performance metrics for varying Scaling Thresholds.*

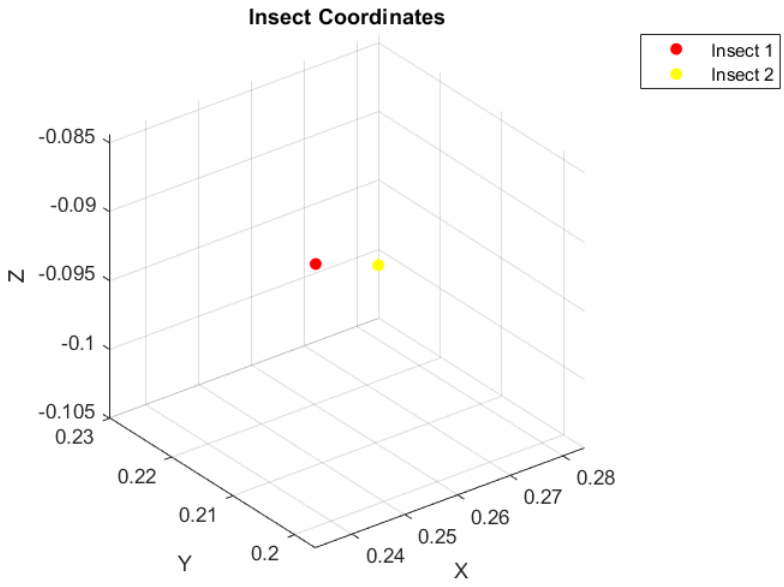


Figure 5.12: *3D plot denoting the coordinates of the insects depicted in Figure 5.11 as red and yellow markings at some point in time.*

It can be observed that the precision of the system decreases substantially from the previous experiments conducted. This could be correlated to the increased number of false positives in the system. However, it can also be visualized that as the scaling threshold is increased, the false positive rate also reduced. This trend substantiates our theory that when the scaling threshold increases, lesser number of false detections will be performed by the radar system and as a result, the system performance is improved. An elaborate discussion regarding the parameters that affect the various performance metrics will be carried out in Section 7.5.

Chapter 6

Results

This chapter introduces the reader to the results obtained from conducting the experiments for non insect targets. The reader is also introduced to the results obtained from evaluating the performance metrics described in Table 4.5 for airborne insect detection in various environments.

6.1 Non Insect Target Detection

Figure 6.1 shows the relation between maximum range of detection and the radius of the object. It can be observed that a target having a radius of 1cm, was detected at a maximum range of 2.85m, whereas, a dome shaped earbud having a similar radius to that of a spherical battery was detected at a lower range compared to a spherical battery by the radar system. This proves that the material under test also plays an important role in determining the maximum detection range. As materials made of rubber absorb a portion of the electromagnetic wave and reflect back only a small portion towards the radar's receiver.

Figure 6.2 shows the measured range from the mmWave radar system for a set of continuous 20 measurements performed. This graph was plotted from the data collected in Table 5.1.

Table 6.1 shows the average standard deviation and the average error that is measured for the range obtained from the radar system for targets having different radius kept at multiple range namely, 0.5m, 1.0m and 1.5m from the radar system. The average standard deviation could be observed to be in the range of $\pm$ 0.05 and $\pm$ 0.06m and the average error calculated from the measured data could be observed to be in the range of $\pm$0.012 and $\pm$0.05m. It can be interpreted that the average standard deviation and error is considerably

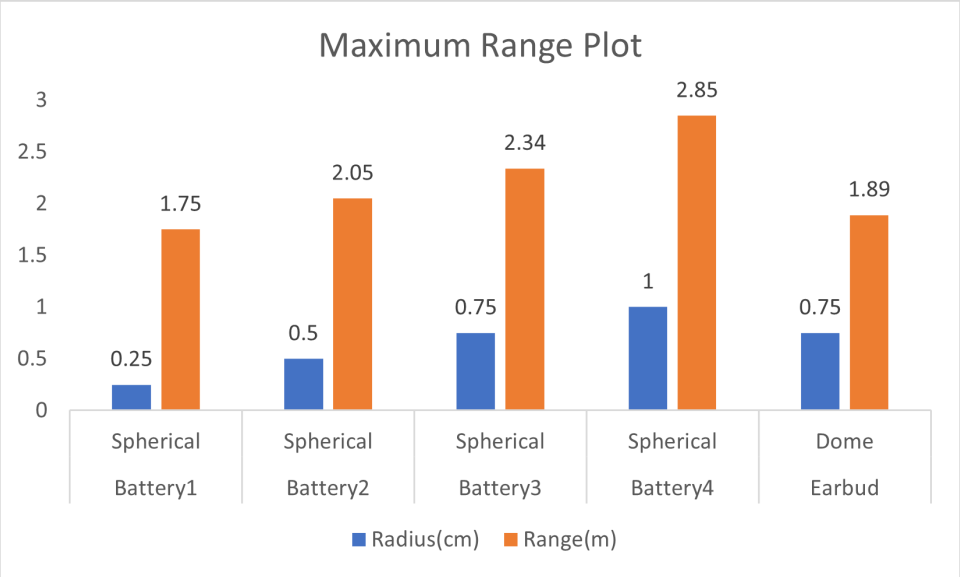
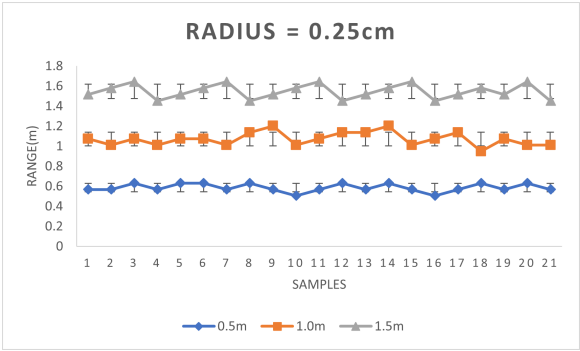


Figure 6.1: *Figure Denoting the maximum range detected by the mmWave radar for different targets utilised in this experiment.*

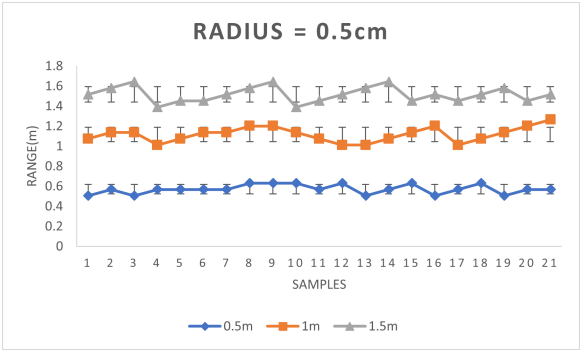
low for all the detections performed. The average standard deviation and error obtained in the mmWave radar system is estimated from the data collected in Section 5.1.

Radius (cm)	Average Standard Deviation (m)	Average Error (m)
0.25	± 0.059	± 0.012
0.5	± 0.065	± 0.013
1	± 0.063	± 0.013

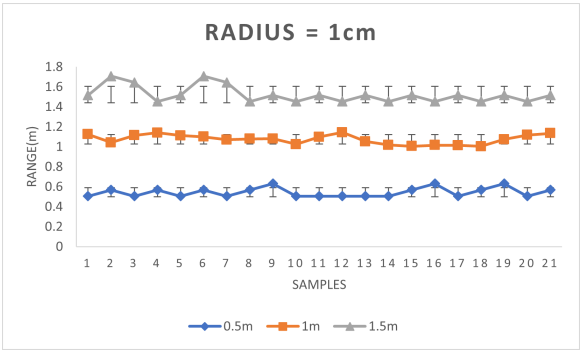
Table 6.1: *Overall performance of the system in determining the true range of small targets having different radius and size.*



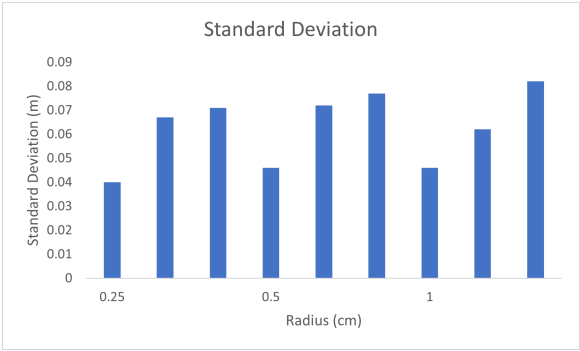
(a) *Measured range at radius = 0.25cm*



(b) *Measured range at radius = 0.5cm*



(c) *Measured range at radius = 1cm*



(d) *Variation of standard deviation with radius*

Figure 6.2: *Figure 6.2a 6.2b and 6.2c show the measured range from the mmWave radar with standard deviation as error bars. Figure 6.2d depicts the total standard deviation obtained for each radius of the battery.*

6.2 Airborne Insect Detection

Table 6.2 realises the performance metrics estimated pertaining to the environments, where the experiments were conducted. The data used for constructing this table was obtained from Section 5.2. It can be interpreted that the Average recall rate obtained in the different environments to be 60%, 66% and 65% respectively. The average precision is estimated to be 76%, 87% and 40% respectively. The average false positive rate can be depicted to be 23%, 12% and 59% respectively. An elaborate discussion regarding the evaluation and reasoning of the obtained results will be performed in Section 7.5.

Experiment	Average Recall Rate	Average Precision Rate	Average FPR	Average FNR
Urban Environment	0.60	0.76	0.23	0.46
Suburban Environment	0.66	0.87	0.12	0.33
Artis Experimental Site	0.65	0.40	0.59	0.34

Table 6.2: *Overall performance of the mmWave radar system in detecting airborne insects in all the environments.*

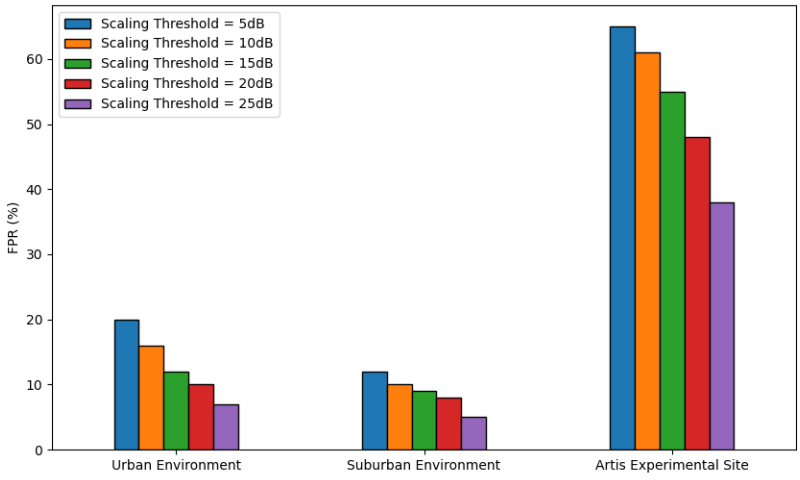


Figure 6.3: *Figure depicting the relation between the False Positive Rate and the Scaling Threshold in different test environments.*

Figure 6.3 shows the effect of the scaling threshold parameter on the false positive rate obtained in all the environments. The scaling threshold parameter is varied from 5dB to

25dB and the respective plots for false positive rate can be observed.

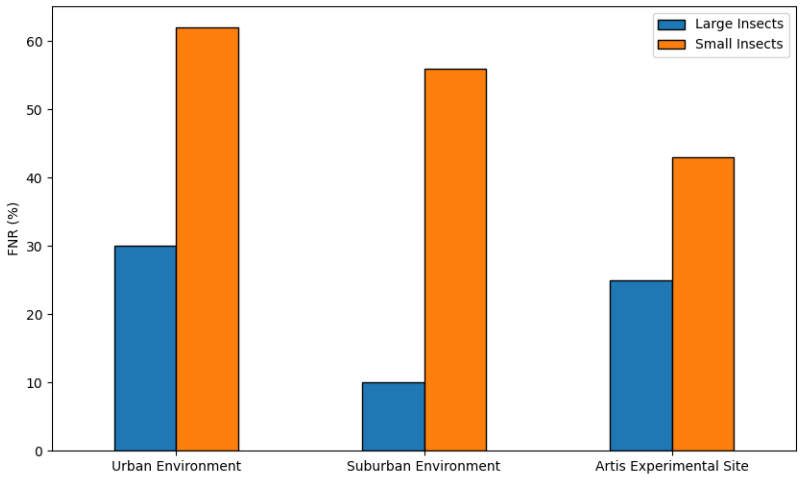


Figure 6.4: *figure representing the effect of size of the insects on the false negative rate achieved by the system.*

Figure 6.4 shows the effect of the size of the insects that occurred during the course of the experiment to the false negative ratio obtained in the the system. Larger insects are visually observed to be greater than (> 2cm in Size) and smaller insects are observed to be (< 2cm in size). However, this is only an approximate estimation of the size based on the visual data recorded by the camera module and not an accurate estimation of the actual size of the insect target.

Figure 6.5 shows the effect of the environment on the performance obtained by the system. The data used for estimating the average performance in an urban environment can be observed in Table 5.4. Similarly, the data utilised for estimating the average performance in a suburban environment can be noticed in Table 5.6. On the other hand, the data collected for estimating the performance in Artis Experimental site can be perceived in Table 5.9.

An elaborate discussion pertaining to the effect of each parameter on the performance of the mmWave radar's detection algorithm would be explained in Section 7.5.

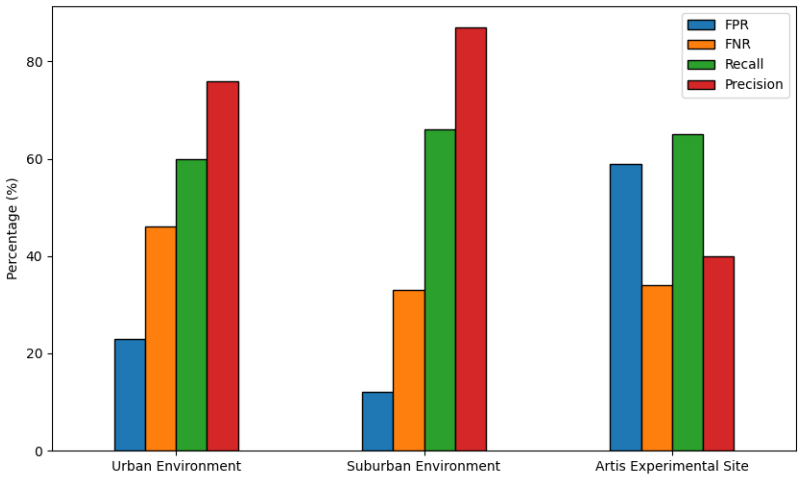


Figure 6.5: *Figure illustrates the effect of the external environment on the performance obtained in the system.*

Chapter 7

Discussion, Conclusion and Future Work

This chapter provides a comparative analysis on the performance of the mmWave radar's detection and the clustering algorithm to ascertain airborne insects successfully in distinct environments. This chapter also draws out the important conclusions from this research and proposes future solutions to improve the limitations and the performance of the mmWave radar system in adverse environments.

7.1 CFAR Detection Algorithm

A cursory review of the CFAR detection algorithm incorporated in the mmWave radar system indicates a reasonably moderate performance of the radar system in detecting small insect-like targets and airborne insects successfully. Thus, validating our hypothesis that a mmWave radar system can aid in detecting insects flying near a certain light source in discrete environments and weather conditions. The CASO-CFAR detection algorithm as explained in 4.4.1 was incorporated as the CFAR algorithm in this thesis because of its high competence in resolving and detecting weak targets with adjacent noise sources and subsequently, improving the overall performance. However, it also becomes important to note that this detection algorithm was designed in mmWave radar's SDK by default and incorporating other alternative algorithms could result in exhausting the device's memory and eventually leading to unexpected results and errors. Although employing other CFAR algorithms in the current mmWave radar's SDK was not tested practically in our thesis because of significant time constraints in understanding the depth of complex underlying concepts and the limitations involved, it could be regarded as an important future prospect in employing additional CFAR algorithms to further optimise the detection performance

of the radar. The scaling threshold parameter of the CFAR algorithm was considered to be one of the fundamental parameters that defined the performance of the detection algorithm in different environments. However, from the results obtained from the experiments, it was analysed that various external factors also contributed to reducing the performance of the detection algorithm in the mmWave radar system. The effect of these factors will be elaborated in the upcoming Section 7.5. One unanticipated finding was that when the scaling threshold was set below 5dB for conducting experiments, continuous ghost detections were generated inside the radar system even when there were not any moving targets present in the RoI.This was the case with both the experiments, the non insect target and actual airborne insect targets. However, for the battery experiment, these ghost detections were considerably low compared to the airborne insect detection experiments. Although the exact reason behind this is not known, this anomaly could be attributed to the ground clutter generated by the floor or the ground on which the radar was deployed in the outdoor environments where the radar was deployed. This information also indicates that for a scaling threshold below 5dB, it becomes intricate to distinguish actual insect targets from these ghost detections and eventually leading to a degradation in the system performance. Therefore, it is always recommended to have a threshold higher than or equal to 5dB.

7.2 Clustering Algorithm

The Gtrack algorithm was employed for clustering point cloud data obtained from the back end processing of the mmWave radar system. This clustering algorithm was developed by Texas Instruments and has similar functionality compared to the Density Based Scanning Algorithm (DBSCAN) clustering algorithm. However, in DBSCAN clustering, the point cloud data is grouped based on only the distance and the minimum number of points in a cluster [55], but in Gtrack algorithm extended improved functionalities for clustering are provided which presumably makes it more suitable for detecting smaller targets as well. These extended functionalities and parameters can be visualised in Section 4.4b in which the working principle of this algorithm is explained comprehensively. The existing values defined for each parameter in the Gtrack algorithm by Texas Instruments only enabled the mmWave radar to detect larger objects and thus, were required to be tuned and modified based on our application requirement to detect smaller targets and airborne insects. One of the major advantages of employing the clustering algorithm in our research was to reduce the point cloud data obtained from the environment by defining certain thresholds in the allocation, gating and scenery parameters respectively and consequently decreasing the computational complexity for the system. However, one major shortcoming of

this algorithm is that the values considered for each parameter were based on certain assumptions observed from previous studies performed regarding insects. Although these assumptions showed adequate results for our thesis, they might become ineffective in the long run because of their ambiguous nature as insect targets vary largely in shape, size and speed with respect to each other. Thus, it becomes critical to define thresholds for each parameter by taking into account the actual dimensions and the velocity of the interested insect targets. This could further increase the performance of the mmWave radar system in tagging distinct insect species showing non-linear behaviour in the RoI.

7.3 Spread Estimation Algorithm

A spread estimation algorithm described in Section 4.4.3 was designed to estimate an appropriate size of an point cloud cluster obtained from the clustering algorithm. The size of an appropriate cluster was evaluated by calculating the distance between the maximum and minimum point cloud of the X-Y coordinates in the point cloud cluster. The fundamental importance of this algorithm is that it can be used to differentiate insect targets from other larger targets that are detected by the radar system. Although a smaller distance between the points indicate a smaller target as the coordinates reflected from a certain small target will be close to each other, there is no exact way of validating this data as larger size targets can also reflect multiple point cloud coordinates with closely packed points. The only method of validating this data would be to utilise a vision based sensor integrated with the radar module. However, this limitation of the algorithm was improved by setting a maximum threshold for the amount of point cloud data reflected from a certain target. As larger targets will reflect higher number of point cloud data compared to smaller insect targets, they can be compared with the set threshold and discarded. This filtering would also reduce the frequency of the spread parameter estimation and in turn reduce the computational complexity of the system. In addition, another major shortcoming of this algorithm is that this estimate cannot be quantified as the distance between two specific coordinates in the point cloud cluster will not have any unit associated to them. Similarly, clutter generated from vegetation such as from small leaves and shrubs in the RoI can also generate similar properties as insects and thus, produce some amount of erroneous data in real time. Although, a moving branch or leaf is also relatively stationary to the radar node, small swaying movements are generated by them in the radar's FoV. This limitation of the algorithm can be improved by utilising machine learning algorithms to detect these swaying movements in its FoV and eliminating them. These movements may be discovered by analyzing and assessing the Doppler velocity and range acquired from a time series data.

7.4 Performance of the mmWave Radar in Detecting Small Non Insect Targets.

The results from the experiments conducted in Section 6.1 show that the mmWave radar shows high performance in detecting small insect like targets dynamic in motion. The maximum practical range obtained by the radar system in detecting these targets was observed to be equal to the maximum theoretical range estimated for the radar system. It was observed from the experiments that for different materials, range of detection was dependent on the radius of the target under test. The range was directly proportional to the radius and as the radius increased, the range of detection also increased. This relation is evidently true as larger objects will emit a stronger electromagnetic signature from the backscattered radio waves and thus, will have a higher reflectivity factor compared to smaller objects. The RCS also plays an important role as larger targets will have a larger target area for the radar waves to reflect from.

It can be observed in Figure 6.2 that the average deviation increases as the range of the targets are increased. This trend could be correlated to the fact that at farther ranges, the backscatter size of the target available to the radar to reflect or hit upon, hypothetically decreases and as a result, affects the range accuracy of the radar system. This minimal standard deviation and margin of error obtained from the measurements depicted in Table 6.1 provide an insight into the high precision that the mmWave radar could achieve in detecting the range at which small targets were present. This high performance of the mmWave radar system could be correlated to the fact that the targets under test were made of metal and followed a linear pendulum type of motion.

Although, these targets are not actual airborne insects, the high performance observed in this scenario will tend to degrade as airborne insects would have higher velocity, smaller size and would follow a non-linear motion compared to these targets. This degradation of the system performance would also depend on various other factors such as the environmental conditions, the surrounding area and the interference present in the RoI. Therefore, due to the aforementioned reasons, it becomes important to know that the mmWave radar would not be able to reproduce such high performance in detecting airborne insect targets when compared to insect like small targets.

7.5 Overall Performance of the mmWave Radar in Detecting Airborne Insects

Approximately 150 insects were attracted to the light source over the course of days during which the experiments were carried out. Out of these 150 insects, 70 insects were lured in the urban environment, 50 insects in the suburban environment and 30 insects in Artis experimental site. The fewer amount of insects attracted to the light source in Artis Experimental site could attribute to two reasons. The test was taken during the end of October, which marks the end of insect season as temperatures got decreased, compared to the tests taken in urban and suburban environments during the month of September, when the temperature was warmer. The second reason could be related to the fact that the experiment in Artis was conducted in daylight, and hence, the light source was not able to attract a large number of insects. The light source utilised for these experiments emitted an UV light and this created a phenomenon called the "**Fixated or Capture Effect**" [56] which drew the neighbouring insects towards the light source. This effect of light on insects act as a catalyst for the final "**Vacuum cleaner effect**", which eventually results in the death and declination of insect species. The number and the characteristics of insects attracted to the light source depends on the experiments that were carried out over the course of multiple days. Since most of the experiments were conducted in an urban environment, a larger proportion of insects attracted were from surrounding urban areas. The results from Section 6.2 show that the mmWave radar system displays moderate performance in detecting airborne insects that were attracted to the light source.

A visual glance at Table 6.2 gives an overview of the performance of the radar in multiple environments. It can be depicted that the radar shows high precision in urban and suburban environments compared to its performance in Artis. It also becomes important to note that the performance and the detectability of the system not only depends on the external environmental and experimental conditions but also on the scaling threshold parameter and the size of the insects being lured near the radar system. The average recall rate obtained from all test environments is estimated to be around 65%. Generally, optimal sensing systems in detecting flying insects [57] [58] have shown to have a recall rate of 65 to 90%. This comparison shows that our system shows an acceptable performance in achieving a moderate recall rate. The average precision obtained from the system in all test environments observed from Table 6.2 is around 70%. This rate of precision obtained can be considered to be a reasonable performance accomplished by the radar system in detecting insects successfully.

7.5.1 Effect of the Scaling Threshold Parameter

The scaling threshold parameter defines the minimum detectability of the radar system. Targets in the RoI having a higher SNR than the set scaling threshold will only be regarded as viable targets by the radar system. Since, the scaling threshold is directly proportional to the SNR obtained from insect targets, it is regarded as one of the fundamental parameters that define the performance of the system. The scaling threshold parameter will mainly affect the recall, precision and the false positive rate of the system. The results from experiments conducted in an urban environment in Figure 6.3 show that the higher the scaling threshold is defined, lower number of false positives will be detected by the system. On the other hand, the number of insects detected by the radar system could also decrease if the scaling threshold is set at a higher value. As depicted in Table 5.4, the Recall rate escalated by 35% when the scaling threshold was decreased from 7dB to 5dB respectively. This increase in recall factor, shows that more insects were detected by the radar system when the threshold was decreased. This correlates to the fact that insects produce a relatively weak signature for the radar to detect and hence, a lower threshold allows more insects could be detected. On the contrary, the false positive rate rose by 23% when the threshold was decreased. This proves that as the scaling threshold is decreased, a higher number of small movements generated by non-insect matter such as large leaves and shrubs will also be detected by the radar system and eventually affect the performance of the system. The precision of the system depends on the number of true and the false positives in the system. Therefore, as the threshold is decreased, the precision also degraded owing to an increase in the number of false positives generated by the system.

However, from the experiments conducted in Katwijk Aan Zee and Artis Zoo referred in Section 5.2.1 we can infer that the performance of the system not only depends on the scaling threshold but also on the external environmental conditions. Although the precision obtained in Katwijk Aan Zee increased by 16% compared to an urban environment, there were noticeable differences in the false positive rate obtained in both scenarios. The increase in precision could be associated with the larger size of insects being attracted, thereby, increasing the detection capability of the system, as the presence of larger buildings in the vicinity of the urban environment prevented the light stimuli in reaching all the distant insects and only the ones closer to the test environment would have been attracted. As depicted in Figure 6.3, in Artis experimental site, the false-positive rate saw a growth of approximately 45% from the experiments conducted in an urban environment. This increase in false-positive rate could be attributed to a large amount of vegetation and interference present in the area at which the experiment was conducted.

7.5.2 Effect of the Size of the Insects

The size of the insects attracted and lured in by the light source will mainly affect the false-negative rate that is achieved by the system in detecting insect targets. The false negative rate infers as to how many insects present near the radar system were not detected by the radar. The general assumption is that the radar system will be capable of detecting insects larger in size. The premise for this assumption is that larger insects will have a higher RCS because of their larger body cross-section and hence, will increase the probability of detection by the radar system.

It can be observed from Figure 6.4 and the experiments conducted that the average false negative rate obtained in suburban and Artis environments, reduced by 10% compared to an urban environment. This decrease could be attributed to larger insects (>2cm in size) being attracted to the light source from the wild. These environments were situated in areas where breeding and migration was common between larger insects. Thus, this could have been one reason behind the attraction of larger insects to the light source. The attraction of larger insects subsequently increased the precision of the system and this can be readily observed in Table 5.7 as the number of true positives obtained would be increased substantially. A higher number of small insects (<2 cm in Size) such as *Mosquitoes*, *House Flies* etc.. near the radar will not reflect enough energy for the radar to pick up because of their small body cross-sections and hence, will result in a higher number of missed detections and a higher false-negative ratio. As a result, the performance of the system is degraded by large amounts of small airborne insects. Since Insects like *Moths* and *Butterflies* are of higher emphasis as they are the most vulnerable species attracted to light sources at night [11], the presence of these insects near the radar system were detected with a higher probability. This proves that the mmWave radar shows better performance in detecting larger insects compared to smaller insects and can contribute effectively to monitor the decline of these important insect species across the globe.

7.5.3 Effect of External Environmental Conditions

The external environmental conditions have a fundamental impact on the performance of the system. This impact was visible in our experiments as the threshold that produced better results in an urban environment could not reproduce similar results in Artis as observed in Tables 5.4 and 5.9. The average false positive rate saw a 60% increase in Artis when compared to the obtained value in an urban environment. This trend is mainly associated with the external environmental conditions in an urban environment, where there weren't many obstructions present compared to the experimental site in Artis, which contained a large number of small leaves and shrubs that acted as a fundamental source of clutter. The presence of vegetation near the system contributes to environmental clutter and directly

affects the false positive rate obtained from the system. Therefore, this clutter present around the system will lead to a higher false positive rate and impact the performance. This increased false positive rate will also harm the precision and thereby, it can be deduced that the precision decreases by 40% as the false positive rate increases as observed in Figure 6.5. The total average false positive rate of around 30% observed in Table 6.2 for different environments proves that our system is moderately sensitive to the external clutter and the environmental conditions present around the system.

However, it is also important to note that these results are also dependent on the weather conditions on the particular day and whether the experiments are performed in an insect season. Therefore, recreating these tests on an other day, might not reproduce the same results as observed above and could generate exceptional or poor results comparatively. The premise for this inference is that dynamic circumstances such as strong winds might also lead to the system generating high number of false positives. Although, the wind conditions noted at the start of the experiment were labeled as gentle breeze, they might have increased over time and indirectly influenced the performance of the system. On the other hand, the presence of smaller insects near the system also degrades the performance of the system. Therefore, it is important to comprehend that the heterogeneity of the environment also plays an important role in determining and influencing the performance of the system.

7.6 Conclusion

This thesis aimed to investigate the performance of a mmWave radar system in effectively detecting airborne insects in a realistic urban and suburban environment.

It was observed that the theoretical maximum range obtained in the mmWave radar system in ideal conditions to be around 2m for detecting small targets. However, this is considered to be a low range and cannot be effectively used to determine the large scale effect of ALAN on airborne insect species. Therefore, an array of mmWave sensor nodes would need to be deployed to enhance the maximum range and investigate the effect of ALAN competently. By addressing our second research question of determining the performance of the mmWave radar in detecting insect-like targets, we were able to observe that the mmWave radar exhibited high performance and accuracy in determining the range of dynamic small targets closer to its ground truth with a minimal margin of error. This provides an insight into how the high reliability of the mmWave radar in measuring the actual range of airborne insect targets and how it could effectively aid in researching the range at which they are attracted to ALAN. From analyzing the perfor-

mance of the mmWave radar in detecting airborne insects, we observed that it displayed moderate performance in detecting insects as the recall and precision rates were estimated to be around 65% and 70% respectively in various environments. Although, the mmWave radar displays high accuracy in measuring the range of small insect-like targets, the moderate recall and precision rate suggest that its capability in detecting airborne insects is still under question and more research needs to be conducted regarding the same. Thus, we can infer that this technology at its current starting stage cannot be reliably used by ecologists around the world to monitor and track insect populations due to its various external dependencies and unpredictability in adverse conditions, However, the performance of the mmWave radar can be certainly improved by addressing its limitations and conducting more experiments in different environmental conditions to gain an even better insight into the working of the system.

The fundamental research questions proposed at the start of the research in Section 1.4 were accomplished and this research introduced us to a new domain of monitoring ecology and biodiversity with the state of the art commercially available mmWave radar modules.

7.7 Future Work and Recommendations

There are several shortcomings of this technology that are required to be addressed in the upcoming future. As discussed in 7.5, the radar system has displayed a moderate performance in detecting insects in noisy and obstreperous environments. This performance of the system can be enhanced by developing and implementing machine learning algorithms that could distinguish airborne insect targets from various environmental clutter such as vegetation, leaves and animals. Besides, the following recommendations could further increase the performance of the radar system and extend this research in detecting and counting insects to estimate the broader scale **Vacuum Cleaner Effect** of light on insects.

- The mmWave radar sensor can be configured to have a higher range compared to the maximum range of 2m achieved in this thesis. This can be accomplished by redesigning the antenna specifications to obtain a higher antenna gain and transmitting power to extend the transmission range of the radiowaves. However, as the transmitting power increases, the power consumption of the mmWave radar would also increase.

- The real time coordinates obtained for certain insects from the mmWave radar system depicted in Section 5.2.1 can be further validated by integrating the mmWave radar with a vision based sensor and developing a vision based algorithm to extract

insect features from the video and tracking those features subsequently. This validation can provide an insight into the accuracy of the mmWave radar in tracking real time coordinates of an insect target.

- By leveraging machine learning and deep learning models, accurate identification of the detected insect species can be performed. This process can be achieved by extracting specific features of an insect such as its Doppler signature, SNR and frequency from the raw data available in the mmWave radar system [44]. These characteristics could then be used to train an ML model and identify specific insects based on an existing dataset that contain annotated data from multiple different insect species. These algorithms could also help in the re-identification of insects to prevent repetitive counting of the same insect flying in front of the radar frequently.

- The CFAR performance of the mmWave radar's processor could be improved by employing artificial intelligence algorithms namely the AI-CFAR prototype [58]. The basic assumption behind this technique is that the radar's processor consists of multiple CFAR algorithms. Based on the external environment where the radar is deployed, the system could dynamically select its CFAR processing algorithm to enhance the detectability of the radar system. The different types of environments could be presumed to be cluttered and noiseless environments. Fundamental and appropriate CFAR parameters such as the reference and guard window size can learn from its previous configurations through supervised and unsupervised techniques and decide the most optimal value for a particular environment.

- The radar system can be integrated with a mini-computer such as Raspberry PI which would act as a gateway and a memory device for seamless acquisition and storing of data from the radar when it is deployed in remote and inaccessible locations where insect activity is abundant.

- **Vacuum Cleaner Effect** is a large scale phenomenon that would be intricate to measure with a single mmWave sensor. Therefore, multiple sensor would be required to work in tandem to determine this effect. mmWave radars could be mounted on an array of lightpoles to identify an insect and track its respective position in time. However, as the distance between these multiple light poles may not be enough to effectively investigate the effect of ALAN, it also becomes important to mount the mmWave sensor nodes in a grid or a network away from the lightpoles in the natural environment where there is no light. This will enable the mmWave radar module to track an insect as it approaches a lightpole from a certain distance and identify it continuously by following its trail. This operation of the mmWave radar module will allow it to investigate the effect of ALAN on different insect species

effectively. The operation of mounting the radar on an elevated grid or a lightpole would also reduce its environmental dependency as there wouldn't be large amounts of clutter generating sources such as trees and leaves present at that elevation. Nevertheless, birds could still generate some amount of clutter at this height, but will produce a high SNR as compared to insects and can be readily distinguished based on the SNR calculated from the radar device. However, incorporating ML algorithms inside the radar's processor would increase the performance of the system at the expense of complexity. Therefore, this trade-off would need to be considered in future applications of this technology.

The results obtained from evaluating the performance of the mmWave radar system in multiple small scale environments in this thesis can be further extended to estimate the vacuum cleaner effect of insects in large scale environments by deploying this system in insect abundant areas for longer periods.

Bibliography

[1] Nigel E Stork. "How many species are there?" In: *Biodiversity Conservation* 2 (3 1993), pp. 215–232. ISSN: 1572-9710. DOI: 10.1007/BF00056669. URL: https://doi.org/10.1007/BF00056669.

[2] Bruce Heming. "BOOK REVIEW: Grimaldi D. Engel M. 2005: Evolution of the Insects." In: *European Journal of Entomology* 103 (Jan. 2006), pp. 273–275. DOI: 10.14411/eje.2006.034.

[3] Gene R. DeFoliart. "The Human Use of Insects as Food and as Animal Feed". In: *Bulletin of the Entomological Society of America* 35.1 (Mar. 1989), pp. 22–36. ISSN: 0013-8754. DOI: 10.1093/besa/35.1.22. eprint: https://academic.oup.com/ae/article-pdf/35/1/22/18812731/besa35-0022.pdf. URL: https://doi.org/10.1093/besa/35.1.22.

[4] Geoffrey G. E. Scudder. "The Importance of Insects". In: (2017), pp. 9–43. DOI: https://doi.org/10.1002/9781118945568.ch2. eprint: https://onlinelibrary.wiley.com/doi/pdf/10.1002/9781118945568.ch2. URL: https://onlinelibrary.wiley.com/doi/abs/10.1002/9781118945568.ch2.

[5] Maja Grubisic et al. "Insect declines and agroecosystems: does light pollution matter?" In: *Annals of Applied Biology* 173 (Sept. 2018), pp. 180–189. DOI: 10.1111/aab.12440.

[6] Emmanuel Desouhant et al. "Mechanistic, ecological, and evolutionary consequences of artificial light at night for insects: review and prospective". In: *Entomologia Experimentalis et Applicata* 167.1 (2019), pp. 37–58. DOI: https://doi.org/10.1111/eea.12754. eprint: https://onlinelibrary.wiley.com/doi/pdf/10.1111/eea.12754. URL: https://onlinelibrary.wiley.com/doi/abs/10.1111/eea.12754.

[7] Kathryn L G Russart and Randy J Nelson. "Light at night as an environmental endocrine disruptor". In: *Physiology behavior* 190 (June 2018), pp. 82–89. ISSN: 1873-507X. DOI: 10.1016/j.physbeh.2017.08.029. URL: https://pubmed.ncbi.nlm.nih.gov/28870443%20https://www.ncbi.nlm.nih.gov/pmc/articles/PMC5839924/.

[8] Eric J. Warrant. "The remarkable visual capacities of nocturnal insects: vision at the limits with small eyes and tiny brains". In: *Philosophical Transactions of the Royal Society B: Biological Sciences* 372.1717 (2017), p. 20160063. DOI: 10.1098/rstb.2016.0063. URL: https://royalsocietypublishing.org/doi/abs/10.1098/rstb.2016.0063.

[9] Marc Rhainds and Stephen Heard. "Sampling procedures and adult sex ratios in spruce budworm". In: *Entomologia Experimentalis et Applicata* 154 (Dec. 2014). DOI: 10.1111/eea.12257.

[10] Florian Altermatt. "Diversity in riverine metacommunities: A network perspective". In: *Aquatic Ecology* 47 (Sept. 2013). DOI: 10.1007/s10452-013-9450-3.

[11] Frank van Langevelde et al. "Declines in moth populations stress the need for conserving dark nights". In: *Global Change Biology* 24.3 (2018), pp. 925–932. DOI: https://doi.org/10.1111/gcb.14008. eprint: https://onlinelibrary.wiley.com/doi/pdf/10.1111/gcb.14008. URL: https://onlinelibrary.wiley.com/doi/abs/10.1111/gcb.14008.

[12] Avalon CS Owens et al. "Light pollution is a driver of insect declines". In: *Biological Conservation* 241 (2020), p. 108259.

[13] Phillip Stepanian et al. "Dual-polarization Radar Products for Biological Applications". In: *Ecosphere* 7 (Nov. 2016). DOI: 10.1002/ecs2.1539.

[14] Liang Mei and Mikkel Brydegaard. "Atmospheric aerosol and gas sensing using Scheimpflug lidar". In: EGU General Assembly Conference Abstracts, 7305 (Apr. 2015), p. 7305.

[15] Carsten Kirkeby, Maren Wellenreuther, and Mikkel Brydegaard. "Observations of movement dynamics of flying insects using high resolution lidar". In: *Scientific Reports* 6 (1 2016), p. 29083. ISSN: 2045-2322. DOI: 10.1038/srep29083. URL: https://doi.org/10.1038/srep29083.

[16] Ziwei Song et al. "Application of lidar remote sensing of insects in agricultural entomology on the Chinese scene". In: *Journal of Applied Entomology* 144.3 (2020), pp. 161–169. DOI: https://doi.org/10.1111/jen.12714. eprint: https://onlinelibrary.wiley.com/doi/pdf/10.1111/jen.12714. URL: https://onlinelibrary.wiley.com/doi/abs/10.1111/jen.12714.

[17] Yanping Chen et al. "Flying Insect Classification with Inexpensive Sensors". In: *Journal of Insect Behavior* 27 (5 2014), pp. 657–677. ISSN: 1572-8889. DOI: 10.1007/s10905-014-9454-4. URL: https://doi.org/10.1007/s10905-014-9454-4.

[18] Ilyas Potamitis and Iraklis Rigakis. "Novel Noise-Robust Optoacoustic Sensors to Identify Insects Through Wingbeats". In: *IEEE Sensors Journal* 15 (8 Aug. 2015), pp. 4621–4631. ISSN: 1530437X. DOI: 10.1109/JSEN.2015.2424924.

[19] Xu Shi et al. "Seasonal Trends in Movement Patterns of Birds and Insects Aloft Simultaneously Recorded by Radar". In: *Remote Sensing* 13 (May 2021), p. 1839. DOI: 10.3390/rs13091839.

[20] Frank Bellrose. "Radar Ornithology. Eric Eastwood. Methuen, London, 1967 (distributed in the U.S. by Barnes and Noble, New York). xii + 278 pp., illus. 12". In: *Science* 160.3830 (1968), pp. 869–869. ISSN: 0036-8075. DOI: 10.1126/science.160.3830.869. eprint: https://science.sciencemag.org/content/160/3830/869.1.full.pdf. URL: https://science.sciencemag.org/content/160/3830/869.1.

[21] W Ruhe. "ASR—Bird observation program at German airports". In: 2 (2000), pp. 157–165.

[22] Sidney Gauthreaux, Carroll Belser, and Donald Blaricom. "Using a Network of WSR-88D Weather Surveillance Radars to Define Patterns of Bird Migration at Large Spatial Scales". In: (Jan. 2003), pp. 335–346. DOI: 10.1007/978-3-662-05957-9_23.

[23] R. Day and B. A. Cooper. "Patterns of movement of Dark-rumped Petrels and Newell's shearwaters on Kauai". In: *The Condor* 97 (1995), pp. 1011–1027.

[24] V. Alistair Drake and Bruno Bruderer. "Aeroecological observation methods". English. In: (2017). Ed. by Phillip B. Chilson et al., pp. 201–237. DOI: 10.1007/978-3-319-68576-2_9.

[25] HU Cheng et al. "Analysis of Insect RCS Characteristics". In: 42.1 (2020), pp. 140–153.

[26] Tianran Zhang et al. “Insect wing-beat frequency automatic extraction and experimental verification with a Ku-band insect radar system”. In: *The Journal of Engineering* 2019.21 (2019), pp. 7973–7976.

[27] S. E. Hobbs and W. W. Wolf. “An airborne radar technique for studying insect migration”. In: *Bulletin of Entomological Research* 79.4 (1989), pp. 693–704. DOI: 10.1017/S000748530001885X.

[28] Jason Chapman, Don Reynolds, and ALAN SMITH. “Vertical-Looking Radar: A New Tool for Monitoring High-Altitude Insect Migration”. In: *BioScience* 53 (Jan. 2009), pp. 503–511. DOI: 10.1641/0006-3568(2003)053[0503:VRANTF]2.0.CO;2.

[29] Denis Poffo et al. “Migration monitoring of Ascia monuste (Lepidoptera) and Schistocerca cancellata (Orthoptera) in Argentina using RMA1 weather radar”. In: *ISPRS Journal of Photogrammetry and Remote Sensing* 145 (May 2018). DOI: 10.1016/j.isprsjprs.2018.05.011.

[30] Cheng Hu et al. “Insect speed extraction method based on a high resolution and full polarisation radar with vertical-looking mode”. In: *The Journal of Engineering* 2019 (May 2019). DOI: 10.1049/joe.2019.0385.

[31] Anna Katharina Knuff et al. “Insect abundance in managed forests benefits from multi-layered vegetation”. In: *Basic and Applied Ecology* 48 (2020), pp. 124–135. ISSN: 1439-1791. DOI: https://doi.org/10.1016/j.baae.2020.09.002. URL: https://www.sciencedirect.com/science/article/pii/S143917912030092X.

[32] Simon J Grove. “Saproxylic insect ecology and the sustainable management of forests”. In: *Annual review of ecology and systematics* 33.1 (2002), pp. 1–23.

[33] Woody Turner et al. “Remote sensing for biodiversity science and conservation”. In: *Trends in ecology & evolution* 18.6 (2003), pp. 306–314.

[34] Kevin Lim et al. “LiDAR remote sensing of forest structure”. In: *Progress in Physical Geography: Earth and Environment* 27.1 (2003), pp. 88–106. DOI: 10.1191/0309133303pp360ra.

[35] Michael Lefsky et al. “Revised method for forest canopy height estimation from Geoscience Laser Altimeter System waveforms”. In: *Journal of Applied Remote Sensing* 1 (Sept. 2007). DOI: 10.1117/1.2795724.

[36] Shiming Zhu et al. “Insect abundance over Chinese rice fields in relation to environmental parameters, studied with a polarization-sensitive CW near-IR lidar system”. In: *Applied Physics B* 123 (7 2017), p. 211. ISSN: 1432-0649. DOI: 10.1007/s00340-017-6784-x. URL: https://doi.org/10.1007/s00340-017-6784-x.

[37] Dave Raman, R.R. Gerhardt, and J.B. Wilkerson. “Detecting Insect Flight Sounds in the Field: Implications for Acoustical Counting of Mosquitoes”. In: *Transactions of the ASABE* 50 (July 2007), pp. 1481–1485. DOI: 10.13031/2013.23606.

[38] L. A. Klein et al. “MMW radar for dedicated bird detection at airports and airfields”. In: (2004), pp. 157–160.

[39] Samiur Rahman and Duncan A Robertson. “Radar micro-Doppler signatures of drones and birds at K-band and W-band”. In: *Scientific reports* 8.1 (2018), pp. 1–11.

[40] J. R. Riley. “A millimetric radar to study the flight of small insects”. In: *Electronics and Communication Engineering Journal* 4 (1 1992). ISSN: 09540695. DOI: 10.1049/ecej:19920011.

[41] Nazifa Tahir and Graham Brooker. “Towards The Development of Millimeter Wave Harmonic Sensors for Tracking Small Insects”. In: *IEEE Sensors Journal* 15 (Oct. 2015), pp. 1–1. DOI: 10.1109/JSEN.2015.2445933.

[42] Yu-Ting Liu et al. “A differential miniature transponder for 9.4/18.8 GHz harmonic bee searching radar with low gain degradation from bee’s body”. In: (2016), pp. 1–4. DOI: 10.1109/MWSYM.2016.7540016.

[43] J. Yang et al. “Development of Millimeter-wave FMCW Vertical-looking Entomological Radar System”. In: (2019), pp. 1–2. DOI: 10.1109/iWEM.2019.8887884.

[44] Rui Wang et al. “Micro-Doppler measurement of insect wing-beat frequencies with W-band coherent radar”. In: *Scientific Reports* 7 (Dec. 2017). DOI: 10.1038/s41598-017-01616-4.

[45] J. -. Muñoz-Ferreras et al. “Coherent Deramping-Based Multi-FMCW Radar Architecture”. In: (2019), pp. 1–4. DOI: 10.1109/WISNET.2019.8711795.

[46] S. H. Dokhanchi et al. “A mmWave Automotive Joint Radar-Communications System”. In: *IEEE Transactions on Aerospace and Electronic Systems* 55.3 (2019), pp. 1241–1260. DOI: 10.1109/TAES.2019.2899797.

[47] Holger Zeltwanger. *Advanced Vision with mmWave Sensors*. https://can-newsletter.org/uploads/media/raw/f903557d04f5d2ae891-d6a5304756708.pdf. [Online; accessed 28-September-2021]. 2017.

[48] Long Cai et al. “Performance Analysis of Some New CFAR Detectors under Clutter.” In: *J. Comput.* 6.6 (2011), pp. 1278–1285.

[49] Ryszard Wawruch. “Experimental evaluation of the Constant False Alarm Rate (CFAR) algorithms used in maritime FM-CW radars”. In: *Zeszyty Naukowe/Akademia Morska w Szczecinie* 36 (108) z. 1 (2013), pp. 177–181.

[50] Texas Instruments. *mmWave Sensing Estimator*. https://dev.ti.com/gallery/view/mmwave/mmWaveSensingEstimator/ver/1.4.0/. [Online; accessed 23-June-2021]. 2020.

[51] Mirabel. C. Rezende et al. “Radar Cross Section Measurements (8-12 GHz) of Magnetic and Dielectric Microwave Absorbing Thin Sheets”. In: (2002).

[52] C.R. Vaughn. “Birds and insects as radar targets: A review”. In: *Proceedings of the IEEE* 73.2 (1985), pp. 205–227. DOI: 10.1109/PROC.1985.13134.

[53] Huafeng Mao et al. “Fully Polarimetric Radar Observing Insects Flight”. In: (2019), pp. 1–4. DOI: 10.1109/ICSIDP47821.2019.9172916.

[54] Xin Cheng and Mao Sun. “Wing-kinematics measurement and aerodynamics in a small insect in hovering flight”. In: *Scientific reports* 6.1 (2016), pp. 1–12.

[55] Nidhi and Km Archana Patel. “An Efficient and Scalable Density-based Clustering Algorithm for Normalize Data”. In: *Procedia Computer Science* 92 (2016). 2nd International Conference on Intelligent Computing, Communication Convergence, ICCC 2016, 24-25 January 2016, Bhubaneswar, Odisha, India, pp. 136–141. ISSN: 1877-0509. DOI: https://doi.org/10.1016/j.procs.2016.07.336. URL: https://www.sciencedirect.com/science/article/pii/S1877050916315824.

[56] Travis Longcore and Catherine Rich. “LIGHTS OUT! FOR NATURE”. In: (June 2007).

[57] Carsten Kirkeby et al. “Advances in automatic identification of flying insects using optical sensors and machine learning”. In: *Scientific reports* 11.1 (2021), pp. 1–8.

[58] W. Baldygo et al. “Artificial intelligence applications to constant false alarm rate (CFAR) processing”. In: *The Record of the 1993 IEEE National Radar Conference*. 1993, pp. 275–280. DOI: 10.1109/NRC.1993.270451.

Appendix A

Theory

A.1 Cell-averaging CFAR

The CASO-CFAR detection algorithm discussed in 3.5.1 employed in our thesis is derived from the CA-CFAR algorithm. Even though, the CA-CFAR algorithm has not been applied in our thesis and does not significantly contribute to the results obtained from our system. However, it is necessary to understand the working behind the CA-CFAR algorithm to gain a deeper understanding of underlying concepts involved in the design of a CFAR algorithm.

Cell-averaging CFAR (CA-CFAR) is a detection scheme, where the threshold level is calculated by estimating the noise level under the floor around the Cell under test (CUT). The CUT is determined as the range cell in which the target's signal is present, for which the detection is required. This is done by estimating the average power level around the neighbouring cells of the CUT. However, this estimation is error prone as the immediate adjacent cells of the CUT could have the same power level and result in an error induced average power level. Thus, the immediate adjacent cells are ignored and are referred to as guard cells. A target is declared present in the CUT if the threshold is greater than all its adjacent cells (Excluding the guard cells) and its local average power level. This local average power level is what is known as the scaling threshold which can be further increased or decreased depending on the target scene and characteristics.

Figure A.1 shows the principle of a cell averaging CFAR system. It can be observed that the threshold for cell under test Y in the reference window can be evaluated by averaging the power level of the neighbouring cells from X1 to Xn. It can also be depicted that the immediate adjacent cells of the CUT have been considered as guard cells. The

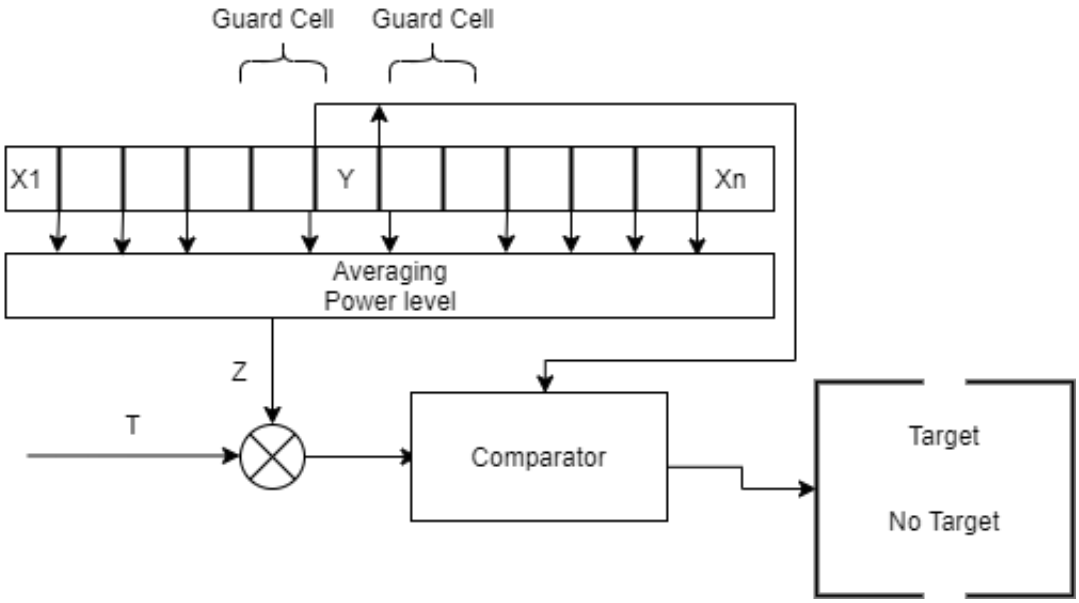


Figure A.1: *Working of the CA-CFAR algorithm*

resultant mean of values in the reference window can be given by Z

$$Z = \frac{1}{N} \sum_{i=1}^{N} X_i \tag{A.1}$$

The scaling threshold is then multiplied by the resultant mean Z in a mixer circuit and the value of cell under test Y is fed into a comparator circuit. The comparator circuit then compares the value of Y with the multiplication factor of Z x T and if this value of Y is greater than the multiplication factor, then it would be recognised as a viable target.

Paper	Goal	Technology used	Data and Information	System Setup	Data Analysis	Results obtained
Kirkeby, et al, 2016[14]	Tracking and classifying Insect population abundance	CW KHz LIDAR, and UV light trap for attracting insects.	808nm near Infrared 3.2W CW laser. 12-bit line scan camera sensor.	Light trap setup at 65m from the Laser beam. The termination box at 140m from the laser beam.	Data reduction and parametrization algorithm[21]	Small Insects abundant near light trap (wing size < 2.5mm2, WBF > 300Hz) large insect abundant near LIDAR system
Song, et al, 2020[15]	Tracking insect abundance on a Chinese rice paddy field	CW Scheimpflug LIDAR, and UV light trap for attracting insects.	808nm two semiconductor lasers, 2048 pixel CMOS linear array.	UV lamp setup at 180m from the laser beam. Termination box at 513m from the laser beam.	FFT to indicate wingbeat frequencies around 200 and 375Hz.	Twelve species of insects and more than 2400 insects were abundant near the LIDAR system
Chen, et al, 2014[17]	Identify and classify insects based on their WB sound.	Pseudo Acoustic Optical Sensor.	Data is recorded into MP3 format.	Laser pointing at a phototransistor array inside a chamber.	Nearest neighbor (KNN), Bayesian classifier.	Maximum accuracy of 95.2% in classifying insects.
I. Potamitis, et al, 2015[18]	To achieve insect species classification through wingbeats	Opto-electronic sensor.	Wingbeat sound measured with a microphone. 3KHz LPF.	60KHz laser emitter, photodiode array as receiver.	Distance measures: Log spectral distance, Itakura Saito distance.	Spectrogram of various species of insects plotted.
J.Yang, 2019[22]	To detect insects flying 200m above the ground.	mmWave - FMCW based VLR	34.5 GHz sampling frequency of radar, 30MHz BPF	mmWave FMCW based vertical radar, waveguide placed on a rotating module, 6 turns per second.	ALTERA FPGA, FFT.	Flying orientation, velocity and body shape obtained from insects every 15 minutes
Riley , 1992[19]	Study the flight of small insects.	mmWave based Radar.	34.1 GHz sampling frequency of radar.	Thyratron-driven pulse radar. Horn antenna.	Quantitative analysis of Radar returns[22]	Aerial density of small insects were analyzed.
J. Mu-noz ferreras, 2019[23]	Estimating the range and radial velocities of illuminated targets.	Coherent FMCW based Radar	24.18 GHz sampling frequency of radar.	Dual FMCW based RADAR with multiple FMCW modes.	Fourier processing or raw data with respect to relevant FMCW modes.	Doppler maps for the targets are obtained
RuiWang, 2016[23]	Measure wingbeat frequency using amplitude and phase modulation.	Coherent Radar	3.2mm Wavelength W-band, 90mm S-band.	W-band and S-band radar. Polystyrene adhered to insect. Dual antenna for transmit and receive.	Micro-doppler analysis, STFT signal processing	Spectrum component analysis was performed. Phase modulation of signal proven to be more effective.

Figure A.2: *Literature Review Summary*